The Pennsylvania State University
The Graduate School
College of Earth and Mineral Sciences

ESSAYS ON MARKET IMPACTS OF NATURAL GAS PIPELINE EXPANSION AND CROSS-PRODUCT MANIPULATION IN ELECTRICITY MARKETS

A Dissertation in
Energy and Mineral Engineering
by
Nongchao Guo

Submitted in Partial Fulfillment
of the Requirements
for the Degree of

Doctor of Philosophy

August 2018

The dissertation of Nongchao Guo was reviewed and approved* by the following:

Chiara Lo Prete
Assistant Professor of Energy Economics
Dissertation Advisor, Chair of Committee

Andrew N. Kleit
Professor of Energy and Environmental Economics

Mort D. Webster
Professor of Energy Engineering

Uday V. Shanbhag
Gary and Sheila Bello Chair Professor of Industrial and Manufacturing Engineering

Luis F. Ayala H.
Professor of Petroleum and Natural Gas Engineering
Associate Department Head for Graduate Education

*Signatures are on file in the Graduate School.

Abstract

This dissertation explores market impacts of natural gas pipeline expansion and cross-product manipulation in electricity markets.

With the surge of production of natural gas in the Marcellus region of Pennsylvania, several expansion projects have been proposed to address the scarcity of pipeline capacity out of the region. Chapter 1 focuses on one of these projects, Williams Company's Atlantic Sunrise project. A fine-grained spatial model based on the arbitrage cost approach is developed to study the potential economic impacts of the project. Over the 30-month period examined, we estimate that consumers from Alabama to New Jersey would have enjoyed about $3.0 billion in total benefits because of the expansion, while producers would have lost about $1.3 billion.

Chapter 2 and 3 look into virtual transactions and cross-product manipulation in wholesale electricity markets in the U.S. Virtual transactions are financial positions that allow market participants to exploit arbitrage opportunities arising when day-ahead electricity prices are predictably higher or lower than expected real-time prices. Unprofitable virtual transactions may be used to move day-ahead prices in a direction that enhances the value of related positions, like financial transmission rights (FTRs). This constitutes cross-product manipulation, and has emerged as a central policy concern of the Federal Energy Regulatory Commission in recent years. Chapter 2 presents a three-stage equilibrium model in a two-node setting to study cross-product manipulation in two-settlement energy markets. Chapter 3 extends the equilibrium model by incorporating a network with loop flows and generator unit commitment problems. Numerical results from the two-node system in Chapter 2 show that uneconomic bidding at the FTR contract sink is an equilibrium strategy for financial trader, if the gains from FTRs exceed the losses from virtual bids. This strategy further diverges the day-ahead price from its expected real-time level at the node being manipulated. Moreover, the trader has a greater incentive to do so as the day-ahead demand becomes more inelastic. Chapter 3 shows that uneconomic bidding could take place at nodes other than the FTR sink. This is because, when loop flows are introduced, price separation between the source and sink of the FTR

path can be induced by congestion of transmission lines different from the FTR path. Since uneconomic manipulation increases the day-ahead prices at certain nodes, a higher fracture of capacity from generators located at these nodes will be dispatched, resulting in higher commitment costs for these generators.

Contents

List of Figures viii

List of Tables x

Acknowledgments xii

Chapter 1
Welfare Impacts of Natural Gas Pipeline Expansion in the Northeastern U.S. 1
1.1 Introduction . . . 1
1.2 Model . . . 5
1.2.1 An Arbitrage Cost Model to Examine Natural Gas Pipeline Expansions . . . 5
1.2.2 Algorithm . . . 7
1.2.2.1 Scenarios . . . 7
1.2.2.2 Price Relations and Supply Demand Balance Conditions . . . 8
1.2.2.3 Verification Conditions . . . 12
1.3 Data . . . 25
1.4 Results . . . 26
1.4.1 Impacts of Atlantic Sunrise on January 28, 2014 . . . 27
1.4.2 Consumer and Producer Surplus Analysis . . . 28
1.4.3 Sensitivity Analysis . . . 31
1.5 Conclusions . . . 31

Chapter 2
Cross-product Manipulation in Electricity Markets: A Three-stage, Two-node Equilibrium Model 34
2.1 Introduction . . . 34
2.2 Literature Review . . . 38

2.3 Model . . . 41
2.3.1 Real-time Market Model Formulation . . . 43
2.3.2 Day-ahead and FTR Markets Model Formulation . . . 48
2.3.2.1 Case 1: Two Competitive Generators and Two Competitive Traders (One with FTR) . . . 49
2.3.2.2 Case 2: Two Competitive Generators, One Cournot Trader with FTR, One Competitive Trader without FTR . . . 54
2.3.2.3 Case 3: Two Cournot Generators, Two Cournot Traders (One with FTR) . . . 55
2.3.2.4 Case 4: Two Cournot Generators, One Cournot Traders with FTR, Multiple Cournot Traders without FTR . . . 57
2.3.2.5 Case 5 (Benchmark): Two Cournot Generators, One Cournot Trader without FTR . . . 61
2.3.2.6 Case 6 (Benchmark): Two Cournot Generators, Two Cournot Traders (without FTR) . . . 63
2.3.2.7 Case 7 (Benchmark): Two Cournot Generators, Two Competitive Traders (One with FTR) . . . 64
2.3.2.8 Case 8: Two Cournot Generators, Two Cournot Traders with FTRs . . . 68
2.4 Solution Method and Metrics . . . 70
2.5 Results . . . 72
2.5.1 Short-run MPEC Results . . . 72
2.5.2 Sensitivity Analysis . . . 74
2.5.3 Long-run MPEC Results . . . 75
2.5.4 EPEC Results . . . 76
2.6 Conclusions . . . 77

Chapter 3
Cross-product Manipulation in Electricity Markets: A Two-stage, Multi-node Equilibrium Model with Intertemporal Constraints **85**
3.1 Introduction . . . 85
3.2 Model . . . 87
3.2.1 Case 1: Real-time Competitive, Day-ahead Competitive Model Formulation . . . 91
3.2.1.1 Real-time Market Model Formulation . . . 91
3.2.1.2 Day-ahead Market Model Formulation . . . 93

3.2.2 Case 2: Real-time Competitive, Day-ahead Cournot Model Formulation . . . 96
3.2.2.1 Real-time Market Model Formulation . . . 96
3.2.2.2 Day-ahead Market Model Formulation . . . 96
3.2.3 Case 4: Real-time Cournot, Day-ahead Cournot Model Formulation . . . 97
3.2.3.1 Real-time Market Model Formulation . . . 98
3.2.3.2 Day-ahead Market Model Formulation . . . 99
3.3 Solution Method and Metrics . . . 99
3.4 Parameters and Results . . . 100
3.4.1 Parameters . . . 100
3.4.2 Results . . . 102
3.4.3 Sensitivity Analysis . . . 111
3.4.3.1 Trader 5's Collateral . . . 111
3.4.3.2 Ramping Capabilities . . . 111
3.4.3.3 Trader 4's FTR Position . . . 112
3.4.3.4 Reference Prices at Node C . . . 112
3.4.3.5 Relationship between Trader 4's Profitability and Day-ahead Load at Node C . . . 114
3.5 Conclusions . . . 114

Bibliography **117**

List of Figures

1.1 Rate Zones on the Transco System 2
1.2 Possible equilibria after the Atlantic Sunrise expansion, when Station 90 is unconstrained before Atlantic Sunrise ("#" refers to the scenarios) 16
1.3 Possible equilibria after the Atlantic Sunrise expansion, when Station 90 is constrained before Atlantic Sunrise and the constraint is eliminated after the expansion ("#" refers to the scenarios) 17
1.4 Possible equilibria after the Atlantic Sunrise expansion, when Station 90 is constrained before and after the Atlantic Sunrise expansion ("#" refers to the scenarios) 18
1.5 Equilibrium Flows on January 28, 2014 27

2.1 Time Frame and Market Participants of the Three-stage Game . . . 42
2.2 Scenario Tree of the Three-stage Game 43
2.3 Consumer Surplus Calculation when Real-time Load is Greater than Day-ahead Load 71
2.4 Consumer Surplus Calculation when Real-time Load is Less than Day-ahead Load 72
2.5 Case 4: Day-ahead Price Premium versus Number of Trader(s) 4 (Slope = 0.1) 75
2.6 Case 3: Trader 3's Profit on Virtual Positions at Node B versus Slopes of Inverse Demand Functions 76
2.7 Reaction Functions when $c_f = 0$ 77
2.8 Reaction Functions when $c_f = 3,000$ 78

3.1 Game Structure 90
3.2 Consumer Surplus Calculation when Generators Behave à la Cournot in the Real-time Market, and Real-time Load is Greater than Day-ahead Load 100
3.3 Illustration on Simultaneous Feasibility Test 102
3.4 Real-time Load at Node A for RT Competitive Cases 104

3.5 Real-time Load at Node B for RT Competitive Cases 105
3.6 Real-time Load at Node C for RT Competitive Cases 106
3.7 Price Divergence at Node C for Case 2 108
3.8 Price Divergence at Node C for Case 4 108
3.9 Relationship between Trader 5's Collateral and Day-ahead Price at Node C 111
3.10 Trader 5's Profits vs Collateral 112
3.11 Relationship between Trader 4's Profitability and Day-ahead Load at Node C 115

List of Tables

1.1 Possible equilibria after the Atlantic Sunrise expansion, when Station 90 is unconstrained before Atlantic Sunrise . . . 19
1.1 Possible equilibria after the Atlantic Sunrise expansion, when Station 90 is unconstrained before Atlantic Sunrise . . . 20
1.2 Possible equilibria after the Atlantic Sunrise expansion, when Station 90 is constrained before Atlantic Sunrise and the constraint is eliminated after the expansion . . . 21
1.2 Possible equilibria after the Atlantic Sunrise expansion, when Station 90 is constrained before Atlantic Sunrise and the constraint is eliminated after the expansion . . . 22
1.3 Possible equilibria after the Atlantic Sunrise expansion, when Station 90 is constrained before and after the Atlantic Sunrise expansion . . 23
1.3 Possible equilibria after the Atlantic Sunrise expansion, when Station 90 is constrained before and after the Atlantic Sunrise expansion . . 24
1.4 Elasticities of Demand . . . 25
1.5 Elasticities of Supply . . . 26
1.6 Comparison of Flows Before and After Atlantic Sunrise, January 28, 2014 (thousand MMBtu) . . . 29
1.7 Comparison of Withdrawals, Injections and Prices Before and After Atlantic Sunrise on January 28, 2014 . . . 29
1.8 Change of Consumer Surplus Under Medium Elasticities (thousand dollars) . . . 30
1.9 Change of Producer Surplus Under Medium Elasticities (thousand dollars) . . . 31
1.10 Change of Consumer Surplus and Producer Surplus Under Different Elasticities (million dollars) . . . 32

2.1 Average Cleared Virtual Bids as A Percentage of Average Real-time Load by ISO (2014-2015) . . . 36

2.2 Percentage of Total Submitted Virtual Bids by Participant Type in PJM (2014-2015) . . . 36
2.3 Percentage of Average Cleared Virtual Bids by Participant Type in CAISO (2014-2015) . . . 37
2.4 Assumed Parameters for Two-generator Cases . . . 79
2.5 Numerical Results for Two-generator Case 1 to Case 7 (slope = 0.1), (B) denotes Benchmark cases . . . 80
2.6 Numerical Results for Two-generator Case 1 to Case 7 (slope = 0.1), (B) denotes Benchmark cases . . . 81
2.7 Numerical Results for Two-generator Case 1 to Case 7 (slope = 0.1), (B) denotes Benchmark cases . . . 82
2.8 Sensitivity Analysis for Long-term effects (Case 3, Hourly) . . . 83
2.9 Sensitivity Analysis for Long-term effects (Case 3, Quarterly) . . . 84

3.1 Modeling Differences between Chapter 2 and Chapter 3 . . . 87
3.2 Assumed Parameters for Base Cases . . . 105
3.3 Hourly Real-time Load (MW) . . . 106
3.4 Intercepts of Hourly Day-ahead Inverse Demand Functions ($/MW) 107
3.5 Numerical Results . . . 109
3.5 Numerical Results . . . 110
3.6 Sensitivity Analysis of Trader 4's FTR Positions . . . 113
3.7 Trader 4's Virtual Positions and Profits under Different Reference Prices at Node C . . . 113

Acknowledgments

I would like to first express my sincere gratitude to my advisor, Dr. Chiara Lo Prete. During my years as a Ph.D. student at Penn State, Dr. Lo Prete spent countless hours in advising me and gave me priceless advice on my dissertation. She is a role model who constantly inspires me to become an independent and diligent researcher. This dissertation would not be possible without her tremendous help.

I would also like to thank my committee members, Dr. Andrew N. Kleit, Dr. Mort D. Webster and Dr. Uday V. Shanbhag for their guidance and feedback on my dissertation. Every discussion I had with them broadened my horizon and motivated me to keep moving my research forward.

To my family and friends, especially Xiumei Wang, Shengxi Jin, Qiujia Jin, James Spencer Lundh, Cody Hohl, Gireesh Subramaniam Sankara Raman and Brayam D'leonid Valqui Ordoñez. Thanks for celebrating with me in good times and cheering me up in bad times. I truly appreciate your company and support during this challenging and rewarding journey.

Last but not least, to my late father Senlin Guo and mother Lang Wang, I know deeply in my heart you are proud of me. Your son misses you very much.

Chapter 1
Welfare Impacts of Natural Gas Pipeline Expansion in the Northeastern U.S.

1.1 Introduction

The emergence of unconventional natural gas plays in North America has dramatically changed commodity flow patterns. While nearly all of the natural gas consumed in the United States is produced on the North American continent,[1] historically the bulk of that production has occurred in the Gulf of Mexico region.[2] A gas transmission system was built to transport natural gas from the Gulf producing area to consumption areas in other parts of the U.S. For example, the Transcontinental Natural Gas Transmission System (Transco), owned and operated by Williams, moves gas from the Gulf producing region to consumption centers along the Atlantic seaboard.

Production from the Marcellus Shale and other unconventional gas plays now accounts for more than 40% of U.S. natural gas production [4], but the ability of the gas transmission system to connect these new supplies to demand centers on the east coast is limited. In Transco's case, as shown in Figure 1.1, bottlenecks have

[1] According to EIA, the total U.S. natural gas consumption in 2015 was 27,473,081 Million Cubit Feet [1], while the U.S. dry natural gas production was 27,095,010 Million Cubit Feet [2], which is 98.6% of the total consumption.

[2] The coastal states that have a shoreline on the Gulf of Mexico are Texas, Louisiana, Mississippi, Alabama, and Florida, and thus are known as the Gulf States. In 2001, the total dry natural gas production in the above five Gulf States and Federal Offshore Gulf of Mexico was 11,743,404 Million Cubit Feet, which is about 60% of the total U.S. dry natural gas production in that year. This percentage drops to 41% in the year of 2014 [3].

occurred in two areas: first, the Leidy Line from the Marcellus region eastward into New Jersey is typically constrained, limiting gas flows out of Pennsylvania;[3] secondly, Transco is currently not configured to allow southward flow south of Transco Station 195 (located near the borders of Pennsylvania, Maryland and Delaware).

Figure 1.1: Rate Zones on the Transco System

Source: Williams, http://www.1line.williams.com/

Insufficient pipeline infrastructure in the Marcellus region not only limited the economic gains from new unconventional resources, but also induced price separation between Pennsylvania and the surrounding states. The impacts of gas transmission constraints were felt particularly hard in the winter of 2014, when prices in surrounding states surpassed $100/MMBtu, while gas prices in Pennsylvania remained at less than one tenth these levels.[4] In turn, low prices in Pennsylvania have economically suppressed the completion of new Marcellus wells.[5]

To alleviate the constraints mentioned above, Williams has proposed a natural

[3] A comparison between daily operating capacity and available capacity at Station 515 on the Leidy line shows that Station 515 was constrained almost 90% of the time between the end of December 2012 and June 2014 [5].

[4] For example, on January 22, 2014, the natural gas price at the Dominion South hub in Pennsylvania was $5.03/MMBtu, while the price at the Transco-Z6 hub in New York was $120.70/MMBtu.

[5] There are 15,721 permitted horizontal wells in Pennsylvania, but only 9,789 are drilled or under development [6].

gas transmission pipeline expansion project called Atlantic Sunrise. This expansion would connect the Marcellus shale region to the Transco mainline near Station 195 in southeastern Pennsylvania. Two new pipelines would provide 1,700,000 MMBtu/day of additional gas transportation capacity from the Marcellus Region. The increased system capacity associated with this expansion has already been allocated to market participants via contracts that are typically 20 years in duration. In addition, the Atlantic Sunrise expansion would enable the reversal of flows along the Transco system in the Mid-Atlantic Region. While gas has historically flowed from south to north, modifications at existing compressor stations in Maryland, Virginia, and North Carolina would enable north-to-south flows when economically advantageous.

In this chapter, we evaluate the welfare impacts of the Atlantic Sunrise expansion. More specifically, we are interested in quantifying changes in gas prices, flows, and consumer and producer surplus in the Transco regions, assuming the Atlantic Sunrise expansion were in operation and the local gas market at any point along the Transco system is in equilibrium.[6]

A number of models have been developed for the analysis of natural gas market on a continental scale, with most applications covering the North American and European continents, or the global gas trade system as a whole. We identify two types of approaches to gas transmission economics in the existing literature.

A first type of approach has been the construction of large-scale optimization models of trade on natural gas transmission systems. These models are often formulated as mixed complementarity problems (MCPs).[7] For example, [7–10] compute market equilibria by maximizing social welfare (sum of producer and consumer surplus) subject to network constraints, assuming perfect competition or Nash-Cournot behavior of market agents. Mixed complementarity models have also been used for the analysis of European natural gas markets [11–13].

A second approach has been to develop dynamic general or partial equilibrium trade models of natural gas markets. For example, the Rice World Gas Trade Model (RWGTM) [14] is a general equilibrium model that combines regional resource

[6]Consumer surplus is an economic measure of consumer satisfaction, which is calculated by analyzing the difference between what consumers are willing to pay for a good or service relative to its market price. Producer surplus is an economic measure of the difference between the amount that a producer of a good receives and the minimum amount that he or she would be willing to accept for the good.

[7]Mixed complementarity problems present the optimization problems of each market participant. The combination of the KKT conditions associated with all decision variables and market-clearing conditions defines the equilibrium solution.

estimates at the country and sub-country level with econometric forecasts of natural gas demand. On the other hand, the FRISBEE model [15,16] is a partial equilibrium model of the international energy markets that divides the world in thirteen regions. Similarly to the Rice Gas Model, market power is not considered in FRISBEE, and bilateral trade takes place until all arbitrage opportunities are fully exploited.

Our approach relies on the concept of cost arbitrage[8] and takes an equilibrium approach in a competitive environment, as in the RWGTM. However, unlike the literature above, our study focuses on calculating daily equilibrium gas flows along a specific pipeline, the Transco. Since we only focus on the transportation sector rather than the entire gas supply chain, our problem is not a multi-agent problem; we also do not consider the possibility of strategic behaviour. For these two reasons, formulating MCP is not necessary for our modeling purposes. Our approach solves for location-specific equilibria on a constrained pipeline system, and can be used to estimate how these equilibria are affected by changes in pipeline capacity availability. Furthermore, it allows us to identify solutions in which no trade between regions occurs, because the price difference between regions is lower than the cost of trade, making arbitrage not profitable.[9] Although we focus our attention on the Atlantic Sunrise expansion of Transco, the model proposed in this chapter can be applied to the evaluation of welfare impacts for other natural gas pipeline expansions.

The rest of the chapter is organized as follows. Section 2 presents the modeling approach, Section 3 explains the data used in the model, Section 4 describes the results, and Section 5 concludes.

[8]The theory of arbitrage states that if a product moves from Market A to Market B, and there is no shortage of transportation capacity between the two markets, the price in Market A plus the costs of transportation from Market A to Market B will equal the price in Market B. Thus, for example, assume that the price of natural gas in Market A is $5.00 per unit (MMBtu), we observe that gas is shipped from A to B, and that the transportation cost from A to B is $0.30/MMBtu. This implies that the price of gas in Market B will be $5.30/MMBtu. The intuition behind the theory of arbitrage is that if the price of gas in Market B rose above $5.30/MMBtu, there would be profit opportunities in increasing shipments of gas from Market A to Market B.

[9]A state of no trade between regions is known as autarky.

1.2 Model

1.2.1 An Arbitrage Cost Model to Examine Natural Gas Pipeline Expansions

Our approach is to develop a spatial equilibrium model of natural gas flows in the northeastern U.S. that utilizes the principle of arbitrage [17–19], under which frictionless trade between geographically separate markets will cause price differences between markets to converge to transportation costs.

Our model considers a single natural gas pipeline, Transco, with several locational points. Denote P_n as the price of natural gas at point n, and T_{mn} as the cost of transportation from point m to point n (with T_{mn} not necessarily equal to T_{nm} for any points).

Demand for natural gas at any point k along the pipeline, if different from zero, is assumed to take on the constant elasticity form $Q_k^D = A_k(P_k^D)^{\varepsilon_k}$, where Q_k^D represents quantity demanded at point k, ε_k is the price elasticity of demand at point k and A_k is a point specific parameter. Supply of natural gas at any point h along the pipeline, if different from zero, is assumed to come from three alternate sources. The first is an infinitely elastic supply from markets located east of Station 90 in Alabama.[10] The second is a fixed supply from the Transco pipeline expansion. The third is supply from other pipelines connected to Transco. Supply of natural gas from these other pipelines at each point h is assumed to take on the constant elasticity form $Q_h^S = B_h(P_h^S)^{\gamma_h}$, where Q_h^S represents quantity supplied at point h, γ_h is the price elasticity of supply at point h and B_h is a point specific parameter.

While injections and withdrawals occur at locational points along a pipeline, the Federal Energy Regulatory Commission (FERC) has approved dividing natural gas markets into zones for rate purposes, as shown in Figure 1.1. Station 195, where Atlantic Sunrise would connect with the main Transco line, is on the western side of Zone 6. For modeling purposes, we assume Station 195 is on the border between Zone 5 and Zone 6. Bottlenecks on the Transco system can occur east of Station 90, precluding more gas from flowing northeastward. For this reason, the scope of

[10] This assumption is reasonable since gas sent through Transco at Station 90 represents a relatively small amount of production in the states on Transco system that are to the southwest of Station 90. According to EIA, gas flows through Station 90 represented about 10% of natural gas marketed production in Texas and Louisiana in 2012-2014 [3].

this study will be on the market impacts of the Atlantic Sunrise expansion in Zone 4 (east of Station 90), Zone 5 and Zone 6 along Transco.

Prices of demand points k and supply points h in a Zone X are set equal by regulation. Further, transportation costs are generally set by regulation. Therefore, equilibrium is not defined at the point level. Rather, due to regulations, the price is equal across all demand and supply points in a defined zone. Let P_X be the price in relevant Zone X, with P_X^D equaling the demand price in Zone X, and P_X^S equaling the supply price in X. Equilibrium occurs in each zone when $P_X^D = P_X^S$ and demand at that price equals supply, or $\sum_{k \in X} Q_k^D(P_X^D) = \sum_{h \in X} Q_h^S(P_X^S)$.

Under the arbitrage conditions and assuming away the existence of uneconomic gas flows (i.e., flows from a high-priced location to a low-priced location), in the absence of any flow constraints on the pipeline system, we expect one of the following conditions to hold for gas flows between Zones X, Y:

- $P_X = P_Y + T_{YX}$ would prevail if gas was flowing from Zone Y to Zone X.
- $P_Y = P_X + T_{XY}$ would prevail if gas was flowing from Zone X to Zone Y.
- Both $P_Y - P_X < T_{XY}$ and $P_X - P_Y < T_{YX}$ would prevail if no gas flowed between Zone X to Zone Y in either direction.

The first two conditions are arbitrage conditions, and would hold if gas was flowing in any direction between Zone X and Y. The third condition defines an autarky scenario, where there is no gas flowing between Zone X and Y in either direction because it is not profitable to trade.

With constraints on the pipeline system, however, we may observe deviations from the three conditions above. Suppose that there is a constraint along the pipeline at point j in Zone X, which limits the amount of flow that could move to neighboring point $j + 1$ in Zone Y. In this case, $P_X + T_{YX} < P_Y$. The price difference between X and Y does not decline to the cost of transportation because it is not physically possible to move additional gas from Zone X to Zone Y. In this case, trade between regions is constrained by capacity.

If gas flows from an injection point z to its adjacent Zones X, Y, one of the following conditions should hold:

- $P_X - T_{zX} > P_Y - T_{zY}$ would prevail if gas flows from point z to Zone X.

- $P_Y - T_{zY} > P_X - T_{zX}$ would prevail if gas flows from point z to Zone Y.
- $P_Y - T_{zY} = P_X - T_{zX}$ would prevail if gas flows from point z to both Zone X and Zone Y.

1.2.2 Algorithm

In this section, we describe the algorithm used to obtain the daily natural gas flows and zonal prices at equilibrium, assuming the completion of Atlantic Sunrise Expansion project. The algorithm consists of three steps:

- Choose a scenario that identifies a unique equilibrium pattern of natural gas flows;
- Apply scenario-specific arbitrage, autarky and capacity-constrained conditions, as well as supply demand balance conditions to define a system of equations. This system is solved for the natural gas prices in Zone 4, 5 and 6;
- Verify if the prices from the second step can yield withdrawals and injections in each zone that satisfy the scenario we designated. Note that the prices obtained from the scenario-specific conditions and supply demand balance conditions do not necessarily satisfy that scenario. This is because these conditions and supply demand balance conditions are only a subset of all the conditions that a specific pattern should meet. If the solved prices do satisfy all the conditions of the scenario specified in the first step, we claim that this is the new equilibrium after Atlantic Sunrise.

We notice that it is theoretically possible to have more than one equilibrium on a particular day after Atlantic Sunrise. For this reason, we repeat the three steps described above for all the potential scenarios we identified. In practice, however, we find only one equilibrium for each day after Atlantic Sunrise in our sample of data. Below is a detailed description of each step.

1.2.2.1 Scenarios

Figures 1.2 to 1.4 below present the 55 potential scenarios we identified. Each scenario identifies a unique equilibrium pattern of gas flows at the following key points along the Transco:

- **East of Station 90**: capacity along the Transco east of Station 90 could be unconstrained or constrained before the Atlantic Sunrise expansion. After Atlantic Sunrise, the constraint could remain or be eliminated;

- **Zone 4 and Zone 5**: gas could flow from Zone 4 to Zone 5, from Zone 5 to Zone 4 or there could be no gas flowing between Zone 4 and Zone 5 (autarky). When gas flows from Zone 5 to Zone 4, the null point[11] may be either in Zone 4 or to the west of Station 90. However, if Station 90 is constrained after Atlantic Sunrise, the null point can not be west of Station 90. This is because a null point west of Station 90 would imply that gas flows from east to west across that station, but that can't be possible if the station remains constrained after the expansion;

- **Station 195 between Zone 5 and Zone 6**: new supply from the Marcellus play injected at Station 195 can flow only north to Zone 6, both south and north, or only south to Zone 5. When Station 195 gas only flows north, there could be additional gas flowing from Zone 5 to Zone 6, or no gas flowing from Zone 5 to Zone 6. Similarly, when Station 195 gas only flows south, there could be additional gas flowing from Zone 6 to Zone 5, or no gas flowing from Zone 6 to Zone 5.

1.2.2.2 Price Relations and Supply Demand Balance Conditions

Based on the flow pattern, we define price relations among the three Transco rate zones from arbitrage, autarky and capacity-constrained conditions, and supply demand balance conditions. These are discussed below. The system of equations we solve for each of the 55 scenarios are detailed in Table 2.4 to 2.6 part (a). Note that all natural gas zonal prices here refer to prices after beginning the operation of Atlantic Sunrise.

East of Station 90

- Station 90 is unconstrained before Atlantic Sunrise

[11] A null point is defined as a physical location where gas flowing one way and gas flowing the other way meet, and across which there is no net flow. The null point may occur at a regulatory zone boundary or, more commonly, within a zone. In our model, we are able to identify the exact point where inward and outward flows meet along the pipeline. On the other hand, if gas flow is unidirectional along the entire length of the pipeline, there would be no null point.

If pipeline capacity east of Station 90 is unconstrained before Atlantic Sunrise, as shown in Figure 1.2, the natural gas price in Zone 4 is assumed to be equal to that at Station 90, or:

$$P_4 = P_{90} \tag{1.1}$$

- Station 90 is constrained before Atlantic Sunrise, and the constraint is eliminated after the expansion

If Station 90 is constrained before the Atlantic Sunrise expansion, but that constraint is eliminated after the Atlantic Sunrise project, as shown in Figure 1.3, equation (1.1) still holds: that is, we assume prices across Zone 4 are equal to those at Station 90.

- Station 90 is constrained before and after Atlantic Sunrise

If the flow east of Station 90 is constrained after the Atlantic Sunrise project, as shown in Figure 1.4, we assume that the flow at Station 90 remains fixed:

$$I_{90,before} = I_{90,after} \tag{1.2}$$

where $I_{90,before}$ represents the flow at Station 90 before Atlantic Sunrise, and $I_{90,after}$ represents the flow at Station 90 after Atlantic Sunrise. In this chapter, we denote a northbound (i.e. west to east) flow with positive values and a southbound (i.e. east to west) flow with negative values.

A flow constraint at Station 90 after Atlantic Sunrise also imposes the supply-demand balance condition that the total net withdrawals in the three zones must be equal to the sum of injections at Station 90 and at Station 195:

$$\sum_{i \in 4,5,6} NW_i = I_{90} + I_{195} \tag{1.3}$$

where NW_i represents the net withdrawal in Zone i, I_{90} and I_{195} represent the injections at Station 90 and Station 195, respectively.

Zone 4 and Zone 5

- Gas flows from Zone 4 to Zone 5

As in scenario 1, where gas flows north and east from Zone 4 to Zone 5, so that owners of gas will be indifferent between selling their gas in Zone 4 and selling it in Zone 5. This implies:

$$P_4 + T_{45} = P_5 \tag{1.4}$$

Where T_{45} is the cost of gas transportation from Zone 4 to Zone 5. For example, assume that the price of gas in Zone 4 is \$5.70/MMBtu and the cost of transportation of gas from Zone 4 to Zone 5 is \$0.30/MMBtu, and that gas flows from Zone 4 to Zone 5. This implies that the price of gas in Zone 5 will be \$5.70+\$0.30 = \$6.00/MMBtu.

- Gas flows from Zone 5 to Zone 4

As in scenario 6 and 11, where gas flows south and west across the Zone 4-5 border. This implies gas owners in Zone 5 are indifferent between selling in Zone 5, or paying the transport cost and selling in Zone 4, or:

$$P_5 + T_{54} = P_4 \tag{1.5}$$

- No gas flows between Zone 4 and Zone 5

If there are gas flows between Zone 5 and Zone 6 (like scenario 16), or Station 195 flows both north and south (like scenario 18), no gas flows between Zone 4 and Zone 5 as in both scenario 16 and 18 indicate that the total net withdrawals in Zone 5 and Zone 6 must be equal to the injection at Station 195 from the Marcellus region, 1,700,000 MMBtu/day:

$$\sum_{i \in 5,6} NW_i = I_{195} \tag{1.6}$$

Station 195 between Zone 5 and Zone 6

- Gas injected at Station 195 flows north, and additional gas flows from Zone 5 to Zone 6

As in scenario 1, gas flowing north from Zone 5 to Zone 6 implies that owners of gas in Zone 5 are indifferent between selling in Zone 5, or paying the transport cost and selling in Zone 6, or:

$$P_5 + T_{56} = P_6 \tag{1.7}$$

- Gas injected at Station 195 flows north, but no additional gas flows from Zone 5 to Zone 6

As in scenario 2, this implies that the net withdrawal in Zone 6 must be equal to the injection at Station 195 from the Marcellus region:

$$NW_6 = I_{195} \tag{1.8}$$

- Gas injected at Station 195 flows both north and south

If gas injected at Station 195 flows both north and south as in scenario 3, under the theory of arbitrage, owners of natural gas injected at Station 195 should be indifferent between their gas going north or south. This implies that the net return from a northbound gas flow must be equal to the net return from a southbound flow.

$$P_6 - T_{195,6} = P_5 - T_{195,5} \tag{1.9}$$

where $T_{195,5}$ is the cost of gas transportation from Station 195 to Zone 5, and $T_{195,6}$ is the cost of gas transportation from Station 195 to Zone 6. For instance, assume the price in Zone 5 is \$6.00/MMBtu, the cost of transporting gas from Station 195 to Zone 5 is \$0.20/MMBtu, while the cost of transporting cost from Station 195 to Zone 6 is \$0.15/MMBtu. Further, assume that injected gas at Station 195 goes both north and south. Under the arbitrage assumption, gas owners at Station 195 are indifferent between sending their gas north to Zone 6, or south to Zone 5. Thus, the prevailing prices in Zones 5 and Zone 6 would need to satisfy (1.9) above, or $P_6 - \$0.15 = \$6.00 - \$0.20$, implying that the price of gas in Zone 6 was \$5.95/MMBtu.

- Gas injected at Station 195 flows south, and additional gas flows from Zone 6 to Zone 5

Given that all the injected gas flows south, it is also possible that Zone 6 gas would also flow south as in scenario 4. In this circumstance:

$$P_6 + T_{65} = P_5 \tag{1.10}$$

- Gas injected at Station 195 flows south, but no additional gas flows from Zone 6 to Zone 5

As in scenario 5, this implies that supply must equal demand in Zone 6, which is in autarky state:

$$NW_6 = 0 \tag{1.11}$$

1.2.2.3 Verification Conditions

After obtaining the natural gas prices in each of the three zones by solving the scenario-specific system of equations in Table 2.4 to 2.6 part (a), we have to verify if the calculated prices will yield injections and withdrawals in each zone that satisfy the same flow pattern specified at step 1. Below is a discussion of the conditions that need to be satisfied under each scenario. These conditions are listed for each of the 55 scenarios in Table 2.4 to 2.6 part (b).

East of Station 90

- Station 90 is unconstrained before Atlantic Sunrise

In this case, we have assigned the price in Zone 4 equal to that at Station 90. No additional verification conditions are needed.

- Station 90 is constrained before Atlantic Sunrise, and the constraint is eliminated after the expansion

As shown in Figure 1.3, if Station 90 is constrained before the Atlantic Sunrise expansion, but that constraint is eliminated after the Atlantic Sunrise project, the following condition has to be true:

$$I_{90,before} > I_{90,after} \tag{1.12}$$

- Station 90 is constrained before and after Atlantic Sunrise

In the case of constrained flow east of station 90 as shown in Figure 1.4, we must verify that the following relationship between prices at station 90 and in Zone 4 holds:

$$P_{90} < P_4 \tag{1.13}$$

Because of the constraint east of Station 90, arbitrage is not possible between Station 90 and the rest of Zone 4, and prices in the rest of Zone 4 must be higher than at Station 90.

Zone 4 and Zone 5

- Gas flows from Zone 4 to Zone 5

In this case, gas flows north and east from Zone 4 to Zone 5, implying that the sum of local supply in Zone 5 and Zone 6, and injections at Station 195 is not enough to meet the demand in Zone 5 and Zone 6. Therefore, the net withdrawal in Zone 5 and Zone 6 must be greater than the injection at Station 195:

$$\sum_{i \in 5,6} NW_i > I_{195} \tag{1.14}$$

- Gas flows from Zone 5 to Zone 4

In this case, the sum of supply in Zone 5 and Zone 6, and injections at Station 195 is more than enough to meet the demand in Zone 5 and Zone 6. Therefore, we should verify that the above condition is reversed:

$$\sum_{i \in 5,6} NW_i < I_{195} \tag{1.15}$$

Moreover, if the null point in this case is in Zone 4 as in scenario 6, the total net withdrawal in the three zones must be greater than the injection at Station 195, so that additional gas supply from east of Station 90 is needed. In this case:

$$\sum_{i \in 4,5,6} NW_i > I_{195} \tag{1.16}$$

Otherwise, if the null point is to the southwest of Station 90 as in scenario 11, we must verify that the above condition is reversed:

$$\sum_{i \in 4,5,6} NW_i < I_{195} \tag{1.17}$$

- No gas flows between Zone 4 and Zone 5

Owners of gas in Zone 4 would prefer to sell it in Zone 4, while owners of gas in Zone 5 would prefer to sell the gas in Zone 5. Here, the transportation costs between two zones are greater than their price difference, and arbitrage is not profitable. From Section 1.2.1 we have that $P_4 - P_5 < T_{54}$ and $P_5 - P_4 < T_{45}$ when we have

autarky. This can be combined as:

$$P_4 - T_{54} < P_5 < P_4 + T_{45} \tag{1.18}$$

For example, assume that the price in Zone 4 is \$4.00/MMBtu, the price in Zone 5 is \$4.10/MMBtu, and the transportation costs from Zone 4 to Zone 5 and Zone 5 to Zone 4 are both \$0.30/MMBtu. In this case, gas owners prefer not to ship gas between the two zones, and autarky exists between the zones.

Station 195 between Zone 5 and Zone 6

- Gas injected at Station 195 flows northbound, and additional gas flows from Zone 5 to Zone 6

Owners of gas at Station 195 prefer selling gas in Zone 6 more than in Zone 5. Thus the following must be true:

$$P_6 - T_{195,6} > P_5 - T_{195,5} \tag{1.19}$$

For example, if the price in Zone 6 is \$5/MMBtu, and the two transport costs both equal \$0.25/MMBtu, this implies that the price in Zone 5 is less than \$5/MMBtu.

Furthermore, gas flowing from Zone 5 to Zone 6 implies that the net withdrawal in Zone 6 is greater than the total injection at Station 195:

$$NW_6 > I_{195} \tag{1.20}$$

- Gas injected at Station 195 flows north, but no additional gas flows from Zone 5 to Zone 6

In this case, condition (1.19) still applies. In addition, Zone 5 gas owners prefer not to send their gas to Zone 6, or:

$$P_5 + T_{56} > P_6 \tag{1.21}$$

and Zone 6 gas owners prefer not to send their gas to Zone 5, or:

$$P_6 + T_{65} > P_5 \tag{1.22}$$

Combining the two, we have:

$$P_6 - T_{56} < P_5 < P_6 + T_{65} \tag{1.23}$$

In this case, we say that Zone 6 is in autarky with respect to Zone 5.

- Gas injected at Station 195 flows both north and south

If gas injected at Station 195 goes both north and south, this implies that the net withdrawal in Zone 6 should be greater than zero but less than the total injection at Station 195:

$$0 < NW_6 < I_{195} \tag{1.24}$$

- Gas injected at Station 195 flows south, and additional gas flows from Zone 6 to Zone 5

Assume that all of the gas injected at Station 195 goes south. This implies

$$P_6 - T_{195,6} < P_5 - T_{195,5} \tag{1.25}$$

and that the payoff to sending gas south is greater than the payoff to sending gas north.

Given that all the injected gas flows south, it is also possible that Zone 6 gas would also flow south. In this circumstance, Zone 6 must have a net injection so that additional gas can be used for export:

$$NW_6 < 0 \tag{1.26}$$

- Gas injected at Station 195 flows south, but no additional gas flows from Zone 6 to Zone 5

Condition (1.25) would still apply. In addition, autarky between Zone 5 and Zone 6 implies that condition (1.23) must hold as well.

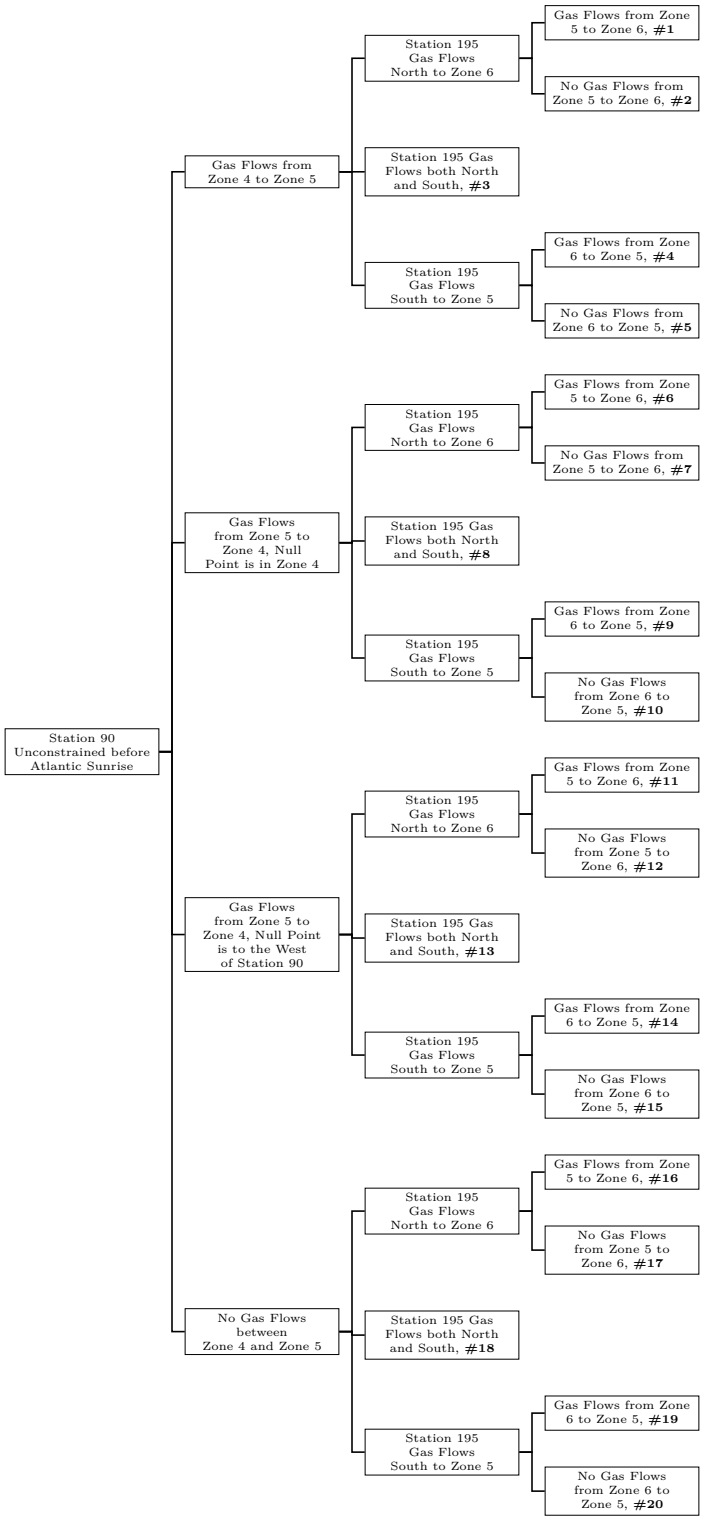

Figure 1.2: Possible equilibria after the Atlantic Sunrise expansion, when Station 90 is unconstrained before Atlantic Sunrise ("#" refers to the scenarios)

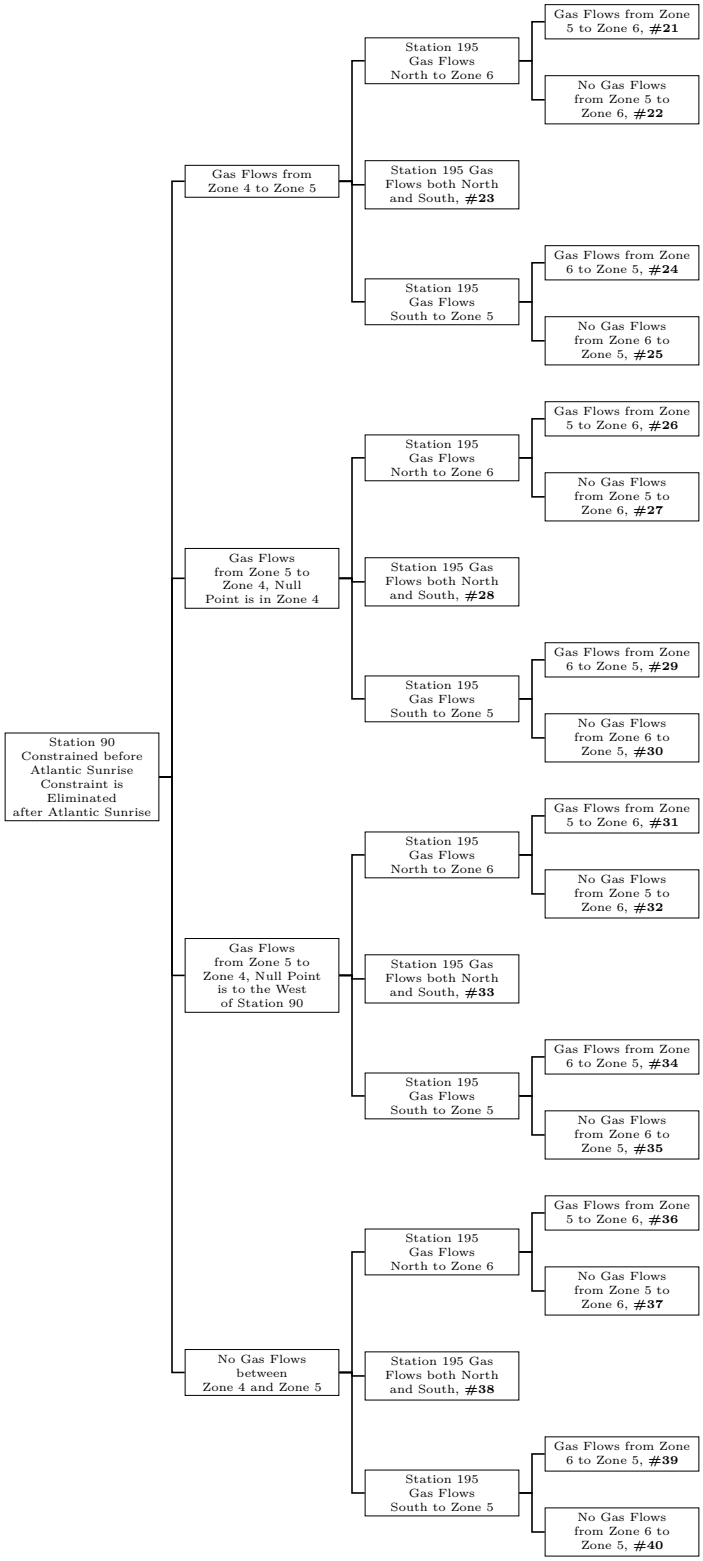

Figure 1.3: Possible equilibria after the Atlantic Sunrise expansion, when Station 90 is constrained before Atlantic Sunrise and the constraint is eliminated after the expansion ("#" refers to the scenarios)

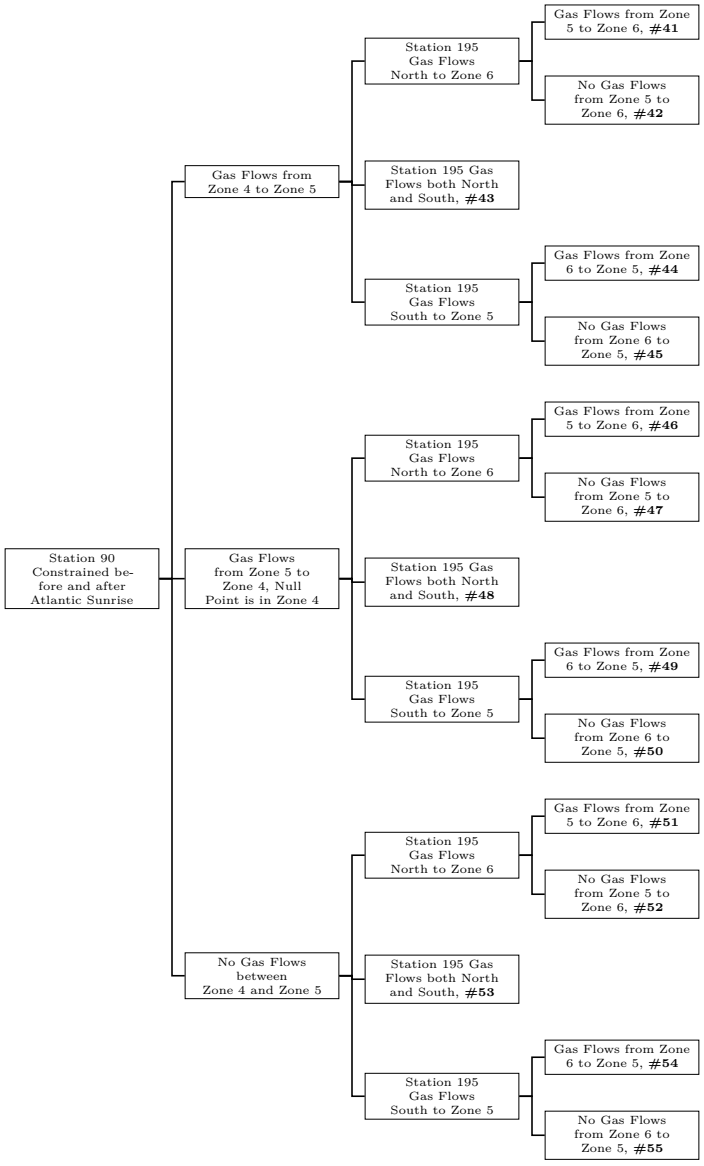

Figure 1.4: Possible equilibria after the Atlantic Sunrise expansion, when Station 90 is constrained before and after the Atlantic Sunrise expansion ("#" refers to the scenarios)

Table 1.1: Possible equilibria after the Atlantic Sunrise expansion, when Station 90 is unconstrained before Atlantic Sunrise

(a) Price Relations

Gas Flow between Zone 4 and Zone 5	Station 195 Gas Flows North, Gas Flows from Zone 5 to Zone 6	Station 195 Gas Flows North, No Gas Flows from Zone 5 to Zone 6	Station 195 Gas Flows Both South and North	Station 195 Gas Flows South, Gas Flows from Zone 6 to Zone 5	Station 195 Gas Flows South, No Gas Flows from Zone 6 to Zone 5
Gas Flows From Zone 4 to Zone 5	$P_{90} = P_4$ $P_4 + T_{45} = P_5$ $P_6 - P_5 = T_{56}$	$P_{90} = P_4$ $P_4 + T_{45} = P_5$ $NW_6 = I_{195}$	$P_{90} = P_4$ $P_4 + T_{45} = P_5$ $P_6 - T_{195,6} = P_5 - T_{195,5}$	$P_{90} = P_4$ $P_4 + T_{45} = P_5$ $P_5 - P_6 = T_{65}$	$P_{90} = P_4$ $P_4 + T_{45} = P_5$ $NW_6 = 0$
Gas Flows From Zone 5 to Zone 4 Null Point in Zone 4	$P_{90} = P_4$ $P_5 + T_{54} = P_4$ $P_6 - P_5 = T_{56}$	$P_{90} = P_4$ $P_5 + T_{54} = P_4$ $NW_6 = I_{195}$	$P_{90} = P_4$ $P_5 + T_{54} = P_4$ $P_6 - T_{195,6} = P_5 - T_{195,5}$	$P_{90} = P_4$ $P_5 + T_{54} = P_4$ $P_5 - P_6 = T_{65}$	$P_{90} = P_4$ $P_5 + T_{54} = P_4$ $NW_6 = 0$
Gas Flows From Zone 5 to Zone 4, Null Point to west of Station 90	$P_{90} = P_4$ $P_5 + T_{54} = P_4$ $P_6 - P_5 = T_{56}$	$P_{90} = P_4$ $P_5 + T_{54} = P_4$ $NW_6 = I_{195}$	$P_{90} = P_4$ $P_5 + T_{54} = P_4$ $P_6 - T_{195,6} = P_5 - T_{195,5}$	$P_{90} = P_4$ $P_5 + T_{54} = P_4$ $P_5 - P_6 = T_{65}$	$P_{90} = P_4$ $P_5 + T_{54} = P_4$ $NW_6 = 0$
No Gas Flows Between Zone 4 and Zone 5	$P_{90} = P_4$ $P_6 - P_5 = T_{56}$ $NW_5 + NW_6 = I_{195}$	$P_{90} = P_4$ $NW_5 = 0$ $NW_6 = I_{195}$	$P_{90} = P_4$ $P_6 - T_{195,6} = P_5 - T_{195,5}$ $NW_5 + NW_6 = I_{195}$	$P_{90} = P_4$ $P_5 - P_6 = T_{65}$ $NW_5 + NW_6 = I_{195}$	$P_{90} = P_4$ $NW_5 = I_{195}$ $NW_6 = 0$

Notation:

NW_i: net withdrawal in Zone i, a negative number indicates a net injection in that zone;

I_j: injection at Station j, a negative number indicates a withdrawal from that station;

P_i: price at Zone/Station i;

T_{mn}: transportation cost from Zone/Station m to Zone/Station n.

Table 1.1: Possible equilibria after the Atlantic Sunrise expansion, when Station 90 is unconstrained before Atlantic Sunrise

(b) Verification Conditions

Gas Flow between Zone 4 and Zone 5	Station 195 Gas Flows North, Gas Flows from Zone 5 to Zone 6	Station 195 Gas Flows North, No Gas Flows from Zone 5 to Zone 6	Station 195 Gas Flows Both South and North	Station 195 Gas Flows South, Gas Flows from Zone 6 to Zone 5	Station 195 Gas Flows South, No Gas Flows from Zone 6 to Zone 5
Gas Flows From Zone 4 to Zone 5	$NW_6 > I_{195}$ $\sum_{i\in 5,6} NW_i > I_{195}$ $P_6 - T_{195,6} > P_5 - T_{195,5}$	$\sum_{i\in 5,6} NW_i > I_{195}$ $P_6 - T_{56} < P_5 < P_6 + T_{65}$ $P_6 - T_{195,6} > P_5 - T_{195,5}$	$0 < NW_6 < I_{195}$ $\sum_{i\in 5,6} NW_i > I_{195}$	$NW_6 < 0$ $\sum_{i\in 5,6} NW_i > I_{195}$ $P_6 - T_{195,6} < P_5 - T_{195,5}$	$\sum_{i\in 5,6} NW_i > I_{195}$ $P_6 - T_{56} < P_5 < P_6 + T_{65}$ $P_6 - T_{195,6} < P_5 - T_{195,5}$
Gas Flows From Zone 5 to Zone 4 Null Point in Zone 4	$NW_6 > I_{195}$ $\sum_{i\in 5,6} NW_i < I_{195}$ $\sum_{i\in 4,5,6} NW_i > I_{195}$ $P_6 - T_{195,6} > P_5 - T_{195,5}$	$\sum_{i\in 5,6} NW_i < I_{195}$ $\sum_{i\in 4,5,6} NW_i > I_{195}$ $P_6 - T_{56} < P_5 < P_6 + T_{65}$ $P_6 - T_{195,6} > P_5 - T_{195,5}$	$0 < NW_6 < I_{195}$ $\sum_{i\in 5,6} NW_i < I_{195}$ $\sum_{i\in 4,5,6} NW_i > I_{195}$	$NW_6 < 0$ $\sum_{i\in 5,6} NW_i < I_{195}$ $\sum_{i\in 4,5,6} NW_i > I_{195}$ $P_6 - T_{195,6} < P_5 - T_{195,5}$	$\sum_{i\in 5,6} NW_i < I_{195}$ $\sum_{i\in 4,5,6} NW_i > I_{195}$ $P_6 - T_{56} < P_5 < P_6 + T_{65}$ $P_6 - T_{195,6} < P_5 - T_{195,5}$
Gas Flows From Zone 5 to Zone 4, Null Point to west of Station 90	$NW_6 > I_{195}$ $\sum_{i\in 5,6} NW_i < I_{195}$ $\sum_{i\in 4,5,6} NW_i < I_{195}$ $P_6 - T_{195,6} > P_5 - T_{195,5}$	$\sum_{i\in 5,6} NW_i < I_{195}$ $\sum_{i\in 4,5,6} NW_i < I_{195}$ $P_6 - T_{56} < P_5 < P_6 + T_{65}$ $P_6 - T_{195,6} > P_5 - T_{195,5}$	$0 < NW_6 < I_{195}$ $\sum_{i\in 5,6} NW_i < I_{195}$ $\sum_{i\in 4,5,6} NW_i < I_{195}$	$NW_6 < 0$ $\sum_{i\in 5,6} NW_i < I_{195}$ $\sum_{i\in 4,5,6} NW_i < I_{195}$ $P_6 - T_{195,6} < P_5 - T_{195,5}$	$\sum_{i\in 5,6} NW_i < I_{195}$ $\sum_{i\in 4,5,6} NW_i < I_{195}$ $P_6 - T_{56} < P_5 < P_6 + T_{65}$ $P_6 - T_{195,6} < P_5 - T_{195,5}$
No Gas Flows Between Zone 4 and Zone 5	$NW_6 > I_{195}$ $P_4 - T_{54} < P_5 < P_4 + T_{45}$ $P_6 - T_{195,6} > P_5 - T_{195,5}$	$P_4 - T_{54} < P_5 < P_4 + T_{45}$ $P_6 - T_{56} < P_5 < P_6 + T_{65}$ $P_6 - T_{195,6} > P_5 - T_{195,5}$	$0 < NW_6 < I_{195}$ $P_4 - T_{54} < P_5 < P_4 + T_{45}$	$NW_6 < 0$ $P_4 - T_{54} < P_5 < P_4 + T_{45}$ $P_6 - T_{195,6} < P_5 - T_{195,5}$	$P_4 - T_{54} < P_5 < P_4 + T_{45}$ $P_6 - T_{56} < P_5 < P_6 + T_{65}$ $P_6 - T_{195,6} < P_5 - T_{195,5}$

Notation:

NW_i: net withdrawal in Zone i, a negative number indicates a net injection in that zone;

I_j: injection at Station j, a negative number indicates a withdrawal from that station;

P_i: price at Zone/Station i;

T_{mn}: transportation cost from Zone/Station m to Zone/Station n.

Table 1.2: Possible equilibria after the Atlantic Sunrise expansion, when Station 90 is constrained before Atlantic Sunrise and the constraint is eliminated after the expansion

(a) Price Relations

Gas Flow between Zone 4 and Zone 5	Station 195 Gas Flows North, Gas Flows from Zone 5 to Zone 6	Station 195 Gas Flows North, No Gas Flows from Zone 5 to Zone 6	Station 195 Gas Flows Both South and North	Station 195 Gas Flows South, Gas Flows from Zone 6 to Zone 5	Station 195 Gas Flows South, No Gas Flows from Zone 6 to Zone 5
Gas Flows From Zone 4 to Zone 5	$P_{90} = P_4$ $P_4 + T_{45} = P_5$ $P_6 - P_5 = T_{56}$	$P_{90} = P_4$ $P_4 + T_{45} = P_5$ $NW_6 = I_{195}$	$P_{90} = P_4$ $P_4 + T_{45} = P_5$ $P_6 - T_{195,6} = P_5 - T_{195,5}$	$P_{90} = P_4$ $P_4 + T_{45} = P_5$ $P_5 - P_6 = T_{65}$	$P_{90} = P_4$ $P_4 + T_{45} = P_5$ $NW_6 = 0$
Gas Flows From Zone 5 to Zone 4 Null Point in Zone 4	$P_{90} = P_4$ $P_5 + T_{54} = P_4$ $P_6 - P_5 = T_{56}$	$P_{90} = P_4$ $P_5 + T_{54} = P_4$ $NW_6 = I_{195}$	$P_{90} = P_4$ $P_5 + T_{54} = P_4$ $P_6 - T_{195,6} = P_5 - T_{195,5}$	$P_{90} = P_4$ $P_5 + T_{54} = P_4$ $P_5 - P_6 = T_{65}$	$P_{90} = P_4$ $P_5 + T_{54} = P_4$ $NW_6 = 0$
Gas Flows From Zone 5 to Zone 4, Null Point to west of Station 90	$P_{90} = P_4$ $P_5 + T_{54} = P_4$ $P_6 - P_5 = T_{56}$	$P_{90} = P_4$ $P_5 + T_{54} = P_4$ $NW_6 = I_{195}$	$P_{90} = P_4$ $P_5 + T_{54} = P_4$ $P_6 - T_{195,6} = P_5 - T_{195,5}$	$P_{90} = P_4$ $P_5 + T_{54} = P_4$ $P_5 - P_6 = T_{65}$	$P_{90} = P_4$ $P_5 + T_{54} = P_4$ $NW_6 = 0$
No Gas Flows Between Zone 4 and Zone 5	$P_{90} = P_4$ $P_6 - P_5 = T_{56}$ $NW_5 + NW_6 = I_{195}$	$P_{90} = P_4$ $NW_5 = 0$ $NW_6 = I_{195}$	$P_{90} = P_4$ $P_6 - T_{195,6} = P_5 - T_{195,5}$ $NW_5 + NW_6 = I_{195}$	$P_{90} = P_4$ $P_5 - P_6 = T_{65}$ $NW_5 + NW_6 = I_{195}$	$P_{90} = P_4$ $NW_5 = I_{195}$ $NW_6 = 0$

Notation:

NW_i: net withdrawal in Zone i, a negative number indicates a net injection in that zone;

I_j: injection at Station j, a negative number indicates a withdrawal from that station;

P_i: price at Zone/Station i;

T_{mn}: transportation cost from Zone/Station m to Zone/Station n.

Table 1.2: Possible equilibria after the Atlantic Sunrise expansion, when Station 90 is constrained before Atlantic Sunrise and the constraint is eliminated after the expansion

(b) Verification Conditions

Gas Flow between Zone 4 and Zone 5	Station 195 Gas Flows North, Gas Flows from Zone 5 to Zone 6	Station 195 Gas Flows North, No Gas Flows from Zone 5 to Zone 6	Station 195 Gas Flows Both South and North	Station 195 Gas Flows South, Gas Flows from Zone 6 to Zone 5	Station 195 Gas Flows South, No Gas Flows from Zone 6 to Zone 5
Gas Flows From Zone 4 to Zone 5	$NW_6 > I_{195}$ $\sum_{i\in5,6} NW_i > I_{195}$ $P_6 - T_{195,6} > P_5 - T_{195,5}$ $I_{90,after} < I_{90,before}$	$\sum_{i\in5,6} NW_i > I_{195}$ $P_6 - T_{56} < P_5 < P_6 + T_{65}$ $P_6 - T_{195,6} > P_5 - T_{195,5}$ $I_{90,after} < I_{90,before}$	$0 < NW_6 < I_{195}$ $\sum_{i\in5,6} NW_i > I_{195}$ $I_{90,after} < I_{90,before}$	$NW_6 < 0$ $\sum_{i\in5,6} NW_i > I_{195}$ $P_6 - T_{195,6} < P_5 - T_{195,5}$ $I_{90,after} < I_{90,before}$	$\sum_{i\in5,6} NW_i > I_{195}$ $P_6 - T_{56} < P_5 < P_6 + T_{65}$ $P_6 - T_{195,6} < P_5 - T_{195,5}$ $I_{90,after} < I_{90,before}$
Gas Flows From Zone 5 to Zone 4 Null Point in Zone 4	$NW_6 > I_{195}$ $\sum_{i\in5,6} NW_i < I_{195}$ $\sum_{i\in4,5,6} NW_i > I_{195}$ $P_6 - T_{195,6} > P_5 - T_{195,5}$ $I_{90,after} < I_{90,before}$	$\sum_{i\in5,6} NW_i < I_{195}$ $\sum_{i\in4,5,6} NW_i > I_{195}$ $P_6 - T_{56} < P_5 < P_6 + T_{65}$ $P_6 - T_{195,6} > P_5 - T_{195,5}$ $I_{90,after} < I_{90,before}$	$0 < NW_6 < I_{195}$ $\sum_{i\in5,6} NW_i < I_{195}$ $\sum_{i\in4,5,6} NW_i > I_{195}$ $I_{90,after} < I_{90,before}$	$NW_6 < 0$ $\sum_{i\in5,6} NW_i < I_{195}$ $\sum_{i\in4,5,6} NW_i > I_{195}$ $P_6 - T_{195,6} < P_5 - T_{195,5}$ $I_{90,after} < I_{90,before}$	$\sum_{i\in5,6} NW_i < I_{195}$ $\sum_{i\in4,5,6} NW_i > I_{195}$ $P_6 - T_{56} < P_5 < P_6 + T_{65}$ $P_6 - T_{195,6} < P_5 - T_{195,5}$ $I_{90,after} < I_{90,before}$
Gas Flows From Zone 5 to Zone 4, Null Point to west of Station 90	$NW_6 > I_{195}$ $\sum_{i\in5,6} NW_i < I_{195}$ $\sum_{i\in4,5,6} NW_i < I_{195}$ $P_6 - T_{195,6} > P_5 - T_{195,5}$ $I_{90,after} < I_{90,before}$	$\sum_{i\in5,6} NW_i < I_{195}$ $\sum_{i\in4,5,6} NW_i < I_{195}$ $P_6 - T_{56} < P_5 < P_6 + T_{65}$ $P_6 - T_{195,6} > P_5 - T_{195,5}$ $I_{90,after} < I_{90,before}$	$0 < NW_6 < I_{195}$ $\sum_{i\in5,6} NW_i < I_{195}$ $\sum_{i\in4,5,6} NW_i < I_{195}$ $I_{90,after} < I_{90,before}$	$NW_6 < 0$ $\sum_{i\in5,6} NW_i < I_{195}$ $\sum_{i\in4,5,6} NW_i < I_{195}$ $P_6 - T_{195,6} < P_5 - T_{195,5}$ $I_{90,after} < I_{90,before}$	$\sum_{i\in5,6} NW_i < I_{195}$ $\sum_{i\in4,5,6} NW_i < I_{195}$ $P_6 - T_{56} < P_5 < P_6 + T_{65}$ $P_6 - T_{195,6} < P_5 - T_{195,5}$ $I_{90,after} < I_{90,before}$
No Gas Flows Between Zone 4 and Zone 5	$NW_6 > I_{195}$ $P_4 - T_{54} < P_5 < P_4 + T_{45}$ $P_6 - T_{195,6} > P_5 - T_{195,5}$ $I_{90,after} < I_{90,before}$	$P_4 - T_{54} < P_5 < P_4 + T_{45}$ $P_6 - T_{56} < P_5 < P_6 + T_{65}$ $P_6 - T_{195,6} > P_5 - T_{195,5}$ $I_{90,after} < I_{90,before}$	$0 < NW_6 < I_{195}$ $P_4 - T_{54} < P_5 < P_4 + T_{45}$ $I_{90,after} < I_{90,before}$	$NW_6 < 0$ $P_4 - T_{54} < P_5 < P_4 + T_{45}$ $P_6 - T_{195,6} < P_5 - T_{195,5}$ $I_{90,after} < I_{90,before}$	$P_4 - T_{54} < P_5 < P_4 + T_{45}$ $P_6 - T_{56} < P_5 < P_6 + T_{65}$ $P_6 - T_{195,6} < P_5 - T_{195,5}$ $I_{90,after} < I_{90,before}$

Notation:

NW_i: net withdrawal in Zone i, a negative number means that there is net injection in that zone;

I_j: injection at Station j, a negative number means that there is withdrawal from that station;

P_i: price at Zone/Station i;

T_{mn}: transportation cost from Zone/Station m to Zone/Station n.

Table 1.3: Possible equilibria after the Atlantic Sunrise expansion, when Station 90 is constrained before and after the Atlantic Sunrise expansion

(a) Price Relations

Gas Flow between Zone 4 and Zone 5	Station 195 Gas Flows North, Gas Flows from Zone 5 to Zone 6	Station 195 Gas Flows North, No Gas Flows from Zone 5 to Zone 6	Station 195 Gas Flows Both South and North	Station 195 Gas Flows South, Gas Flows from Zone 6 to Zone 5	Station 195 Gas Flows South, No Gas Flows from Zone 6 to Zone 5
Gas Flows From Zone 4 to Zone 5	$P_4 + T_{45} = P_5$ $P_6 - P_5 = T_{56}$ $\sum_{i \in 4,5,6} NW_i = I_{90} + I_{195}$	$P_4 + T_{45} = P_5$ $NW_6 = I_{195}$ $\sum_{i \in 4,5} NW_i = I_{90}$	$P_4 + T_{45} = P_5$ $P_6 - T_{195,6} = P_5 - T_{195,5}$ $\sum_{i \in 4,5,6} NW_i = I_{90} + I_{195}$	$P_4 + T_{45} = P_5$ $P_5 - P_6 = T_{65}$ $\sum_{i \in 4,5,6} NW_i = I_{90} + I_{195}$	$P_4 + T_{45} = P_5$ $NW_6 = 0$ $\sum_{i \in 4,5} NW_i = I_{90} + I_{195}$
Gas Flows From Zone 5 to Zone 4 Null Point in Zone 4	$P_5 + T_{54} = P_4$ $P_6 - P_5 = T_{56}$ $\sum_{i \in 4,5,6} NW_i = I_{90} + I_{195}$	$P_5 + T_{54} = P_4$ $NW_6 = I_{195}$ $\sum_{i \in 4,5} NW_i = I_{90}$	$P_5 + T_{54} = P_4$ $P_6 - T_{195,6} = P_5 - T_{195,5}$ $\sum_{i \in 4,5,6} NW_i = I_{90} + I_{195}$	$P_5 + T_{54} = P_4$ $P_5 - P_6 = T_{65}$ $\sum_{i \in 4,5,6} NW_i = I_{90} + I_{195}$	$P_5 + T_{54} = P_4$ $NW_6 = 0$ $\sum_{i \in 4,5} NW_i = I_{90} + I_{195}$
No Gas Flows Between Zone 4 and Zone 5	$P_6 - P_5 = T_{56}$ $NW_4 = I_{90}$ $\sum_{i \in 5,6} NW_i = I_{195}$	$NW_5 = 0$ $NW_4 = I_{90}$ $NW_6 = I_{195}$	$P_6 - T_{195,6} = P_5 - T_{195,5}$ $NW_4 = I_{90}$ $\sum_{i \in 5,6} NW_i = I_{195}$	$P_5 - P_6 = T_{65}$ $NW_4 = I_{90}$ $\sum_{i \in 5,6} NW_i = I_{195}$	$NW_5 = I_{195}$ $NW_4 = I_{90}$ $NW_6 = 0$

Notation:

NW_i: net withdrawal in Zone i, a negative number means that there is net injection in that zone;

I_j: injection at Station j, a negative number means that there is withdrawal from that station;

P_i: price at Zone/Station i;

T_{mn}: transportation cost from Zone/Station m to Zone/Station n.

Table 1.3: Possible equilibria after the Atlantic Sunrise expansion, when Station 90 is constrained before and after the Atlantic Sunrise expansion

(b) Verification Conditions

Gas Flow between Zone 4 and Zone 5	Station 195 Gas Flows North, Gas Flows from Zone 5 to Zone 6	Station 195 Gas Flows North, No Gas Flows from Zone 5 to Zone 6	Station 195 Gas Flows Both South and North	Station 195 Gas Flows South, Gas Flows from Zone 6 to Zone 5	Station 195 Gas Flows South, No Gas Flows from Zone 6 to Zone 5
Gas Flows From Zone 4 to Zone 5	$NW_6 > I_{195}$ $\sum_{i\in 5,6} NW_i > I_{195}$ $P_6 - T_{195,6} > P_5 - T_{195,5}$ $P_{90} < P_4$	$\sum_{i\in 5,6} NW_i > I_{195}$ $P_6 - T_{56} < P_5 < P_6 + T_{65}$ $P_6 - T_{195,6} > P_5 - T_{195,5}$ $P_{90} < P_4$	$0 < NW_6 < I_{195}$ $\sum_{i\in 5,6} NW_i > I_{195}$ $P_{90} < P_4$	$NW_6 < 0$ $\sum_{i\in 5,6} NW_i > I_{195}$ $P_6 - T_{195,6} < P_5 - T_{195,5}$ $P_{90} < P_4$	$\sum_{i\in 5,6} NW_i > I_{195}$ $P_6 - T_{56} < P_5 < P_6 + T_{65}$ $P_6 - T_{195,6} < P_5 - T_{195,5}$ $P_{90} < P_4$
Gas Flows From Zone 5 to Zone 4 Null Point in Zone 4	$NW_6 > I_{195}$ $\sum_{i\in 5,6} NW_i < I_{195}$ $NW_4 > I_{90}$ $P_6 - T_{195,6} > P_5 - T_{195,5}$ $P_{90} < P_4$	$\sum_{i\in 5,6} NW_i < I_{195}$ $P_6 - T_{56} < P_5 < P_6 + T_{65}$ $P_6 - T_{195,6} > P_5 - T_{195,5}$ $P_{90} < P_4$	$0 < NW_6 < I_{195}$ $\sum_{i\in 5,6} NW_i < I_{195}$ $P_{90} < P_4$	$NW_6 < 0$ $\sum_{i\in 5,6} NW_i < I_{195}$ $P_6 - T_{195,6} < P_5 - T_{195,5}$ $P_{90} < P_4$	$\sum_{i\in 5,6} NW_i < I_{195}$ $P_6 - T_{56} < P_5 < P_6 + T_{65}$ $P_6 - T_{195,6} < P_5 - T_{195,5}$ $P_{90} < P_4$
No Gas Flows Between Zone 4 and Zone 5	$NW_6 > I_{195}$ $P_4 - T_{54} < P_5 < P_4 + T_{45}$ $P_6 - T_{195,6} > P_5 - T_{195,5}$ $P_{90} < P_4$	$P_4 - T_{54} < P_5 < P_4 + T_{45}$ $P_6 - T_{56} < P_5 < P_6 + T_{65}$ $P_6 - T_{195,6} > P_5 - T_{195,5}$ $P_{90} < P_4$	$0 < NW_6 < I_{195}$ $P_4 - T_{54} < P_5 < P_4 + T_{45}$ $P_{90} < P_4$	$NW_6 < 0$ $P_4 - T_{54} < P_5 < P_4 + T_{45}$ $P_6 - T_{195,6} < P_5 - T_{195,5}$ $P_{90} < P_4$	$P_4 - T_{54} < P_5 < P_4 + T_{45}$ $P_6 - T_{56} < P_5 < P_6 + T_{65}$ $P_6 - T_{195,6} < P_5 - T_{195,5}$ $P_{90} < P_4$

Notation:

NW_i: net withdrawal in Zone i, a negative number means that there is net injection in that zone;

I_j: injection at Station j, a negative number means that there is withdrawal from that station;

P_i: price at Zone/Station i;

T_{mn}: transportation cost from Zone/Station m to Zone/Station n.

1.3 Data

We utilize two data sets to perform our analysis. The first is composed of natural gas flows, injections and withdrawals along Transco from January 1, 2012 to June 27, 2014. The second includes daily natural gas prices at Station 90 ("Transco-85"), Zone 5 ("non-WGL Transco Z5" near the Virginia/North Carolina border) and Zone 6 ("TETCO-M3" near Philadelphia). All data were supplied by Williams. The gas transportation cost between Zone 4 and Zone 5 is \$0.36/MMBtu plus 1.28% of the natural gas price in the originating zone on that day. The transportation cost between Zone 5 and Zone 6 is \$0.26/MMBtu plus 0.77% of the natural gas price in the originating zone on that day.

To analyze the impact on different type of natural gas consumers, we divide the withdrawal points into three categories (Local Distribution Companies (LDCs) serving residential customers, Power Plants, and Other Industry[12]), and assign an elasticity of demand to each category. A review of the recent literature on natural gas demand elasticity estimates in the U.S. provided lower and upper thresholds for each group's elasticity. These values are presented in Table 2.7 below, along with the midpoint for each range.

Table 1.4: Elasticities of Demand

	High	Medium	Low
Residential	-0.680	-0.361	-0.042
Industrial	-0.269	-0.257	-0.244
Electric Power	-0.290	-0.214	-0.138

Upper and lower bound of demand elasticities for the residential sector are from [20] and [21], respectively; upper and lower bound of demand elasticities for the industrial sector are from [21] and [22], respectively; upper and lower bound of demand elasticities for the electric power sector are from [23] and [21], respectively.

A similar literature review on natural gas supply elasticity estimates in the U.S. provides lower and upper thresholds for elasticity of suppliers. These values are presented in Table 1.5 below, along with the midpoint.

[12]Other Industry includes the following consumer categories: Industrial, Liquids Plant, Municipality, Pipeline Interconnect, Processing Plant and Storage.

Table 1.5: Elasticities of Supply

	High	Medium	Low
Supply	0.81	0.45	0.09

Upper and lower bound of supply elasticities are from [24].

We use the withdrawals and injections at each point on the Transco system, and the prices before the Atlantic Sunrise project to calculate the constants A_k and B_h at each point.

We often observe uneconomic flows of gas between zones in our data. For example, on July 28, 2013, the price in Zone 4 was \$3.54/MMBtu, the Zone 5 price was \$3.61/MMBtu, the transportation cost from Zone 4 to Zone 5 was \$0.41/MMBtu, and yet there were substantial flows of gas from Zone 4 to Zone 5. We assume these uneconomic flows are the result of the difficulties of renegotiating long-term contracts between parties. Our model assumes such flows will not continue following the construction of Atlantic Sunrise.[13]

1.4 Results

We begin this section by illustrating how our model works for one particular day, January 28, 2014, and show the equilibrium results for that day. We then proceed by showing the breakdown of consumer and producer surplus change, assuming the completion of Atlantic Sunrise for the entire data period (from January 1, 2012 to June 27, 2014) and medium supply and demand elasticities from Table 2.7 and 1.5. Finally, a sensitivity analysis is performed using combinations of supply and demand elasticities from Table 2.7 and 1.5.

[13]We take three modeling steps to address the issue of uneconomic flows, which are consistent with our other modeling assumptions. First, in circumstances where the resulting change in Zone 4 and Zone 5 consumer surplus is negative, we set the change in consumer surplus to zero. There is no economic reason to believe that the Atlantic Sunrise project would cause either Zone 4 or Zone 5 prices to rise (since Atlantic Sunrise would increase supply deliverability into Zone 4 and Zone 5). Second, on days where there are no shipments from Zones 6 to 5, and the estimated consumer surplus change in Zone 6 is negative, we set the change in Zone 6 consumer surplus to zero. Finally, on days where we estimate that Atlantic Sunrise would induce shipments of gas from Zone 6 to Zone 5, we allow estimated consumer surplus in Zone 6 to decline.

1.4.1 Impacts of Atlantic Sunrise on January 28, 2014

We provide detailed results of how the Atlantic Sunrise expansion would have impacted flows and prices along the Transco on one particular day, January 28, 2014. On this high demand winter day, the Transco pipeline was constrained at Station 90 prior to Atlantic Sunrise, as the prices in Zones 5 and 6 were significantly higher than the Transco-85 price. Prices in Zones 5 and 6 were \$93.56/MMBtu and \$79.85/MMBtu, respectively, prior to the construction of Atlantic Sunrise. The price at Station 90, was \$5.71/MMBtu. Transportation costs from Zone 4 to Zone 5 equalled \$0.36/MMBtu plus 1.28% of the Station 90 gas price, yielding a daily rate of \$0.43/MMBtu. Thus, we obtain an equilibrium price in Zone 4 equal to \$93.13/MMBtu.

Here we present one of the 55 scenarios we tried, where Station 90 remains constrained after Atlantic Sunrise, and gas flows from Zone 4 to Zone 5. We also assume that the additional injection from the Marcellus region at Station 195 flows both north and south. This scenario is shown in Figure 1.5.

Figure 1.5: Equilibrium Flows on January 28, 2014

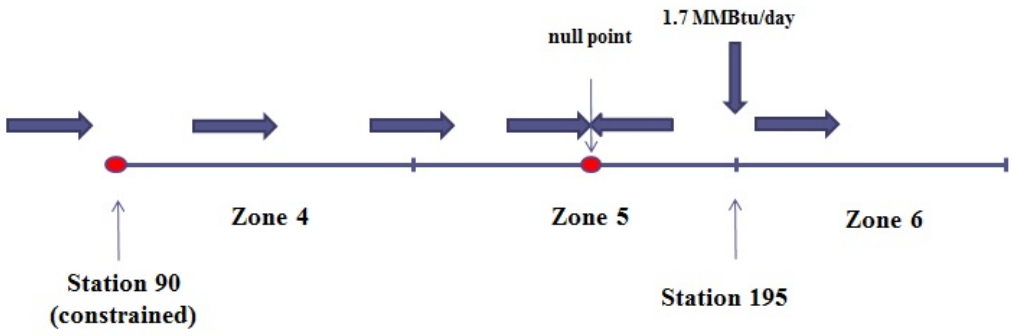

We have three equations to obtain the equilibrium prices in Zone 4, Zone 5 and Zone 6 after the construction of Atlantic Sunrise:

$$P_4 + T_{45} = P_5 \tag{1.27}$$

$$P_6 - T_{195,6} = P_5 - T_{195,5} \tag{1.28}$$

$$\sum_{i \in 4,5,6} NW_i = I_{90} + I_{195} \tag{1.29}$$

The first two equations come from our arbitrage assumption: prices in zones that are connected by uncongested pipelines should differ by the cost of transportation. The last equation follows from setting total withdrawals equal to total injections in the three zones, given that flows downstream of Station 90 remain constant.

Solving for the three equations yields the new zonal prices of $P_4 = \$64.01$/MMBtu, $P_5 = \$64.44$/MMBtu, $P_6 = \$63.71$/MMBtu.

Lastly, we verify if the solved prices can yield the withdrawal and injection amounts that satisfy the specified scenario. The three conditions that need to be verified in this case are:

$$P_{90} = 5.71 < P_4 = 64.01 \tag{1.30}$$

$$\sum_{i \in 5,6} NW_i = 4,413,447 > I_{195} = 1,700,000 \tag{1.31}$$

$$0 < NW_6 = 966,914 < I_{195} = 1,700,000 \tag{1.32}$$

All three conditions are satisfied, so that this is a valid scenario after Atlantic Sunrise for that particular day. In this scenario, gas from Station 90 flows north, while part of gas from station 195 flows south. The null point occurs at EMPORIA in Zone 5.

The zonal consumer surplus changes (ΔCS) for January 28, 2014 are $\Delta CS_4 = \$42.7$million, $\Delta CS_5 = \$113.4$million, $\Delta CS_6 = \$86.9$million, implying the total welfare gain to consumers on this day after the pipeline expansion is \$243 million. Meanwhile, the producer surplus changes (ΔPS) for that day are $\Delta PS_4 = -\$0.7$million, $\Delta PS_5 = -\$28.3$million, $\Delta PS_6 = -\$79.0$million, implying a total welfare loss of \$108 million to producers on this day after the pipeline expansion.

Table 1.6 summarizes the flows at four stations, where Table 1.7 compares prices, withdrawals and injections before and after Atlantic Sunrise on January 28, 2014. As Station 90 remains constrained, flows at that point are fixed and equal to 4,250,000 MMBtu. Nearly one 1,000,000 MMBtu of the Station 195 injection flows north, while the remainder of the 1,700,000 MMBtu injection flows south. Prices fall by \$25.57/MMBtu in Zone 5, and by \$12.60/MMBtu in Zone 6.

1.4.2 Consumer and Producer Surplus Analysis

Using the medium supply and demand elasticities in Table 2.7 and 2.7, we calculate the impact of Atlantic Sunrise on consumer surplus across Zones 4, 5 and 6 for

Table 1.6: Comparison of Flows Before and After Atlantic Sunrise, January 28, 2014 (thousand MMBtu)

Area	Flow Before	Flow After	Flow Change
Station 90	4,250	4,250	0
Station 135	2,885	2,713	-172
Station 195 North Flow	48	967	919
Station 195 South Flow	0	-733	-733

Table 1.7: Comparison of Withdrawals, Injections and Prices Before and After Atlantic Sunrise on January 28, 2014

Area		Withdrawals (000 MMBtu)	Injections (000 MMBtu)	Prices ($/MMBtu)
Zone 4	Before	1,391	26	93.13
	After	1,558	22	64.01
	Change	167	-4	-29.12
Zone 5	Before	3,886	1,049	93.56
	After	4,334	887	64.44
	Change	488	-162	-29.12
Zone 6	Before	5,183	5,134	79.85
	After	5,605	4,638	63.71
	Change	422	-496	-16.14

the period January 1, 2012 to June 27, 2014. Table 1.8 summarizes our results by season across the three zones.

We estimate $64 million in gains for consumers between January and March 2012. For most of the remainder of 2012, however, we estimate very limited consumer gains in Zones 4, 5 and 6. The reason is that the new injection of gas would largely displace gas flowing east of Station 90. In theory, that should have resulted in relatively small consumer gains in Zone 6. Those gains in our model, however, were offset by the assumed cessation of uneconomic gas flows to Zone 6.

From January to March 2013, we estimated consumer gains of about $207

Table 1.8: Change of Consumer Surplus Under Medium Elasticities (thousand dollars)

Months	ΔCS_4	ΔCS_5	ΔCS_6	Total
January - March 2012	7,268	15,803	40,651	63,722
April - June 2012	0	0	253	253
July - September 2012	0	116	931	1,047
October - December 2012	3,053	6,413	14,549	24,015
January - March 2013	22,022	51,954	132,938	206,914
April - June 2013	0	14,839	41,414	56,253
July - September 2013	0	49,202	109,742	158,944
October - December 2013	16,157	61,086	88,395	165,638
January - March 2014	407,904	967,984	1,021,306	2,397,194
April - June 2014	0	62,123	-103,387	-41,264
Total	456,404	1,229,520	1,346,792	3,032,716

million, primarily in Zone 6, from eliminating the network constraint east of Station 90. For the rest of that year consumer gains were about $381 million, as the new injection of gas either results in exports from Zone 5 to 4, or in lower Zone 5 price such that imports from Zone 4 were eliminated.

The largest gains arise from extreme periods such as the polar vortex of the winter of 2014. Consumer gains from January to March 2014 were estimated to be about $2.4 billion, with $1.9 billion occurring in January alone. January gains represent about 64% of the total gains across the period of our study.

From April to June of 2014 the price of gas in Zone 4 was extremely low (often below $5/MMBtu). In these circumstances, the Atlantic Sunrise project would have allowed additional flows from Zone 6 into Zone 5. Thus, prices rise and consumer surplus falls in Zone 6 on those days.

We also calculate the impact of Atlantic Sunrise on producer surplus across Zones 4, 5 and 6. Table 1.9 summarizes our results by season across the three zones.

Producers incur estimated losses of about $1.3 billion due to the Atlantic Sunrise expansion. This corresponds to a little more than 40% of the welfare gains enjoyed

Table 1.9: Change of Producer Surplus Under Medium Elasticities (thousand dollars)

Months	ΔPS_4	ΔPS_5	ΔPS_6	Total
January - March 2012	-290	-5,742	-25,737	-31,769
April - June 2012	0	0	-159	-159
July - September 2012	0	-22	-677	-699
October - December 2012	-115	-1,290	-9,847	-11,252
January - March 2013	-1,479	-11,504	-90,771	-103,754
April - June 2013	0	-3,915	-37,041	-40,956
July - September 2013	0	-14,198	-104,699	-118,897
October - December 2013	-836	-15,323	-75,595	-91,754
January - March 2014	-13,161	-207,287	-802,925	-1,023,373
April - June 2014	0	-15,401	116,797	101,396
Total	-15,881	-274,682	-1,030,654	-1,321,217

by consumers. Roughly 77% of these losses would have occurred during the winter of 2014.

1.4.3 Sensitivity Analysis

We calculate the total change of consumer and producer surplus using the combinations of supply and demand elasticities listed in Table 2.7 and 1.5. Table 1.10 lists our results.

The results show that our estimate of consumer surplus changes associated with Atlantic Sunrise range from 2,099 to 6,442 millions dollars, while the producer surplus changes range from -3,208 to -791 millions dollars, depending on different elasticities.

1.5 Conclusions

Using the arbitrage cost approach of [19] in the context of natural gas pricing, we have modeled the impact of the Atlantic Sunrise pipeline expansion on gas flows and prices across the Transco system (Alabama and Georgia (Zone 4), Carolinas

Table 1.10: Change of Consumer Surplus and Producer Surplus Under Different Elasticities (million dollars)

		High Elasticity of Pipeline Supply	Medium Elasticity of Pipeline Supply	Low Elasticity of Pipeline Supply
High Elasticity of Demand	ΔCS	2,099	2,394	2,834
	ΔPS	-791	-978	-1,256
Medium Elasticity of Demand	ΔCS	2,537	3,033	3,886
	ΔPS	-1,024	-1,321	-1,832
Low Elasticity of Demand	ΔCS	3,287	4,330	6,442
	ΔPS	-1,399	-1,972	-3,208

and Virginia (Zone 5) and Maryland, Delaware, Pennsylvania, and New Jersey (Zone 6)). Over the 30-month period of data used in our study, we estimate that under medium elasticities, consumers in Zones 4, 5 and 6 would have enjoyed $3.0 billion in in total benefits because of the Atlantic Sunrise expansion, while producers would have lost $1.3 billion. The total consumer and producer surplus under high elasticities are $2.1 and -$0.8 billion, respectively, and those under low elasticities are $6.4 and -$3.2 billion.

More than 60 percent of the estimated benefits of Atlantic Sunrise would have accrued in January 2014 alone, because of the "polar vortex". This suggests that in an evaluation year with different weather conditions, our estimates of welfare gains would have been much lower. This was the case with the winters of 2012 and 2013.

Our model also shows that welfare changes are not uniform over space. Consumers in Zones 4 and 5, who would be the recipients of additional gas flowing south due to Atlantic Sunrise, would nearly always benefit from the pipeline expansion project. Because of the location of the constraints at Stations 90 and 195, we estimate that Zone 5 customers would benefit nearly three times as much as Zone 4 customers. Zone 6 customers exhibit the highest benefits overall, but will also be harmed when exports from Zones 6 to 5 cause prices in Zone 6 to increase. These

price increases in Zone 6 occur only rarely, and are orders of magnitude smaller than the price declines in all three zones that can be expected during cold winter days.

Chapter 2
Cross-product Manipulation in Electricity Markets: A Three-stage, Two-node Equilibrium Model

2.1 Introduction

In 1996, the U.S. Federal Energy Regulatory Commission (FERC) issued its landmark Orders 888 and 889, providing a framework for competitive wholesale markets in the electricity industry [25,26]. In Order 888, FERC first introduced the concept of an Independent System Operator (ISO) as an entity whose goal is to "... operate the transmission systems of public utilities in a manner that is independent of any business interest in sales or purchases of electric power by those utilities" [25]. FERC Order 2000, issued in 1999, encouraged transmission-owning public utilities to voluntarily form and participate in a Regional Transmission Organization (RTO), and established a set of twelve technical requirements to obtain RTO status [27]. Although there exist some differences, the basic functions of ISOs and RTOs are the same: both are non-profit and independent organizations that are responsible for ensuring grid reliability, non-discriminatory access for electric generators to the transmission grid, optimal dispatch of the generating system, and running the region's wholesale electricity markets [28]. Nowadays, two-thirds of electricity consumers in the United States are served by ISOs and RTOs [29].

Restructured energy markets run by ISOs and RTOs have a multi-settlement structure including a day-ahead (DA) market, where participants commit to buy or

sell electricity one day before the operating day, and a real-time (RT) market, where deviations from day-ahead market schedules are settled during the day of operation. Both markets are organized as uniform price auctions [30]. ISOs and RTOs clear participants' bids to buy and offers to sell energy, and the market clearing price at each location on the transmission network is called locational marginal price (LMP) [31]. Buyers with cleared purchases (or sellers with cleared sales) in the day-ahead market pay (or receive) the day-ahead price at their location. Purchases (or sales) cleared at the day-ahead prices that are not subsequently converted into physical positions in real-time must be sold back (or bought back) at the real-time market prices [32].

Energy traded in the day-ahead market and in the real-time market are identical products; therefore, the DA price should converge to the expected RT price to eliminate any predictable arbitrage opportunities [33]. Price convergence in the two markets helps mitigate market power and improve the efficiency of serving load [34]. To help improve price convergence, ISOs and RTOs allow entities without physical generation or load to participate in the day-ahead auction via virtual bids [35]. A cleared virtual supply offer (or an increment offer, or INC) is an offer to sell electricity at the day-ahead price and buy back the same amount of energy at the real-time price. On the other hand, a cleared virtual demand bid (or a decrement bid, or DEC) is a bid to buy electricity at the day-ahead price and sell back the same amount of power at the real-time price. Table 2.1 summarizes the average cleared virtual bids as a percentage of average real-time load for five ISOs and RTOs in 2014 and 2015 [36–43]. Even though the percentage is relatively small in most cases, virtual bids can set the DA LMPs, as physical bids do [35]. As shown in Table 2.2 for PJM and Table 2.3 for CAISO, financial entities, such as banks, hedge funds and energy trading firms take a large fraction of virtual positions, and in some cases provide most virtual liquidity [36, 38, 39]. By exploiting predictable arbitrage opportunities between day-ahead and expected real-time prices, virtual bidders should, in principle, help the markets achieve better price convergence. For example, if a virtual bidder expects the real-time price to be higher than the day-ahead price, she would have incentive to place DECs in the DA market to buy power at a lower DA price, and sell it back at a higher RT price. The additional demand in DA market, and corresponding additional supply in the RT market, will raise the day-ahead price and lower the real-time price, helping close the price gap

between the two markets [34].

Table 2.1: Average Cleared Virtual Bids as A Percentage of Average Real-time Load by ISO (2014-2015)

ISO	2014			2015		
	DEC	**INC**	**Load (MW)**	**DEC**	**INC**	**Load (MW)**
PJM	7.4%	3.9%	89,099	4.6%	5.3%	88,594
MISO	5.8%	4.3%	77,317	6.6%	6.7%	76,233
CAISO	5.3%	7.0%	26,440	4.5%	6.7%	26,426
NYISO	5.1%	13.6%	18,300	5.4%	13.6%	18,400
ISO-NE	1.3%	1.6%	14,700	1.4%	1.8%	14,600

Table 2.2: Percentage of Total Submitted Virtual Bids by Participant Type in PJM (2014-2015)

Trading Entities	**2014**	**2015**
Financial	35.8%	44.6%
Physical	64.2%	55.4%
Total	100.0%	100.0%

Despite these theoretical price convergence benefits, the actual performance of virtual transactions and role of financial players in organized electricity markets is a subject of controversy. In a number of high-profile enforcement cases, FERC has accused banks, energy trading firms and other market participants of taking uneconomic virtual positions in the day-ahead energy market to benefit financial positions whose value is tied to day-ahead prices, like financial transmission right (FTR) positions.[1] For example, the Commission levied $135 million in penalties

[1] As noted above, all ISOs and RTOs are profit-neutral entities. However, because of locational marginal pricing, ISOs and RTOs would collect more rents from the LSEs than the payments they make to the generators in the case of transmission congestion. The difference is redistributed through Financial Transmission Rights (FTRs) [44]. A FTR is a unidirectional financial instrument defined in megawatts from a source node (where power is injected into the grid) to a sink node (where power is withdrawn from the grid). Holders of FTRs are entitled to payments equal to the difference between the congestion components of the day-ahead LMPs at the sink node and source node times the awarded megawatts. With FTRs, market participants are able to hedge against congestion risk [45].

Table 2.3: Percentage of Average Cleared Virtual Bids by Participant Type in CAISO (2014-2015)

Trading Entities	**2014**		**2015**	
	DEC	**INC**	**DEC**	**INC**
Financial	68.4%	54.1%	60.1%	43.4%
Marketer	20.9%	19.4%	33.7%	31.8%
Physical	10.7%	26.5%	6.2%	24.8%
Total	100.0%	100.0%	100.0%	100.0%

Marketers include participants on the inter-ties and participants whose portfolios are not primarily focused on physical or financial participation in the ISO markets [39].

and $110 million in disgorgement[2] based on findings that Constellation Energy Commodities Group (CCG) entered uneconomic virtual and physical transactions in the ISO-NE and NYISO markets to affect DA market prices in order to benefit the firm's financial swap positions (138 FERC ¶61,168). Similarly, in the case against Louis Dreyfus Energy Services (LDES), the Commission accused the company of placing uneconomic virtual transactions at a node in MISO to increase the value of the its financial transmission rights sinking at that node. The case was settled with $4,072,257 in penalties and $3.34 million in disgorgement for LDES, and $310,000 in penalties for a LDES trader (146 FERC ¶61,072).

Some studies have considered day-ahead price manipulation through virtual bidding [34, 46–49]. As [34] pointed out, a profit maximizing market participant having FTR positions of sufficient size will have an incentive to create congestion in the day-ahead market via virtual bids. The virtual bid will likely be unprofitable on a stand-alone basis, but the congestion revenues received via the FTRs could exceed the losses from virtual bids, resulting in overall positive profits. [49] discuss how the two-period theoretical model by Kumar and Seppi [50] could be used to explain how this type of manipulation can persist in equilibrium.

In this chapter, we investigate the interactions between generators, financial traders and the ISO in a three-stage game. The first stage is represented by a FTR market, followed by a two-settlement (day-ahead and real-time) energy market. As

[2]Disgorgement represents repayment of unjust profits resulting from violation of statuses, regulations, rules, orders and tariffs of the Federal Energy Regulatory Commission (130 FERC ¶61,220).

discussed below, three-stage games have been rarely considered in the literature.

2.2 Literature Review

Restructured electricity markets run by ISOs and RTOs are organized as uniform price auctions where market participants submit bids and offers to buy and sell energy. An intuitive way to model this type of market is Supply Function Equilibrium (SFE). First introduced by [51], SFE allows each supplier to choose a continuous and smooth supply function to maximize their profits. Equilibrium is obtained by solving a system of differential equations. [52] is the first to apply the SFE model to the electricity industry reforms in England and Wales. Realizing that the supply functions in reality are often not continuous or smooth, [53] propose a multiple-unit auction model to allow discrete cost and bid steps in the supply auction. Although more realistic to suppliers' bidding strategies, both SFE and multiple-unit approaches seek to find the optimal combinations of prices and quantities, and therefore impose difficulties in applying to multi-settlement markets settings [54].

On the other hand, Nash-Cournot models only solve for optimal quantities and are much easier to be applied to multi-settlement electricity markets. The first type of Nash-Cournot models do not have a detailed power flow model. Building on [55, 56], [57] develop an analytical framework to study the Nash-Cournot equilibrium of a two-settlement electricity market. Backward induction is used to obtain the subgame perfect equilibrium. [58] present a theoretical model to understand the effects of speculators on market prices and firm's production decision in a two-settlement electricity market.

To provide a better representation of power flows, two-settlement electricity markets models are often cast as Mathematical Program with Equilibrium Constraints (MPEC), or Equilibrium Problem with Equilibrium Constraints (EPEC). An MPEC is an optimization problem with constraints representing equilibrium conditions. These equilibrium conditions are often expressed as the Karush-Kuhn-Tucker (KKT) conditions for one or several interrelated optimization problems. An EPEC is an equilibrium problem where each player solves an MPEC. Most of these two-settlement electricity markets models feature an ISO's social welfare maximization problem or a collection of each player's profit maximization problem at the spot

market (lower level), and the profit maximization problem of Stackelberg leaders at the forward market (upper level), subject to the lower level problem. [59–61] present a typical two-settlement electricity market model with transmission constraints. On the lower level, demand and generation/transmission capacity uncertainty is realized. Generators then act as Nash-Cournot players by choosing generation amounts to maximize their profits, taking into account the state of nature as well as their forward positions. Meanwhile, the ISO maximizes social welfare by choosing the power transferred between nodes. On the top level (forward market), generators choose their forward positions to maximize total profit (the sum of profits from forward market and expected profits from spot market), taking into account their spot market decisions. The forward market is assumed to be efficient so that the forward price is equal to the expected spot price. Each generator is solving an MPEC, and the equilibrium problem becomes an EPEC. [62] consider a stochastic multi-leader multi-follower equilibrium problem with application to the two-settlement electricity markets. The intercept of the inverse demand function is assumed to be a random variable to reflect the randomness of demand at the spot market. The ISO's optimal dispatch problem is also included in the spot market. Other examples of applying MPECs and EPECs to model restructured electricity markets are in [63–66].

Some papers in the literature have considered three-stage market models. [67] add generator capacity expansion decisions before a two-settlement market without transmission constraints. The intercept of the inverse demand function is assumed to be a random variable. The three-stage problem is reduced to the two-stage one by solving the last stage (the spot market) analytically, and substituting the results in the second stage. They find that by adding generation capacity constraints, the result that forward contracts mitigate market power on the spot market claimed by [56] no longer holds. The impact of contracts is further discussed in a serial paper [68]. [69] propose a three-stage proactive transmission investment valuation model, where the network planner evaluates different transmission expansion projects first, then generating firms invest in new generation capacity based on the transmission expansion decision. Lastly, the energy market operates subject to the constraints determined in the previous two stages. The energy market equilibrium is modeled as in [59–61], where nature picks the state of the world, and firms then compete in a Nash-Cournot fashion by selecting production quantities to maximize their profit.

The problem is solved using backwards induction, resulting in an EPEC for the last two stages. Instead of solving the first stage transmission expansion problem, the authors evaluated the alternative predetermined transmission expansion proposals to see which one returns the highest social benefits. [70] analyze the equilibrium encompassing an electricity futures market and a sequence of spot markets. Despite the appearance of a multi-stage (more than two) setup, spot markets are independent from each other, so that the model is actually a two-stage game (futures market and spot markets). The authors solve the equilibrium in each spot market analytically and substitute the results in the futures market, therefore reducing an EPEC model to an MCP model.

Although algorithms on the global solution of linear programs with linear complementarity constraints have been developed [71], efficient methods for computing global optimal solutions to MPEC are generally not available [72]. An MPEC is a nonlinear program (NLP) with nonconvex feasible regions because of the equilibrium constraints. There are three methods to apply NLP algorithms to solve MPECs: regularization, penalization and sequential quadratic programming (SQP) [73]. Regularization relaxes the complementarity constraints by defining a larger feasible region so that NLP algorithms can work. The penalization method drops complementarity conditions from the constraints, and adds them to the upper-level objective as a penalty term. Complementarity conditions are enforced by penalizing the violation of these conditions. Finally, SQP is an iterative algorithm that replaces the nonlinear objective function by a quadratic approximation of the Lagrangian of the NLP, and approximates the nonlinear constraints by linear expression in the Newton fashion in each iteration. Diagonalization is the most common algorithm to solve an EPEC [63, 64]. It is an iterative method that solves one leader's MPEC at a time, taking other leaders' decision variables as given (either from user-supplied initial values or previous iteration results). The algorithm loops over all leaders' problems until convergence is achieved. However, in some cases, diagonalization could converge to a point that is not an equilibrium, if the leader's MPEC is solved by an algorithm that doesn't guarantee a global optimum. In other cases, the algorithm might not converge because there is no pure strategy equilibrium. By contrast, a centralized approach solves a collection of KKT conditions derived from each agent's MPEC problem [66, 74–76].

2.3 Model

We propose a three-stage sequential game (FTR, day-ahead and real-time markets) to investigate the manipulation of day-ahead electricity prices using uneconomic virtual bids, absent control of real-time prices. In this section, we describe the model assumptions and formulations.

Market Structure and Behavioral Assumptions

Consider a two-node network where a cheap generator 1 is located at node A, and an expensive generator 2 is located at node B. The marginal cost of each generator is assumed to be constant and denoted by C_j for generator j ($C_1 < C_2$). Let K_j denote generator j's capacity. There is demand at both nodes. The transmission capacity is denoted by T_{AB}. The first stage of the sequential game is the FTR stage where a financial trader acts as a Stackelberg leader with respect to FTR position.

The FTR stage is followed by a day-ahead market where generators make bilateral sales to customers with elastic demand, traders submit virtual bids to arbitrage price difference between day-ahead and real-time markets, and a system operator provides transmission services to generators and performs spatial arbitrage (i.e., price differences between two nodes). In the day-ahead market, we make different behavioral assumptions for generators and financial traders: market participants either act competitively or behave à la Cournot. The spatial arbitrage function of ISO is an essential assumption to ensure price difference between two nodes equal to the transmission cost when market participants behave à la Cournot.

Lastly, demand is realized in real-time market and generators provide residual sales (or buy back their positions) at real-time prices. Generators are assumed to be competitive in the real-time market. This assumption serves for two purposes: first, it is consistent with our general notion that we seek to understand traders' uneconomic manipulation behavior in the day-ahead market, absent control of real-time prices; secondly, a competitive setting for the real-time market makes it possible to derive analytical solutions for the real-time variables. Therefore, the three-stage problem can be reduced to two-stage which can be formulated as an MPEC. Since transmission price is equal to the nodal price difference under perfect competition, there is no need for the ISO to perform spatial arbitrage in the real-time market.

Figure 2.1 summarizes the time frame of the three-stage sequential game, as

well as the market participants at each stage.

Figure 2.1: Time Frame and Market Participants of the Three-stage Game

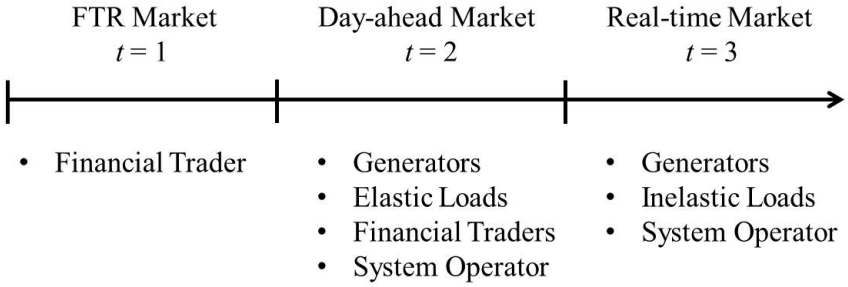

Demand Uncertainty

We assume for both nodes an elastic demand in the day-ahead market, and an inelastic demand in the real-time market. Elastic demand in the day-ahead market allows bids and offers to influence the day-ahead prices so that a potential manipulation attempt could be sustained in equilibrium, while inelastic demand in the real-time market makes our three-stage problem tractable. In the day-ahead market, we assume the intercept of inverse demand function at node B to be random and has a uniform distribution. 100 samples were drawn from the uniform distribution. For each realization of day-ahead demand, we assume the real-time demand at both nodes are random, corresponding to the 2 real-time scenarios where the transmission line in real-time can be either uncongested or congested. In both cases, let the real-time load at node A be less than the difference between generator 1's capacity and transmission capacity ($0 < L_A < K_1 - T_{AB}$) so that the cheap generator always has enough capacity to serve the load at its own node as well as ship power to the other node. For the real-time uncongestion case, the real-time load at node B is less than the transmission capacity ($0 < L_B < T_{AB}$). For the real-time congestion case, the real-time load at node B is greater than the transmission capacity and less than the sum of generator 2's generation capacity and the transmission capacity ($T_{AB} < L_B < K_2 + T_{AB}$). Figure 2.2 shows the scenario tree for our three-stage model.

Cases

For the day-ahead market, we simulate eight cases:

- Case 1: Two Competitive Generators and Two Competitive Traders (One with FTR)

Figure 2.2: Scenario Tree of the Three-stage Game

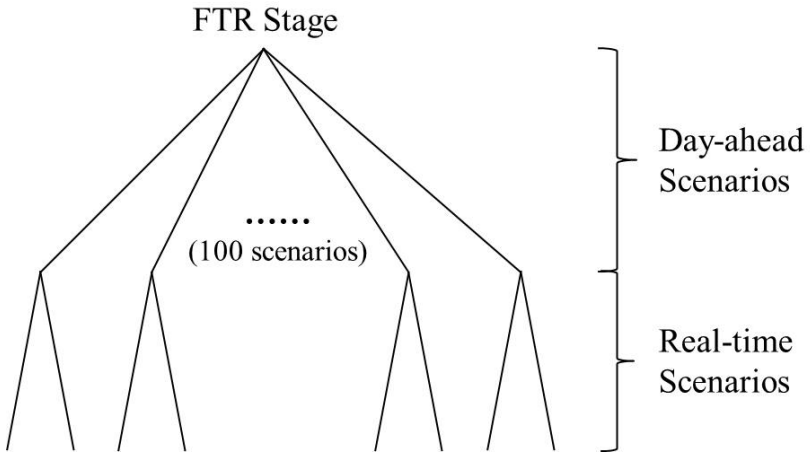

- Case 2: Two Competitive Generators, One Cournot Trader with FTR, One Competitive Trader without FTR
- Case 3: Two Cournot Generators, Two Cournot Traders (One with FTR)
- Case 4: Two Cournot Generators, One Cournot Traders with FTR, Multiple Cournot Traders without FTR
- Case 5: Two Cournot Generators, One Cournot Trader without FTR
- Case 6: Two Cournot Generators, Two Cournot Traders (without FTR)
- Case 7: Two Cournot Generators, Two Competitive Traders (One with FTR)
- Case 8: Two Cournot Generators, Two Cournot Traders (both with FTR)

2.3.1 Real-time Market Model Formulation

The real-time market formulation is the same for all cases. We formulate the real-time problem as both a complementarity problem and an optimization problem. We also show the equivalence between the two formulations. Superscript ω and ψ are used to denote real-time and day-ahead variables, respectively.

Complementarity formulation:

- Generator 1

Generator 1 is a strategic player that chooses the amount of power to sell at each node in both real-time and day-ahead markets. In the real-time market, she chooses the residual sales at node i (denoted by s^{ω}_{1i}, where $i = A, B$) to maximize her total profit from both real-time and day-ahead markets. The real-time residual sales at node i is defined as the difference between the total sales and the day-ahead scheduled sales at node i, and is paid the real-time locational marginal price (LMP) at that node (p^{ω}_i). If generators want to sell power to node other than their own location, a transmission price has to be paid to the ISO for transporting power. In generator 1's real-time case, since it is located at node A, real-time residual sales to node B needs to pay a real-time transmission price w^{ω}_{AB} for every unit of the residual sales to node B from generator 1. Similarly, generator 1's day-ahead scheduled sales at node i (denoted by s^{ψ}_{1i}) is paid the day-ahead LMP at that node (p^{ψ}_i), and every unit of day-ahead sales to node B needs to pay a day-ahead transmission charge w^{ψ}_{AB} to the ISO. The sum of real-time residual sales and day-ahead scheduled sales is the total sales and is produced at the constant marginal cost C_1. The total sales from generator 1 is bounded by its generation capacity K_1. We also require each generator's total sales at each location to be positive. Following the description above, generator 1's real-time problem is formulated below:

$$
\begin{aligned}
\underset{s^{\omega}_{1A}, s^{\omega}_{1B}}{\text{maximize}} \quad & p^{\omega}_A s^{\omega}_{1A} + (p^{\omega}_B - w^{\omega}_{AB}) s^{\omega}_{1B} + p^{\psi}_A s^{\psi}_{1A} + (p^{\psi}_B - w^{\psi}_{AB}) s^{\psi}_{1B} \\
& - C_1(s^{\omega}_{1A} + s^{\omega}_{1B} + s^{\psi}_{1A} + s^{\psi}_{1B}) && \text{(2.1a)} \\
\text{subject to} \quad & s^{\omega}_{1A} + s^{\omega}_{1B} \leqslant K_1 - s^{\psi}_{1A} - s^{\psi}_{1B}\,, \ (\mu^{\omega}_1) && \text{(2.1b)} \\
& s^{\omega}_{1A} + s^{\psi}_{1A} \geqslant 0\,, && \text{(2.1c)} \\
& s^{\omega}_{1B} + s^{\psi}_{1B} \geqslant 0\,, && \text{(2.1d)}
\end{aligned}
$$

- Generator 2

Generator 2's problem is mostly the same as generator 1's. The only difference is that, generator 2 is located at node B, therefore its sales to node A has to pay a transmission charge to the ISO. We have defined the transmission charge from node A to node B as w_{AB}, thus the transmission charge from node B to node A is $-w_{AB}$. Generator 2's real-time problem is formulated below:

$$
\underset{s^{\omega}_{2A}, s^{\omega}_{2B}}{\text{maximize}} \quad (p^{\omega}_A + w^{\omega}_{AB}) s^{\omega}_{2A} + p^{\omega}_B s^{\omega}_{2B} + (p^{\psi}_A + w^{\psi}_{AB}) s^{\psi}_{2A} + p^{\psi}_B s^{\psi}_{2B}
$$

$$
\begin{aligned}
& - C_2(s_{2A}^{\omega} + s_{2B}^{\omega} + s_{2A}^{\psi} + s_{2B}^{\psi}) && \text{(2.2a)} \\
\text{subject to} \quad & s_{2A}^{\omega} + s_{2B}^{\omega} \leqslant K_2 - s_{2A}^{\psi} - s_{2B}^{\psi}\,, \ (\mu_2^{\omega}) && \text{(2.2b)} \\
& s_{2A}^{\omega} + s_{2A}^{\psi} \geqslant 0\,, && \text{(2.2c)} \\
& s_{2B}^{\omega} + s_{2B}^{\psi} \geqslant 0\,, && \text{(2.2d)}
\end{aligned}
$$

- Independent System Operator (ISO)

The ISO's problem is to maximize the value the market receives from the transmission assets, subject to network constraints. The ISO provides MW of transmission services from A to B to power suppliers. Denote real-time transmission services as y_{AB}^{ω}. ISO charges w_{AB}^{ω} for every unit of y_{AB}^{ω}. Similarly, we denote the day-ahead transmission services as y_{AB}^{ψ}, and w_{AB}^{ψ} is charged for every unit of y_{AB}^{ψ} by the ISO.

We also assume that ISO performs spatial arbitrage function in day-ahead market, so that it can buy power at the node with lower LMP and sell it to the node with higher LMP. We introduce variable m^{ψ} to represent the load flow from node A to node B due to ISO's spatial arbitrage function. This means that in addition to generators' sales choices, ISO buys m^{ψ} amount of power at node A and sell it to node B in the day-ahead market. Allowing ISO to perform spatial arbitrage in the day-ahead market is necessary to eliminate any arbitrage opportunities at equilibrium, and therefore yield a transmission price equal to the price difference between the two nodes. Since we assume perfect competition in the real-time market, the assumption of ISO performing spatial arbitrage function is not needed.

The sum of the real-time residual load flow from transmission and the day-ahead scheduled load flow from both transmission and arbitrage functions is the total load flow at real-time and should be bounded by the transmission line's capacity.

Therefore, the ISO's real-time problem becomes:

$$
\begin{aligned}
\underset{y_{AB}^{\omega}}{\text{maximize}} \quad & w_{AB}^{\omega} y_{AB}^{\omega} && \text{(2.3a)} \\
\text{subject to} \quad & y_{AB}^{\omega} + y_{AB}^{\psi} + m^{\psi} \leqslant T_{AB}\,, \ (\lambda_{AB}^{\omega}) && \text{(2.3b)} \\
& y_{AB}^{\omega} + y_{AB}^{\psi} + m^{\psi} \geqslant -T_{AB}\,, \ (\lambda_{BA}^{\omega}) && \text{(2.3c)}
\end{aligned}
$$

- Market clearing

Let l_i^{ω} and l_i^{ψ} represent the real-time residual demand and day-ahead scheduled demand at node i, respectively. And denote L_i as the total demand at node i in

the real-time. In the real-time market, total demand at node i should be equal to the total supply to that node. Moreover, the total power flow due to ISO's transportation service at real-time should be equal to the difference between total sales from generator 1 to node B and that from generator 2 to node A:

$$L_A = l_A^\omega + l_A^\psi = s_{1A}^\omega + s_{2A}^\omega + s_{1A}^\psi + s_{2A}^\psi - m^\psi \,, \ (p_A^\omega) \tag{2.4a}$$
$$L_B = l_B^\omega + l_B^\psi = s_{1B}^\omega + s_{2B}^\omega + s_{1B}^\psi + s_{2B}^\psi + m^\psi \,, \ (p_B^\omega) \tag{2.4b}$$
$$y_{AB}^\omega + y_{AB}^\psi = (s_{1B}^\omega - s_{2A}^\omega) + (s_{1B}^\psi - s_{2A}^\psi) \,, \ (w_{AB}^\omega) \tag{2.4c}$$

Optimization formulation

The real-time problem can also be formulated as a cost minimization problem as follows:

$$\underset{s_{1A}^\omega, s_{1B}^\omega, s_{2A}^\omega, s_{2B}^\omega, y_{AB}^\omega}{\text{minimize}} \quad C_1(s_{1A}^\omega + s_{1B}^\omega + s_{1A}^\psi + s_{1B}^\psi) + C_2(s_{2A}^\omega + s_{2B}^\omega + s_{2A}^\psi + s_{2B}^\psi) \tag{2.5a}$$
$$\text{subject to} \quad s_{1A}^\omega + s_{1B}^\omega \leqslant K_1 - s_{1A}^\psi - s_{1B}^\psi \,, \ (\mu_1^\omega) \tag{2.5b}$$
$$s_{1A}^\omega + s_{1A}^\psi \geqslant 0 \,, \tag{2.5c}$$
$$s_{1B}^\omega + s_{1B}^\psi \geqslant 0 \,, \tag{2.5d}$$
$$s_{2A}^\omega + s_{2B}^\omega \leqslant K_2 - s_{2A}^\psi - s_{2B}^\psi \,, \ (\mu_2^\omega) \tag{2.5e}$$
$$s_{2A}^\omega + s_{2A}^\psi \geqslant 0 \,, \tag{2.5f}$$
$$s_{2B}^\omega + s_{2B}^\psi \geqslant 0 \,, \tag{2.5g}$$
$$y_{AB}^\omega + y_{AB}^\psi + m^\psi \leqslant T_{AB} \,, \ (\lambda_{AB}^\omega) \tag{2.5h}$$
$$y_{AB}^\omega + y_{AB}^\psi + m^\psi \geqslant -T_{AB} \,, \ (\lambda_{BA}^\omega) \tag{2.5i}$$
$$L_A = l_A^\omega + l_A^\psi = s_{1A}^\omega + s_{2A}^\omega + s_{1A}^\psi + s_{2A}^\psi - m^\psi \,, \ (p_A^\omega) \tag{2.5j}$$
$$L_B = l_B^\omega + l_B^\psi = s_{1B}^\omega + s_{2B}^\omega + s_{1B}^\psi + s_{2B}^\psi + m^\psi \,, \ (p_B^\omega) \tag{2.5k}$$
$$y_{AB}^\omega + y_{AB}^\psi = (s_{1B}^\omega - s_{2A}^\omega) + (s_{1B}^\psi - s_{2A}^\psi) \,, \ (w_{AB}^\omega) \tag{2.5l}$$

Both formulations will result in KKT conditions below:

$$0 \leqslant s_{1A}^\omega + s_{1A}^\psi \perp - p_A^\omega + C_1 + \mu_1^\omega \geqslant 0 \,, \tag{2.6a}$$
$$0 \leqslant s_{1B}^\omega + s_{1B}^\psi \perp - (p_B^\omega - w_{AB}^\omega) + C_1 + \mu_1^\omega \geqslant 0 \,, \tag{2.6b}$$
$$0 \leqslant \mu_1^\omega \perp K_1 - s_{1A}^\psi - s_{1B}^\psi - s_{1A}^\omega - s_{1B}^\omega \geqslant 0 \,, \tag{2.6c}$$
$$0 \leqslant s_{2A}^\omega + s_{2A}^\psi \perp - (p_A^\omega + w_{AB}^\omega) + C_2 + \mu_2^\omega \geqslant 0 \,, \tag{2.6d}$$

$$0 \leqslant s^{\omega}_{2B} + s^{\psi}_{2B} \perp - p^{\omega}_{B} + C_2 + \mu^{\omega}_{2} \geqslant 0\,, \tag{2.6e}$$

$$0 \leqslant \mu^{\omega}_{2} \perp K_2 - s^{\psi}_{2A} - s^{\psi}_{2B} - s^{\omega}_{2A} - s^{\omega}_{2B} \geqslant 0\,, \tag{2.6f}$$

$$w^{\omega}_{AB} - \lambda^{\omega}_{AB} + \lambda^{\omega}_{BA} = 0\,, \tag{2.6g}$$

$$0 \leqslant \lambda^{\omega}_{AB} \perp T_{AB} - y^{\omega}_{AB} - y^{\psi}_{AB} - m^{\psi} \geqslant 0\,, \tag{2.6h}$$

$$0 \leqslant \lambda^{\omega}_{BA} \perp T_{AB} + y^{\omega}_{AB} + y^{\psi}_{AB} + m^{\psi} \geqslant 0\,, \tag{2.6i}$$

$$L_A = l^{\omega}_{A} + l^{\psi}_{A} = s^{\omega}_{1A} + s^{\omega}_{2A} + s^{\psi}_{1A} + s^{\psi}_{2A} - m^{\psi}\,, \tag{2.6j}$$

$$L_B = l^{\omega}_{B} + l^{\psi}_{B} = s^{\omega}_{1B} + s^{\omega}_{2B} + s^{\psi}_{1B} + s^{\psi}_{2B} + m^{\psi}\,, \tag{2.6k}$$

$$y^{\omega}_{AB} + y^{\psi}_{AB} = (s^{\omega}_{1B} - s^{\omega}_{2A}) + (s^{\psi}_{1B} - s^{\psi}_{2A})\,, \tag{2.6l}$$

Assume that generator 1 serves the load at node A first before transporting any power to node B. We also assume $0 < L_A < K_1$ and $T_{AB} < K_1 - L_A$. Because of this, generator 1 is turned on but not at its capacity, so $s^{\omega}_{1A} + s^{\psi}_{1A} > 0$ and $\mu^{r}_{1} = 0$.

We have two cases for the stochastic real-time demand at node B:

Case a: $0 < L_B < T_{AB}$ with probability $\Pr(\Omega_a)$

In this case, generator 2 is not turned on, so $s^{\omega}_{2A} + s^{\psi}_{2A} = 0$, $s^{\omega}_{2B} + s^{\psi}_{2B} = 0$ and $\mu^{\omega}_{2} = 0$. Also, this means generator 1 is transporting power to node B, so that $s^{\omega}_{1B} + s^{\psi}_{1B} > 0$. The transmission line will not be congested on either direction, so $\lambda^{\omega}_{AB} = \lambda^{\omega}_{BA} = 0$.

Given the above information, we can solve the KKT conditions analytically:

$$p^{\omega}_{A} = C_1$$
$$\mu^{\omega}_{1} = 0$$
$$p^{\omega}_{B} = C_1$$
$$\mu^{\omega}_{2} = 0$$
$$w^{\omega}_{AB} = 0$$
$$\lambda^{\omega}_{AB} = 0$$
$$\lambda^{\omega}_{BA} = 0$$
$$s^{\omega}_{1A} = L_A - s^{\psi}_{1A} + m^{\psi} = l^{\omega}_{A} + l^{\psi}_{A} - s^{\psi}_{1A} + m^{\psi}$$
$$s^{\omega}_{1B} = L_B - s^{\psi}_{1B} - m^{\psi} = l^{\omega}_{B} + l^{\psi}_{B} - s^{\psi}_{1B} - m^{\psi}$$
$$s^{\omega}_{2A} = -s^{\psi}_{2A}$$
$$s^{\omega}_{2B} = -s^{\psi}_{2B}$$

$$y^{\omega}_{AB} = L_B - y^{\psi}_{AB} - m^{\psi} = l^{\omega}_B + l^{\psi}_B - y^{\psi}_{AB} - m^{\psi}$$

Case b: $T_{AB} < L_B < K_2 + T_{AB}$ with probability $\Pr(\Omega_b)$

In this case, generator 2 is turned on but not at its capacity, so $s^{\omega}_{2B} + s^{\psi}_{2B} > 0$ and $\mu^{\omega}_2 = 0$. Also, this means generator 1 is transporting power to node B, so that $s^{\omega}_{1B} + s^{\psi}_{1B} > 0$. Generator 2 is not going to transport power to node A, so $s^{\omega}_{2A} + s^{\psi}_{2A} = 0$. Since the transmission line will be congested from A to B, so $T_{AB} - y^{\omega}_{AB} - y^{\psi}_{AB} - m^{\psi} = 0$ and $\lambda^{\omega}_{BA} = 0$.

Given the above information, we can solve the KKT conditions analytically:

$$\begin{aligned}
&p^{\omega}_A = C_1 \\
&\mu^{\omega}_1 = 0 \\
&p^{\omega}_B = C_2 \\
&\mu^{\omega}_2 = 0 \\
&w^{\omega}_{AB} = C_2 - C_1 \\
&\lambda^{\omega}_{AB} = C_2 - C_1 \\
&\lambda^{\omega}_{BA} = 0 \\
&s^{\omega}_{1A} = L_A - s^{\psi}_{1A} + m^{\psi} = l^{\omega}_A + l^{\psi}_A - s^{\psi}_{1A} + m^{\psi} \\
&s^{\omega}_{1B} = T_{AB} - s^{\psi}_{1B} - m^{\psi} \\
&s^{\omega}_{2A} = -s^{\psi}_{2A} \\
&s^{\omega}_{2B} = L_B - T_{AB} - s^{\psi}_{2B} = l^{\omega}_B + l^{\psi}_B - T_{AB} - s^{\psi}_{2B} \\
&y^{\omega}_{AB} = T_{AB} - y^{\psi}_{AB} - m^{\psi}
\end{aligned}$$

2.3.2 Day-ahead and FTR Markets Model Formulation

We simulate eight cases for the day-ahead and FTR markets. In particular, Cases 5, 6 and 7 represent benchmarks to assess changes in prices and other equilibrium market outcomes. These benchmarks differ with regard to day-ahead market behavioral assumptions and participants, but are all characterized by no uneconomic virtual bidding at the FTR sink. Further, while in Cases 1-7 the trader's problem is cast as an MPEC, Case 8 is a EPEC. For each case, we allow the intercept of the inverse demand function at node B to be stochastic, denoted by a^{ψ}_B. Blow is the model formulation for each case.

2.3.2.1 Case 1: Two Competitive Generators and Two Competitive Traders (One with FTR)

- Demand at Node A

$$p_A^{\psi} = p_A^{\psi}(d_A^{\psi}) = a_A - b_A(s_{1A}^{\psi} + s_{2A}^{\psi} + s_{3A}^{inc,\psi} + s_{4A}^{inc,\psi} - s_{3A}^{dec,\psi} - s_{4A}^{dec,\psi} - m^{\psi}) \tag{2.7a}$$

- Demand at Node B

$$p_B^{\psi} = p_B^{\psi}(d_B^{\psi}) = a_B^{\psi} - b_B(s_{1B}^{\psi} + s_{2B}^{\psi} + s_{3B}^{inc,\psi} + s_{4B}^{inc,\psi} - s_{3B}^{dec,\psi} - s_{4B}^{dec,\psi} + m^{\psi}) \tag{2.8a}$$

- Generator 1

$$\begin{aligned}
\underset{s_{1A}^{\psi}, s_{1B}^{\psi}}{\text{maximize}} \quad & \mathbb{E}[p_A^{\omega} s_{1A}^{\omega} + (p_B^{\omega} - w_{AB}^{\omega}) s_{1B}^{\omega} + p_A^{\psi} s_{1A}^{\psi} + (p_B^{\psi} - w_{AB}^{\psi}) s_{1B}^{\psi} \\
& - C_1(s_{1A}^{\omega} + s_{1B}^{\omega} + s_{1A}^{\psi} + s_{1B}^{\psi})] && \text{(2.9a)} \\
\text{subject to} \quad & s_{1A}^{\psi} + s_{1B}^{\psi} \leqslant K_1\,, \ (\mu_1^{\psi}) && \text{(2.9b)} \\
& s_{1A}^{\psi} \geqslant 0\,, && \text{(2.9c)} \\
& s_{1B}^{\psi} \geqslant 0\,, && \text{(2.9d)}
\end{aligned}$$

Substitute the real-time analytical solution, the above formulation can be written as the optimization problem below:

$$\begin{aligned}
\underset{s_{1A}^{\psi}, s_{1B}^{\psi}}{\text{maximize}} \quad & p_A^{\psi} s_{1A}^{\psi} + (p_B^{\psi} - w_{AB}^{\psi}) s_{1B}^{\psi} - C_1(s_{1A}^{\psi} + s_{1B}^{\psi}) && \text{(2.10a)} \\
\text{subject to} \quad & s_{1A}^{\psi} + s_{1B}^{\psi} \leqslant K_1\,, \ (\mu_1^{\psi}) && \text{(2.10b)} \\
& s_{1A}^{\psi} \geqslant 0\,, && \text{(2.10c)} \\
& s_{1B}^{\psi} \geqslant 0\,, && \text{(2.10d)}
\end{aligned}$$

- Generator 2

$$\underset{s_{2A}^{\psi}, s_{2B}^{\psi}}{\text{maximize}} \quad \mathbb{E}[(p_A^{\omega} + w_{AB}^{\omega}) s_{2A}^{\omega} + p_B^{\omega} s_{2B}^{\omega} + (p_A^{\psi} + w_{AB}^{\psi}) s_{2A}^{\psi} + p_B^{\psi} s_{2B}^{\psi}$$

$$- C_2(s^{\omega}_{2A} + s^{\omega}_{2B} + s^{\psi}_{2A} + s^{\psi}_{2B})] \tag{2.11a}$$

$$\text{subject to} \quad s^{\psi}_{2A} + s^{\psi}_{2B} \leqslant K_2\,,\ (\mu^{\psi}_2) \tag{2.11b}$$

$$s^{\psi}_{2A} \geqslant 0\,, \tag{2.11c}$$

$$s^{\psi}_{2B} \geqslant 0\,, \tag{2.11d}$$

Substitute the real-time analytical solution, the above formulation can be written as the optimization problem below:

$$\underset{s^{\psi}_{2A}, s^{\psi}_{2B}}{\text{maximize}} \quad (p^{\psi}_A + w^{\psi}_{AB})s^{\psi}_{2A} + p^{\psi}_B s^{\psi}_{2B} - C_2(s^{\psi}_{2A} + s^{\psi}_{2B}) + \Pr(\Omega_a)(C_2 - C_1)(s^{\psi}_{2A} + s^{\psi}_{2B}) \tag{2.12a}$$

$$\text{subject to} \quad s^{\psi}_{2A} + s^{\psi}_{2B} \leqslant K_2\,,\ (\mu^{\psi}_2) \tag{2.12b}$$

$$s^{\psi}_{2A} \geqslant 0\,, \tag{2.12c}$$

$$s^{\psi}_{2B} \geqslant 0\,, \tag{2.12d}$$

- Financial Trader 3

In the day-ahead market, Trader 3 maximizes her total profits from both virtual bid and FTR positions, by choosing the virtual bids placed at each node. $s^{inc,\psi}_{3i}$ and $s^{dec,\psi}_{3i}$ represent the virtual supply offers and virtual demand bids at node i, respectively. Virtual supply offers are settled using the difference between day-ahead and real-time LMPs, and virtual demand bids are settled using the difference between real-time and day-ahead LMPs. Trader 3's FTR position is denoted by f_{3AB}, which is settled by the day-ahead price difference between sink node (B) and source node (A), netting the per MW hourly FTR cost. Across this chapter, we assume the FTR position is a quarterly FTR, and therefore divide the FTR cost (c_f) by 2,160 (the number of hours in a quarter) to get the hourly FTR cost. To ensure market participants have enough credits to settle their virtual positions, most ISOs require the current virtual bids exposure of a market participant to be less than their collateral. The current exposure of virtual bids is calculated by the sum of product of virtual bids positions and corresponding reference prices (denoted by R_i in the model formulation). The model formulation for Trader 3's

problem is the following:

$$\begin{aligned}
\underset{s_{3A}^{inc,\psi}, s_{3A}^{dec,\psi}, s_{3B}^{inc,\psi}, s_{3B}^{dec,\psi}}{\text{maximize}} \quad & \mathbb{E}[(p_A^\psi - p_A^\omega)s_{3A}^{inc,\psi} + (p_B^\psi - p_B^\omega)s_{3B}^{inc,\psi} \\
& + (p_A^\omega - p_A^\psi)s_{3A}^{dec,\psi} + (p_B^\omega - p_B^\psi)s_{3B}^{dec,\psi} \\
& + f_{3AB}(p_B^\psi - p_A^\psi - (c_f/2, 160))] \qquad (2.13a) \\
\text{subject to} \quad & s_{3A}^{inc,\psi} \geqslant 0\,, \qquad (2.13b) \\
& s_{3A}^{dec,\psi} \geqslant 0\,, \qquad (2.13c) \\
& s_{3B}^{inc,\psi} \geqslant 0\,, \qquad (2.13d) \\
& s_{3B}^{dec,\psi} \geqslant 0\,, \qquad (2.13e) \\
& R_A s_{3A}^{inc,\psi} + R_A s_{3A}^{dec,\psi} + R_B s_{3B}^{inc,\psi} + R_B s_{3B}^{dec,\psi} \leqslant S_3\,,\ (\theta_3^\psi) \qquad (2.13f)
\end{aligned}$$

Substitute the real-time analytical solution, the above formulation can be written as the optimization problem below:

$$\begin{aligned}
\underset{s_{3A}^{inc,\psi}, s_{3A}^{dec,\psi}, s_{3B}^{inc,\psi}, s_{3B}^{dec,\psi}}{\text{maximize}} \quad & (p_A^\psi - C_1)s_{3A}^{inc,\psi} + [p_B^\psi - (P(\Omega_a)C_1 + P(\Omega_b)C_2)]s_{3B}^{inc,\psi} \\
& + (C_1 - p_A^\psi)s_{3A}^{dec,\psi} + [(P(\Omega_a)C_1 + P(\Omega_b)C_2) - p_B^\psi]s_{3B}^{dec,\psi} \\
& + f_{3AB}[p_B^\psi - p_A^\psi - (c_f/2, 160)] \qquad (2.14a) \\
\text{subject to} \quad & s_{3A}^{inc,\psi} \geqslant 0\,, \qquad (2.14b) \\
& s_{3A}^{dec,\psi} \geqslant 0\,, \qquad (2.14c) \\
& s_{3B}^{inc,\psi} \geqslant 0\,, \qquad (2.14d) \\
& s_{3B}^{dec,\psi} \geqslant 0\,, \qquad (2.14e) \\
& R_A s_{3A}^{inc,\psi} + R_A s_{3A}^{dec,\psi} + R_B s_{3B}^{inc,\psi} + R_B s_{3B}^{dec,\psi} \leqslant S_3\,,\ (\theta_3^\psi) \qquad (2.14f)
\end{aligned}$$

- Financial Trader 4

Trader 4's day-ahead problem is similar to Trader 3's, except for Trader 4 does not have FTR positions:

$$\begin{aligned}
\underset{s_{4A}^{inc,\psi}, s_{4A}^{dec,\psi}, s_{4B}^{inc,\psi}, s_{4B}^{dec,\psi}}{\text{maximize}} \quad & \mathbb{E}[(p_A^\psi - p_A^\omega)s_{4A}^{inc,\psi} + (p_B^\psi - p_B^\omega)s_{4B}^{inc,\psi} \\
& + (p_A^\omega - p_A^\psi)s_{4A}^{dec,\psi} + (p_B^\omega - p_B^\psi)s_{4B}^{dec,\psi}] \qquad (2.15a) \\
\text{subject to} \quad & s_{4A}^{inc,\psi} \geqslant 0\,, \qquad (2.15b)
\end{aligned}$$

$$s_{4A}^{dec,\psi} \geqslant 0\,, \tag{2.15c}$$
$$s_{4B}^{inc,\psi} \geqslant 0\,, \tag{2.15d}$$
$$s_{4B}^{dec,\psi} \geqslant 0\,, \tag{2.15e}$$
$$R_A s_{4A}^{inc,\psi} + R_A s_{4A}^{dec,\psi} + R_B s_{4B}^{inc,\psi} + R_B s_{4B}^{dec,\psi} \leqslant S_4\,,\ (\theta_4^{\psi}) \tag{2.15f}$$

Substitute the real-time analytical solution, the above formulation can be written as the optimization problem below:

$$\underset{s_{4A}^{inc,\psi}, s_{4A}^{dec,\psi}, s_{4B}^{inc,\psi}, s_{4B}^{dec,\psi}}{\text{maximize}} \quad (p_A^{\psi} - C_1)s_{4A}^{inc,\psi} + [p_B^{\psi} - (\Pr(\Omega_a)C_1 + \Pr(\Omega_b)C_2)]s_{4B}^{inc,\psi} + (C_1 - p_A^{\psi})s_{4A}^{dec,\psi} + [(\Pr(\Omega_a)C_1 + \Pr(\Omega_b)C_2) - p_B^{\psi}]s_{4B}^{dec,\psi} \tag{2.16a}$$
$$\text{subject to} \quad s_{4A}^{inc,\psi} \geqslant 0\,, \tag{2.16b}$$
$$s_{4A}^{dec,\psi} \geqslant 0\,, \tag{2.16c}$$
$$s_{4B}^{inc,\psi} \geqslant 0\,, \tag{2.16d}$$
$$s_{4B}^{dec,\psi} \geqslant 0\,, \tag{2.16e}$$
$$R_A s_{4A}^{inc,\psi} + R_A s_{4A}^{dec,\psi} + R_B s_{4B}^{inc,\psi} + R_B s_{4B}^{dec,\psi} \leqslant S_4\,,\ (\theta_4^{\psi}) \tag{2.16f}$$

- ISO

$$\underset{y_{AB}^{\psi}, m^{\psi}}{\text{maximize}} \quad w_{AB}^{\psi} y_{AB}^{\psi} + (p_B^{\psi} - p_A^{\psi})m^{\psi} \tag{2.17a}$$
$$\text{subject to} \quad y_{AB}^{\psi} + m^{\psi} \leqslant T_{AB}\,,\ (\lambda_{AB}^{\psi}) \tag{2.17b}$$
$$y_{AB}^{\psi} + m^{\psi} \geqslant -T_{AB}\,,\ (\lambda_{BA}^{\psi}) \tag{2.17c}$$

- Market clearing

$$y_{AB}^{\psi} = s_{1B}^{\psi} - s_{2A}^{\psi} \tag{2.18a}$$

The KKT conditions for the day-ahead lower level problem are listed below for every ψ:

$$0 \leqslant s_{1A}^{\psi} \perp -p_A^{\psi} + C_1 + \mu_1^{\psi} \geqslant 0\,, \tag{2.19a}$$
$$0 \leqslant s_{1B}^{\psi} \perp -(p_B^{\psi} - w_{AB}^{\psi}) + C_1 + \mu_1^{\psi} \geqslant 0\,, \tag{2.19b}$$

$$0 \leqslant \mu_1^\psi \perp K_1 - s_{1A}^\psi - s_{1B}^\psi \geqslant 0\,, \tag{2.19c}$$

$$0 \leqslant s_{2A}^\psi \perp -(p_A^\psi + w_{AB}^\psi) + C_2 - \Pr(\Omega_a)(C_2 - C_1) + \mu_2^\psi \geqslant 0\,, \tag{2.19d}$$

$$0 \leqslant s_{2B}^\psi \perp -p_B^\psi + C_2 - \Pr(\Omega_a)(C_2 - C_1) + \mu_2^\psi \geqslant 0\,, \tag{2.19e}$$

$$0 \leqslant \mu_2^\psi \perp K_2 - s_{2A}^\psi - s_{2B}^\psi \geqslant 0\,, \tag{2.19f}$$

$$w_{AB}^\psi - \lambda_{AB}^\psi + \lambda_{BA}^\psi = 0\,, \tag{2.19g}$$

$$p_B^\psi - p_A^\psi - \lambda_{AB}^\psi + \lambda_{BA}^\psi = 0\,, \tag{2.19h}$$

$$0 \leqslant \lambda_{AB}^\psi \perp T_{AB} - y_{AB}^\psi - m^\psi \geqslant 0\,, \tag{2.19i}$$

$$0 \leqslant \lambda_{BA}^\psi \perp T_{AB} + y_{AB}^\psi + m^\psi \geqslant 0\,, \tag{2.19j}$$

$$p_A^\psi = a_A - b_A(s_{1A}^\psi + s_{2A}^\psi + s_{3A}^{inc,\psi} + s_{4A}^{inc,\psi} - s_{3A}^{dec,\psi} - s_{4A}^{dec,\psi} - m^\psi)\,, \tag{2.19k}$$

$$p_B^\psi = a_B^\psi - b_B(s_{1B}^\psi + s_{2B}^\psi + s_{3B}^{inc,\psi} + s_{4B}^{inc,\psi} - s_{3B}^{dec,\psi} - s_{4B}^{dec,\psi} + m^\psi)\,, \tag{2.19l}$$

$$y_{AB}^\psi = s_{1B}^\psi - s_{2A}^\psi\,, \tag{2.19m}$$

$$0 \leqslant s_{3A}^{inc,\psi} \perp -p_A^\psi + C_1 + \theta_3^\psi R_A \geqslant 0\,, \tag{2.19n}$$

$$0 \leqslant s_{3A}^{dec,\psi} \perp -C_1 + p_A^\psi + \theta_3^\psi R_A \geqslant 0\,, \tag{2.19o}$$

$$0 \leqslant s_{3B}^{inc,\psi} \perp -p_B^\psi + (\Pr(\Omega_a)C_1 + \Pr(\Omega_b)C_2) + \theta_3^\psi R_B \geqslant 0\,, \tag{2.19p}$$

$$0 \leqslant s_{3B}^{dec,\psi} \perp -(\Pr(\Omega_a)C_1 + \Pr(\Omega_b)C_2) + p_B^\psi + \theta_3^\psi R_B \geqslant 0\,, \tag{2.19q}$$

$$0 \leqslant \theta_3^\psi \perp S_3 - R_A s_{3A}^{inc,\psi} - R_B s_{3B}^{inc,\psi} - R_A s_{3A}^{dec,\psi} - R_B s_{3B}^{dec,\psi} \geqslant 0\,, \tag{2.19r}$$

$$0 \leqslant s_{4A}^{inc,\psi} \perp -p_A^\psi + C_1 + \theta_4^\psi R_A \geqslant 0\,, \tag{2.19s}$$

$$0 \leqslant s_{4A}^{dec,\psi} \perp -C_1 + p_A^\psi + \theta_4^\psi R_A \geqslant 0\,, \tag{2.19t}$$

$$0 \leqslant s_{4B}^{inc,\psi} \perp -p_B^\psi + (\Pr(\Omega_a)C_1 + \Pr(\Omega_b)C_2) + \theta_4^\psi R_B \geqslant 0\,, \tag{2.19u}$$

$$0 \leqslant s_{4B}^{dec,\psi} \perp -(\Pr(\Omega_a)C_1 + \Pr(\Omega_b)C_2) + p_B^\psi + \theta_4^\psi R_B \geqslant 0\,, \tag{2.19v}$$

$$0 \leqslant \theta_4^\psi \perp S_4 - R_A s_{4A}^{inc,\psi} - R_B s_{4B}^{inc,\psi} - R_A s_{4A}^{dec,\psi} - R_B s_{4B}^{dec,\psi} \geqslant 0\,, \tag{2.19w}$$

In the upper level, Trader 3 is choosing her FTR position to maximize profit. The Trader 3's problem is formulated below:

$$\begin{aligned}
&\underset{f_{3AB}, s_{ji}^\psi, m^\psi, \mu_j^\psi, \eta_j^\psi, \zeta_j^\psi, w_{AB}^\psi, \lambda_{AB}^\psi, \lambda_{BA}^\psi, p_j^\psi, y_{AB}^\psi, s_{3A}^{inc,\psi}, s_{3A}^{dec,\psi}, s_{3B}^{inc,\psi}, s_{3B}^{dec,\psi}, s_{4A}^{inc,\psi}, s_{4A}^{dec,\psi}, s_{4B}^{inc,\psi}, s_{4B}^{dec,\psi}, \epsilon}{\text{maximize}} \\
&\quad \mathbb{E}_{\psi,\omega}[(p_A^\psi - p_A^\omega)s_{3A}^{inc,\psi} + (p_B^\psi - p_B^\omega)s_{3B}^{inc,\psi} \\
&\quad + (p_A^\omega - p_A^\psi)s_{3A}^{dec,\psi} + (p_B^\omega - p_B^\psi)s_{3B}^{dec,\psi} + f_{3AB}(p_B^\psi - p_A^\psi - (c_f/2, 160))]
\end{aligned} \tag{2.20a}$$

subject to:

- FTR Position Limit

$$-T_{AB} \leqslant f_{3AB} \leqslant T_{AB}\,, \tag{2.21}$$

- KKT conditions of the DA problem

The variables $(s^{\psi}_{ji}, m^{\psi}, \mu^{\psi}_{j}, \eta^{\psi}_{j}, \zeta^{\psi}_{j}, w^{\psi}_{AB}, \lambda^{\psi}_{AB}, \lambda^{\psi}_{BA}, p^{\psi}_{j}, y^{\psi}_{AB}, s^{inc,\psi}_{3A}, s^{dec,\psi}_{3A}, s^{inc,\psi}_{3B}, s^{dec,\psi}_{3B}, s^{inc,\psi}_{4A}, s^{dec,\psi}_{4A}, s^{inc,\psi}_{4B}, s^{dec,\psi}_{4B}, \theta^{\psi}_{3}, \theta^{\psi}_{4})$ represent a solution to the lower-level day-ahead problem, and solve its associated KKT system as in Equations 2.19.

2.3.2.2 Case 2: Two Competitive Generators, One Cournot Trader with FTR, One Competitive Trader without FTR

In Case 2, we allow the financial trader with FTR position to behave à la Cournot in the day-ahead market. Trader 3's problem formulation is therefore modified by substituting the day-ahead prices with day-ahead inverse demand functions in her objective:

- Financial Trader 3

$$\begin{aligned}
\underset{s^{inc,\psi}_{3A}, s^{dec,\psi}_{3A}, s^{inc,\psi}_{3B}, s^{dec,\psi}_{3B}}{\text{maximize}} \quad & \mathbb{E}[(p^{\psi}_{A}(d^{\psi}_{A}) - p^{\omega}_{A})s^{inc,\psi}_{3A} + (p^{\psi}_{B}(d^{\psi}_{B}) - p^{\omega}_{B})s^{inc,\psi}_{3B} \\
& + (p^{\omega}_{A} - p^{\psi}_{A}(d^{\psi}_{A}))s^{dec,\psi}_{3A} + (p^{\omega}_{B} - p^{\psi}_{B}(d^{\psi}_{B}))s^{dec,\psi}_{3B} && \text{(2.22a)} \\
& + f_{3AB}(p^{\psi}_{B}(d^{\psi}_{B}) - p^{\psi}_{A}(d^{\psi}_{A}) - (c_f/2, 160))] \\
\text{subject to} \quad & s^{inc,\psi}_{3A} \geqslant 0\,, && \text{(2.22b)} \\
& s^{dec,\psi}_{3A} \geqslant 0\,, && \text{(2.22c)} \\
& s^{inc,\psi}_{3B} \geqslant 0\,, && \text{(2.22d)} \\
& s^{dec,\psi}_{3B} \geqslant 0\,, && \text{(2.22e)} \\
& R_A s^{inc,\psi}_{3A} + R_A s^{dec,\psi}_{3A} + R_B s^{inc,\psi}_{3B} + R_B s^{dec,\psi}_{3B} \leqslant S_3\,, \ (\theta^{\psi}_{3}) && \text{(2.22f)}
\end{aligned}$$

After substituting the real-time analytical solutions, we derive the KKT conditions for Cournot Trader 3 as follows:

$$0 \leqslant s^{inc,\psi}_{3A} \perp -a_A + b_A(s^{\psi}_{1A} + s^{\psi}_{2A} + s^{inc,\psi}_{3A} + s^{inc,\psi}_{4A} - s^{dec,\psi}_{3A} - s^{dec,\psi}_{4A} - m^{\psi})$$

$$+ C_1 + b_A s_{3A}^{inc,\psi} - b_A s_{3A}^{dec,\psi} - f_{3AB} b_A + \theta_3^\psi R_A \geqslant 0\,, \tag{2.23a}$$

$$0 \leqslant s_{3A}^{dec,\psi} \perp - C_1 + a_A - b_A(s_{1A}^\psi + s_{2A}^\psi + s_{3A}^{inc,\psi} + s_{4A}^{inc,\psi} - s_{3A}^{dec,\psi} - s_{4A}^{dec,\psi} - m^\psi)$$
$$+ b_A s_{3A}^{dec,\psi} - b_A s_{3A}^{inc,\psi} + f_{3AB} b_A + \theta_3^\psi R_A \geqslant 0\,, \tag{2.23b}$$

$$0 \leqslant s_{3B}^{inc,\psi} \perp - a_B^\psi + b_B(s_{1B}^\psi + s_{2B}^\psi + s_{3B}^{inc,\psi} + s_{4B}^{inc,\psi} - s_{3B}^{dec,\psi} - s_{4B}^{dec,\psi} + m^\psi)$$
$$+ (\Pr(\Omega_a) C_1 + \Pr(\Omega_b) C_2) + b_B s_{3B}^{inc,\psi} - b_B s_{3B}^{dec,\psi} + f_{3AB} b_B + \theta_3^\psi R_B \geqslant 0\,, \tag{2.23c}$$

$$0 \leqslant s_{3B}^{dec,\psi} \perp a_B^\psi - b_B(s_{1B}^\psi + s_{2B}^\psi + s_{3B}^{inc,\psi} + s_{4B}^{inc,\psi} - s_{3B}^{dec,\psi} - s_{4B}^{dec,\psi} + m^\psi)$$
$$- (\Pr(\Omega_a) C_1 + \Pr(\Omega_b) C_2) + b_B s_{3B}^{dec,\psi} - b_B s_{3B}^{inc,\psi} - f_{3AB} b_B + \theta_3^\psi R_B \geqslant 0\,, \tag{2.23d}$$

$$0 \leqslant \theta_3^\psi \perp S_3 - R_A s_{3A}^{inc,\psi} - R_B s_{3B}^{inc,\psi} - R_A s_{3A}^{dec,\psi} - R_B s_{3B}^{dec,\psi} \geqslant 0\,, \tag{2.23e}$$

The upper level problem formulation is the same as Case 1 except for the substitution of Equations 2.19n to 2.19r with Equations 2.23.

2.3.2.3 Case 3: Two Cournot Generators, Two Cournot Traders (One with FTR)

In Case 3, we assume both generators and financial traders behave à la Cournot in the day-ahead market. Both generators' and Trader 5's problem formulations are therefore modified by substituting the day-ahead prices with day-ahead inverse demand functions in their objectives. Trader 3 and ISO's problem formulations and market clearing conditions are the same as in Case 2.

- Generator 1

$$\begin{aligned}
\underset{s_{1A}^\psi, s_{1B}^\psi}{\text{maximize}} \quad & \mathbb{E}[p_A^\omega s_{1A}^\omega + (p_B^\omega - w_{AB}^\omega) s_{1B}^\omega + p_A^\psi(d_A^\psi) s_{1A}^\psi + (p_B^\psi(d_B^\psi) - w_{AB}^\psi) s_{1B}^\psi \\
& - C_1(s_{1A}^\omega + s_{1B}^\omega + s_{1A}^\psi + s_{1B}^\psi)] && (2.24a) \\
\text{subject to} \quad & s_{1A}^\psi + s_{1B}^\psi \leqslant K_1\,,\ (\mu_1^\psi) && (2.24b) \\
& s_{1A}^\psi \geqslant 0\,, && (2.24c) \\
& s_{1B}^\psi \geqslant 0\,, && (2.24d)
\end{aligned}$$

- Generator 2

$$\begin{aligned}
\underset{s^{\psi}_{2A},s^{\psi}_{2B}}{\text{maximize}} \quad & \mathbb{E}[(p^{\omega}_{A}+w^{\omega}_{AB})s^{\omega}_{2A}+p^{\omega}_{B}s^{\omega}_{2B}+(p^{\psi}_{A}(d^{\psi}_{A})+w^{\psi}_{AB})s^{\psi}_{2A}+p^{\psi}_{B}(d^{\psi}_{B})s^{\psi}_{2B} \\
& -C_2(s^{\omega}_{2A}+s^{\omega}_{2B}+s^{\psi}_{2A}+s^{\psi}_{2B})] && \text{(2.25a)} \\
\text{subject to} \quad & s^{\psi}_{2A}+s^{\psi}_{2B}\leqslant K_2\,,\ (\mu^{\psi}_{2}) && \text{(2.25b)} \\
& s^{\psi}_{2A}\geqslant 0\,, && \text{(2.25c)} \\
& s^{\psi}_{2B}\geqslant 0\,, && \text{(2.25d)}
\end{aligned}$$

- Financial Trader 4

$$\begin{aligned}
\underset{s^{inc,\psi}_{4A},s^{dec,\psi}_{4A},s^{inc,\psi}_{4B},s^{dec,\psi}_{4B}}{\text{maximize}} \quad & \mathbb{E}[(p^{\psi}_{A}(d^{\psi}_{A})-p^{\omega}_{A})s^{inc,\psi}_{4A}+(p^{\psi}_{B}(d^{\psi}_{B})-p^{\omega}_{B})s^{inc,\psi}_{4B} \\
& +(p^{\omega}_{A}-p^{\psi}_{A}(d^{\psi}_{A}))s^{dec,\psi}_{4A}+(p^{\omega}_{B}-p^{\psi}_{B}(d^{\psi}_{B}))s^{dec,\psi}_{4B}] && \text{(2.26a)} \\
\text{subject to} \quad & s^{inc,\psi}_{4A}\geqslant 0\,, && \text{(2.26b)} \\
& s^{dec,\psi}_{4A}\geqslant 0\,, && \text{(2.26c)} \\
& s^{inc,\psi}_{4B}\geqslant 0\,, && \text{(2.26d)} \\
& s^{dec,\psi}_{4B}\geqslant 0\,, && \text{(2.26e)} \\
& R_A s^{inc,\psi}_{4A}+R_A s^{dec,\psi}_{4A}+R_B s^{inc,\psi}_{4B}+R_B s^{dec,\psi}_{4B}\leqslant S_4\,,\ (\theta^{\psi}_{4}) && \text{(2.26f)}
\end{aligned}$$

The KKT conditions for the above three players' problems are as follows for every ψ:

$$\begin{aligned}
& 0\leqslant s^{\psi}_{1A}\perp C_1-a_A+b_A(s^{\psi}_{1A}+s^{\psi}_{2A}+s^{inc,\psi}_{3A}+s^{inc,\psi}_{4A}-s^{dec,\psi}_{3A}-s^{dec,\psi}_{4A}-m^{\psi}) \\
& +b_A s^{\psi}_{1A}+\mu^{\psi}_{1}\geqslant 0\,, && \text{(2.27a)} \\
& 0\leqslant s^{\psi}_{1B}\perp C_1-a^{\psi}_{B}+b_B(s^{\psi}_{1B}+s^{\psi}_{2B}+s^{inc,\psi}_{3B}+s^{inc,\psi}_{4B}-s^{dec,\psi}_{3B}-s^{dec,\psi}_{4B}+m^{\psi}) \\
& +w^{\psi}_{AB}+b_B s^{\psi}_{1B}+\mu^{\psi}_{1}\geqslant 0\,, && \text{(2.27b)} \\
& 0\leqslant \mu^{\psi}_{1}\perp K_1-s^{\psi}_{1A}-s^{\psi}_{1B}\geqslant 0\,, && \text{(2.27c)} \\
& 0\leqslant s^{\psi}_{2A}\perp C_2-a_A+b_A(s^{\psi}_{1A}+s^{\psi}_{2A}+s^{inc,\psi}_{3A}+s^{inc,\psi}_{4A}-s^{dec,\psi}_{3A}-s^{dec,\psi}_{4A}-m^{\psi}) \\
& -w^{\psi}_{AB}+b_A s^{\psi}_{2A}-\Pr(\Omega_a)(C_2-C_1)+\mu^{\psi}_{2}\geqslant 0\,, && \text{(2.27d)} \\
& 0\leqslant s^{\psi}_{2B}\perp C_2-a^{\psi}_{B}+b_B(s^{\psi}_{1B}+s^{\psi}_{2B}+s^{inc,\psi}_{3B}+s^{inc,\psi}_{4B}-s^{dec,\psi}_{3B}-s^{dec,\psi}_{4B}+m^{\psi}) \\
& +b_B s^{\psi}_{2B}-\Pr(\Omega_a)(C_2-C_1)+\mu^{\psi}_{2}\geqslant 0\,, && \text{(2.27e)} \\
& 0\leqslant \mu^{\psi}_{2}\perp K_2-s^{\psi}_{2A}-s^{\psi}_{2B}\geqslant 0\,, && \text{(2.27f)} \\
& 0\leqslant s^{inc,\psi}_{4A}\perp -a_A+b_A(s^{\psi}_{1A}+s^{\psi}_{2A}+s^{inc,\psi}_{3A}+s^{inc,\psi}_{4A}-s^{dec,\psi}_{3A}-s^{dec,\psi}_{4A}-m^{,\psi})
\end{aligned}$$

$$+ C_1 + b_A s_{4A}^{inc,\psi} - b_A s_{4A}^{dec,\psi} + \theta_4^\psi R_A \geqslant 0\,, \tag{2.27g}$$

$$0 \leqslant s_{4A}^{dec,\psi} \perp - C_1 + a_A - b_A(s_{1A}^\psi + s_{2A}^\psi + s_{3A}^{inc,\psi} + s_{4A}^{inc,\psi} - s_{3A}^{dec,\psi} - s_{4A}^{dec,\psi} - m^\psi)$$
$$+ b_A s_{4A}^{dec,\psi} - b_A s_{4A}^{inc,\psi} + \theta_4^\psi R_A \geqslant 0\,, \tag{2.27h}$$

$$0 \leqslant s_{4B}^{inc,\psi} \perp - a_B^\psi + b_B(s_{1B}^\psi + s_{2B}^\psi + s_{3B}^{inc,\psi} + s_{4B}^{inc,\psi} - s_{3B}^{dec,\psi} - s_{4B}^{dec,\psi} + m^\psi)$$
$$+ (P(\Omega_a)C_1 + P(\Omega_b)C_2) + b_B s_{4B}^{inc,\psi} - b_B s_{4B}^{dec,\psi} + \theta_4^\psi R_B \geqslant 0\,, \tag{2.27i}$$

$$0 \leqslant s_{4B}^{dec,\psi} \perp a_B^\psi - b_B(s_{1B}^\psi + s_{2B}^\psi + s_{3B}^{inc,\psi} + s_{4B}^{inc,\psi} - s_{3B}^{dec,\psi} - s_{4B}^{dec,\psi} + m^\psi)$$
$$- (\Pr(\Omega_a)C_1 + \Pr(\Omega_b)C_2) + b_B s_{4B}^{dec,\psi} - b_B s_{4B}^{inc,\psi} + \theta_4^\psi R_B \geqslant 0\,, \tag{2.27j}$$

$$0 \leqslant \theta_4^\psi \perp S_4 - R_A s_{4A}^{inc,\psi} - R_B s_{4B}^{inc,\psi} - R_A s_{4A}^{dec,\psi} - R_B s_{4B}^{dec,\psi} \geqslant 0\,, \tag{2.27k}$$

The upper level problem is modified by replacing both generators' and Trader 4's KKT conditions in Case 2 with Equations 2.27.

2.3.2.4 Case 4: Two Cournot Generators, One Cournot Traders with FTR, Multiple Cournot Traders without FTR

In Case 4, we assume there are n traders with no FTR positions who act as Cournot players. The model formulation is the following:

- Demand at Node A

$$p_A^\psi = p_A^\psi(d_A^\psi) = a_A - b_A(s_{1A}^\psi + s_{2A}^\psi + s_{3A}^{inc,\psi} + \sum_n s_{4A,n}^{inc,\psi} - s_{3A}^{dec,\psi} - \sum_n s_{4A,n}^{dec,\psi} - m^\psi) \tag{2.28a}$$

- Demand at Node B

$$p_B^\psi = p_B^\psi(d_B^\psi) = a_B^\psi - b_B(s_{1B}^\psi + s_{2B}^\psi + s_{3B}^{inc,\psi} + \sum_n s_{4B,n}^{inc,\psi} - s_{3B}^{dec,\psi} - \sum_n s_{4B,n}^{dec,\psi} + m^\psi) \tag{2.29a}$$

- Generator 1

$$\underset{s_{1A}^\psi, s_{1B}^\psi}{\text{maximize}} \quad \mathbb{E}[p_A^\omega s_{1A}^\omega + (p_B^\omega - w_{AB}^\omega)s_{1B}^\omega + p_A^\psi(d_A^\psi)s_{1A}^\psi + (p_B^\psi(d_B^\psi) - w_{AB}^\psi)s_{1B}^\psi$$
$$- C_1(s_{1A}^\omega + s_{1B}^\omega + s_{1A}^\psi + s_{1B}^\psi)] \tag{2.30a}$$

$$\text{subject to} \quad s_{1A}^{\psi} + s_{1B}^{\psi} \leqslant K_1\,,\ (\mu_1^{\psi}) \tag{2.30b}$$
$$s_{1A}^{\psi} \geqslant 0\,, \tag{2.30c}$$
$$s_{1B}^{\psi} \geqslant 0\,, \tag{2.30d}$$

- Generator 2

$$\underset{s_{2A}^{\psi}, s_{2B}^{\psi}}{\text{maximize}} \quad \mathbb{E}[(p_A^{\omega} + w_{AB}^{\omega})s_{2A}^{\omega} + p_B^{\omega}s_{2B}^{\omega} + (p_A^{\psi}(d_A^{\psi}) + w_{AB}^{\psi})s_{2A}^{\psi} + p_B^{\psi}(d_B^{\psi})s_{2B}^{\psi} - C_2(s_{2A}^{\omega} + s_{2B}^{\omega} + s_{2A}^{\psi} + s_{2B}^{\psi})] \tag{2.31a}$$
$$\text{subject to} \quad s_{2A}^{\psi} + s_{2B}^{\psi} \leqslant K_2\,,\ (\mu_2^{\psi}) \tag{2.31b}$$
$$s_{2A}^{\psi} \geqslant 0\,, \tag{2.31c}$$
$$s_{2B}^{\psi} \geqslant 0\,, \tag{2.31d}$$

- Financial Trader 3

$$\underset{s_{3A}^{inc,\psi}, s_{3A}^{dec,\psi}, s_{3B}^{inc,\psi}, s_{3B}^{dec,\psi}}{\text{maximize}} \quad \mathbb{E}[(p_A^{\psi}(d_A^{\psi}) - p_A^{\omega})s_{3A}^{inc,\psi} + (p_B^{\psi}(d_B^{\psi}) - p_B^{\omega})s_{3B}^{inc,\psi} + (p_A^{\omega} - p_A^{\psi}(d_A^{\psi}))s_{3A}^{dec,\psi} + (p_B^{\omega} - p_B^{\psi}(d_B^{\psi}))s_{3B}^{dec,\psi} + f_{3AB}(p_B^{\psi}(d_B^{\psi}) - p_A^{\psi}(d_A^{\psi}) - (c_f/2, 160))] \tag{2.32a}$$
$$\text{subject to} \quad s_{3A}^{inc,\psi} \geqslant 0\,, \tag{2.32b}$$
$$s_{3A}^{dec,\psi} \geqslant 0\,, \tag{2.32c}$$
$$s_{3B}^{inc,\psi} \geqslant 0\,, \tag{2.32d}$$
$$s_{3B}^{dec,\psi} \geqslant 0\,, \tag{2.32e}$$
$$R_A s_{3A}^{inc,\psi} + R_A s_{3A}^{dec,\psi} + R_B s_{3B}^{inc,\psi} + R_B s_{3B}^{dec,\psi} \leqslant S_3\,,\ (\theta_3^{\psi}) \tag{2.32f}$$

- Financial Trader 4

For each trader without FTR positions, their problems are formulated below:

$$\underset{s_{4A,n}^{inc,\psi}, s_{4A,n}^{dec,\psi}, s_{4B,n}^{inc,\psi}, s_{4B,n}^{dec,\psi}}{\text{maximize}} \quad \mathbb{E}[(p_A^{\psi}(d_A^{\psi}) - p_A^{\omega})s_{4A,n}^{inc,\psi} + (p_B^{\psi}(d_B^{\psi}) - p_B^{\omega})s_{4B,n}^{inc,\psi} + (p_A^{\omega} - p_A^{\psi}(d_A^{\psi}))s_{4A,n}^{dec,\psi} + (p_B^{\omega} - p_B^{\psi}(d_B^{\psi}))s_{4B,n}^{dec,\psi}] \tag{2.33a}$$
$$\text{subject to} \quad s_{4A,n}^{inc,\psi} \geqslant 0\,, \tag{2.33b}$$

$$s^{dec,\psi}_{4A,n} \geqslant 0\,, \tag{2.33c}$$
$$s^{inc,\psi}_{4B,n} \geqslant 0\,, \tag{2.33d}$$
$$s^{dec,\psi}_{4B,n} \geqslant 0\,, \tag{2.33e}$$
$$R_A s^{inc,\psi}_{4A,n} + R_A s^{dec,\psi}_{4A,n} + R_B s^{inc,\psi}_{4B,n} + R_B s^{dec,\psi}_{4B,n} \leqslant S_4\,,\ (\theta^{\psi}_{4,n}) \tag{2.33f}$$

- ISO

$$\underset{y^{\psi}_{AB}, m^{\psi}}{\text{maximize}} \quad w^{\psi}_{AB} y^{\psi}_{AB} + (p^{\psi}_B - p^{\psi}_A) m^{\psi} \tag{2.34a}$$
$$\text{subject to} \quad y^{\psi}_{AB} + m^{\psi} \leqslant T_{AB}\,,\ (\lambda^{\psi}_{AB}) \tag{2.34b}$$
$$y^{\psi}_{AB} + m^{\psi} \geqslant -T_{AB}\,,\ (\lambda^{\psi}_{BA}) \tag{2.34c}$$

- Market clearing

$$y^{\psi}_{AB} = s^{\psi}_{1B} - s^{\psi}_{2A} \tag{2.35a}$$

The KKT conditions for the day-ahead lower level problem of Case 4 are listed below for every ψ:

$$0 \leqslant s^{\psi}_{1A} \perp C_1 - a_A + b_A(s^{\psi}_{1A} + s^{\psi}_{2A} + s^{inc,\psi}_{3A} + \sum_n s^{inc,\psi}_{4A,n} - s^{dec,\psi}_{3A} - \sum_n s^{dec,\psi}_{4A,n} - m^{\psi}) + b_A s^{\psi}_{1A} + \mu^{\psi}_1 \geqslant 0\,, \tag{2.36a}$$
$$0 \leqslant s^{\psi}_{1B} \perp C_1 - a^{\psi}_B + b_B(s^{\psi}_{1B} + s^{\psi}_{2B} + s^{inc,\psi}_{3B} + \sum_n s^{inc,\psi}_{4B,n} - s^{dec,\psi}_{3B} - \sum_n s^{dec,\psi}_{4B,n} + m^{\psi}) + w^{\psi}_{AB} + b_B s^{\psi}_{1B} + \mu^{\psi}_1 \geqslant 0\,, \tag{2.36b}$$
$$0 \leqslant \mu^{\psi}_1 \perp K_1 - s^{\psi}_{1A} - s^{\psi}_{1B} \geqslant 0\,, \tag{2.36c}$$
$$0 \leqslant s^{\psi}_{2A} \perp C_2 - a_A + b_A(s^{\psi}_{1A} + s^{\psi}_{2A} + s^{inc,\psi}_{3A} + \sum_n s^{inc,\psi}_{4A,n} - s^{dec,\psi}_{3A} - \sum_n s^{dec,\psi}_{4A,n} - m^{\psi}) - w^{\psi}_{AB} + b_A s^{\psi}_{2A} - \Pr(\Omega_a)(C_2 - C_1) + \mu^{\psi}_2 \geqslant 0\,, \tag{2.36d}$$
$$0 \leqslant s^{\psi}_{2B} \perp C_2 - a^{\psi}_B + b_B(s^{\psi}_{1B} + s^{\psi}_{2B} + s^{inc,\psi}_{3B} + \sum_n s^{inc,\psi}_{4B,n} - s^{dec,\psi}_{3B} - \sum_n s^{dec,\psi}_{4B,n} + m^{\psi}) + b_B s^{\psi}_{2B} - \Pr(\Omega_a)(C_2 - C_1) + \mu^{\psi}_2 \geqslant 0\,, \tag{2.36e}$$
$$0 \leqslant \mu^{\psi}_2 \perp K_2 - s^{\psi}_{2A} - s^{\psi}_{2B} \geqslant 0\,, \tag{2.36f}$$
$$w^{\psi}_{AB} - \lambda^{\psi}_{AB} + \lambda^{\psi}_{BA} = 0\,, \tag{2.36g}$$

$$p_B^\psi - p_A^\psi - \lambda_{AB}^\psi + \lambda_{BA}^\psi = 0\,, \tag{2.36h}$$

$$0 \leqslant \lambda_{AB}^\psi \perp T_{AB} - y_{AB}^\psi - m^\psi \geqslant 0\,, \tag{2.36i}$$

$$0 \leqslant \lambda_{BA}^\psi \perp T_{AB} + y_{AB}^\psi + m^\psi \geqslant 0\,, \tag{2.36j}$$

$$p_A^\psi = a_A - b_A(s_{1A}^\psi + s_{2A}^\psi + s_{3A}^{inc,\psi} + \sum_n s_{4A,n}^{inc,\psi} - s_{3A}^{dec,\psi} - \sum_n s_{4A,n}^{dec,\psi} - m^\psi)\,, \tag{2.36k}$$

$$p_B^\psi = a_B^\psi - b_B(s_{1B}^\psi + s_{2B}^\psi + s_{3B}^{inc,\psi} + \sum_n s_{4B,n}^{inc,\psi} - s_{3B}^{dec,\psi} - \sum_n s_{4B,n}^{dec,\psi} + m^\psi)\,, \tag{2.36l}$$

$$y_{AB}^\psi = s_{1B}^\psi - s_{2A}^\psi\,, \tag{2.36m}$$

$$0 \leqslant s_{3A}^{inc,\psi} \perp - a_A + b_A(s_{1A}^\psi + s_{2A}^\psi + s_{3A}^{inc,\psi} + \sum_n s_{4A,n}^{inc,\psi} - s_{3A}^{dec,\psi} - \sum_n s_{4A,n}^{dec,\psi} - m^\psi)$$
$$+ C_1 + b_A s_{3A}^{inc,\psi} - b_A s_{3A}^{dec,\psi} - f_{3AB} b_A + \theta_3^\psi R_A \geqslant 0\,, \tag{2.36n}$$

$$0 \leqslant s_{3A}^{dec,\psi} \perp a_A - b_A(s_{1A}^\psi + s_{2A}^\psi + s_{3A}^{inc,\psi} + \sum_n s_{4A,n}^{inc,\psi} - s_{3A}^{dec,\psi} - \sum_n s_{4A,n}^{dec,\psi} - m^\psi)$$
$$- C_1 + b_A s_{3A}^{dec,\psi} - b_A s_{3A}^{inc,\psi} + f_{3AB} b_A + \theta_3^\psi R_A \geqslant 0\,, \tag{2.36o}$$

$$0 \leqslant s_{3B}^{inc,\psi} \perp - a_B^\psi + b_B(s_{1B}^\psi + s_{2B}^\psi + s_{3B}^{inc,\psi} + \sum_n s_{4B,n}^{inc,\psi} - s_{3B}^{dec,\psi} - \sum_n s_{4B,n}^{dec,\psi} + m^\psi)$$
$$+ (\Pr(\Omega_a) C_1 + \Pr(\Omega_b) C_2) + b_B s_{3B}^{inc,\psi} - b_B s_{3B}^{dec,\psi} + f_{3AB} b_B + \theta_3^\psi R_B \geqslant 0\,, \tag{2.36p}$$

$$0 \leqslant s_{3B}^{dec,\psi} \perp a_B^\psi - b_B(s_{1B}^\psi + s_{2B}^\psi + s_{3B}^{inc,\psi} + \sum_n s_{4B,n}^{inc,\psi} - s_{3B}^{dec,\psi} - \sum_n s_{4B,n}^{dec,\psi} + m^\psi)$$
$$- (\Pr(\Omega_a) C_1 + \Pr(\Omega_b) C_2) + b_B s_{3B}^{dec,\psi} - b_B s_{3B}^{inc,\psi} - f_{3AB} b_B + \theta_3^\psi R_B \geqslant 0\,, \tag{2.36q}$$

$$0 \leqslant \theta_3^\psi \perp S_3 - R_A s_{3A}^{inc,\psi} - R_B s_{3B}^{inc,\psi} - R_A s_{3A}^{dec,\psi} - R_B s_{3B}^{dec,\psi} \geqslant 0\,, \tag{2.36r}$$

$$0 \leqslant s_{4A,n}^{inc,\psi} \perp - a_A + b_A(s_{1A}^\psi + s_{2A}^\psi + s_{3A}^{inc,\psi} + \sum_n s_{4A,n}^{inc,\psi} - s_{3A}^{dec,\psi} - \sum_n s_{4A,n}^{dec,\psi} - m^{,\psi})$$
$$+ C_1 + b_A s_{4A,n}^{inc,\psi} - b_A s_{4A,n}^{dec,\psi} + \theta_{4,n}^\psi R_A \geqslant 0\,, \forall n \tag{2.36s}$$

$$0 \leqslant s_{4A,n}^{dec,\psi} \perp a_A - b_A(s_{1A}^\psi + s_{2A}^\psi + s_{3A}^{inc,\psi} + \sum_n s_{4A,n}^{inc,\psi} - s_{3A}^{dec,\psi} - \sum_n s_{4A,n}^{dec,\psi} - m^\psi)$$
$$- C_1 + b_A s_{4A,n}^{dec,\psi} - b_A s_{4A,n}^{inc,\psi} + \theta_{4,n}^\psi R_A \geqslant 0\,, \forall n \tag{2.36t}$$

$$0 \leqslant s_{4B,n}^{inc,\psi} \perp - a_B^\psi + b_B(s_{1B}^\psi + s_{2B}^\psi + s_{3B}^{inc,\psi} + \sum_n s_{4B,n}^{inc,\psi} - s_{3B}^{dec,\psi} - \sum_n s_{4B,n}^{dec,\psi} + m^\psi)$$
$$+ (P(\Omega_a) C_1 + P(\Omega_b) C_2) + b_B s_{4B,n}^{inc,\psi} - b_B s_{4B,n}^{dec,\psi} + \theta_{4,n}^\psi R_B \geqslant 0\,, \forall n \tag{2.36u}$$

$$0 \leqslant s_{4B,n}^{dec,\psi} \perp a_B^\psi - b_B(s_{1B}^\psi + s_{2B}^\psi + s_{3B}^{inc,\psi} + \sum_n s_{4B,n}^{inc,\psi} - s_{3B}^{dec,\psi} - \sum_n s_{4B,n}^{dec,\psi} + m^\psi)$$
$$- (\Pr(\Omega_a) C_1 + \Pr(\Omega_b) C_2) + b_B s_{4B,n}^{dec,\psi} - b_B s_{4B,n}^{inc,\psi} + \theta_{4,n}^\psi R_B \geqslant 0\,, \forall n \tag{2.36v}$$

$$0 \leqslant \theta_{4,n}^\psi \perp S_4 - R_A s_{4A,n}^{inc,\psi} - R_B s_{4B,n}^{inc,\psi} - R_A s_{4A,n}^{dec,\psi} - R_B s_{4B,n}^{dec,\psi} \geqslant 0\,, \forall n \tag{2.36w}$$

In the upper level, financial trader is choosing her FTR position to maximize profit. The financial trader's problem is formulated below:

$$\underset{f_{3AB},s_{ji}^{\psi},m^{\psi},\mu_j^{\psi},\eta_j^{\psi},\zeta_j^{\psi},w_{AB}^{\psi},\lambda_{AB}^{\psi},\lambda_{BA}^{\psi},p_j^{\psi},y_{AB}^{\psi},s_{3A}^{inc,\psi},s_{3A}^{dec,\psi},s_{3B}^{inc,\psi},s_{3B}^{dec,\psi},s_{4A,n}^{inc,\psi},s_{4A,n}^{dec,\psi},s_{4B,n}^{inc,\psi},s_{4B,n}^{dec,\psi},\theta_3^{\psi},\theta_{4,n}^{\psi},\epsilon}{\text{maximize}}$$
$$\begin{aligned}&\mathbb{E}_{\psi,\omega}[(p_A^{\psi}-p_A^{\omega})s_{3A}^{inc,\psi}+(p_B^{\psi}-p_B^{\omega})s_{3B}^{inc,\psi}\\&+(p_A^{\omega}-p_A^{\psi})s_{3A}^{dec,\psi}+(p_B^{\omega}-p_B^{\psi})s_{3B}^{dec,\psi}+f_{3AB}(p_B^{\psi}-p_A^{\psi}-(c_f/2,160))]\end{aligned} \tag{2.37a}$$

subject to:

- FTR Position Limit

$$-T_{AB}\leqslant f_{3AB}\leqslant T_{AB}\,, \tag{2.38}$$

- KKT conditions of the DA problem

The variables $(s_{ji}^{\psi}, m^{\psi}, \mu_j^{\psi}, \eta_j^{\psi}, \zeta_j^{\psi}, w_{AB}^{\psi}, \lambda_{AB}^{\psi}, \lambda_{BA}^{\psi}, p_j^{\psi}, y_{AB}^{\psi}, s_{3A}^{inc,\psi}, s_{3A}^{dec,\psi}, s_{3B}^{inc,\psi}, s_{3B}^{dec,\psi}, s_{4A,n}^{inc,\psi}, s_{4A,n}^{dec,\psi}, s_{4B,n}^{inc,\psi}, s_{4B,n}^{dec,\psi}, \theta_3^{\psi}, \theta_{4,n}^{\psi})$ represent a solution to the lower-level day-ahead problem, and solve its associated KKT system as in Equations 2.36.

2.3.2.5 Case 5 (Benchmark): Two Cournot Generators, One Cournot Trader without FTR

In Case 5, we remove the financial trader with FTR position. The inverse demand functions are therefore modified as follows:

- Demand at Node A

$$p_A^{\psi}=p_A^{\psi}(d_A^{\psi})=a_A-b_A(s_{1A}^{\psi}+s_{2A}^{\psi}+s_{4A}^{inc,\psi}-s_{4A}^{dec,\psi}-m^{\psi}) \tag{2.39a}$$

- Demand at Node B

$$p_B^{\psi}=p_B^{\psi}(d_B^{\psi})=a_B^{\psi}-b_B(s_{1B}^{\psi}+s_{2B}^{\psi}+s_{4B}^{inc,\psi}-s_{4B}^{dec,\psi}+m^{\psi}) \tag{2.40a}$$

The KKT conditions for every realization of ψ for this problem are listed below:

$$0 \leqslant s_{1A}^{\psi} \perp C_1 - a_A + b_A(s_{1A}^{\psi} + s_{2A}^{\psi} + s_{4A}^{inc,\psi} - s_{4A}^{dec,\psi} - m^{\psi}) + b_A s_{1A}^{\psi} + \mu_1^{\psi} \geqslant 0\,, \tag{2.41a}$$

$$0 \leqslant s_{1B}^{\psi} \perp C_1 - a_B^{\psi} + b_B(s_{1B}^{\psi} + s_{2B}^{\psi} + s_{4B}^{inc,\psi} - s_{4B}^{dec,\psi} + m^{\psi}) + w_{AB}^{\psi} + b_B s_{1B}^{\psi} + \mu_1^{\psi} \geqslant 0\,, \tag{2.41b}$$

$$0 \leqslant \mu_1^{\psi} \perp K_1 - s_{1A}^{\psi} - s_{1B}^{\psi} \geqslant 0\,, \tag{2.41c}$$

$$0 \leqslant s_{2A}^{\psi} \perp C_2 - a_A + b_A(s_{1A}^{\psi} + s_{2A}^{\psi} + s_{4A}^{inc,\psi} - s_{4A}^{dec,\psi} - m^{\psi}) - w_{AB}^{\psi} + b_A s_{2A}^{\psi} - \Pr(\Omega_a)(C_2 - C_1) + \mu_2^{\psi} \geqslant 0\,, \tag{2.41d}$$

$$0 \leqslant s_{2B}^{\psi} \perp C_2 - a_B^{\psi} + b_B(s_{1B}^{\psi} + s_{2B}^{\psi} + s_{4B}^{inc,\psi} - s_{4B}^{dec,\psi} + m^{\psi}) + b_B s_{2B}^{\psi} - \Pr(\Omega_a)(C_2 - C_1) + \mu_2^{\psi} \geqslant 0\,, \tag{2.41e}$$

$$0 \leqslant \mu_2^{\psi} \perp K_2 - s_{2A}^{\psi} - s_{2B}^{\psi} \geqslant 0\,, \tag{2.41f}$$

$$w_{AB}^{\psi} - \lambda_{AB}^{\psi} + \lambda_{BA}^{\psi} = 0\,, \tag{2.41g}$$

$$p_B^{\psi} - p_A^{\psi} - \lambda_{AB}^{\psi} + \lambda_{BA}^{\psi} = 0\,, \tag{2.41h}$$

$$0 \leqslant \lambda_{AB}^{\psi} \perp T_{AB} - y_{AB}^{\psi} - m^{\psi} \geqslant 0\,, \tag{2.41i}$$

$$0 \leqslant \lambda_{BA}^{\psi} \perp T_{AB} + y_{AB}^{\psi} + m^{\psi} \geqslant 0\,, \tag{2.41j}$$

$$p_A^{\psi} = a_A - b_A(s_{1A}^{\psi} + s_{2A}^{\psi} + s_{4A}^{inc,\psi} - s_{4A}^{dec,\psi} - m^{\psi})\,, \tag{2.41k}$$

$$p_B^{\psi} = a_B^{\psi} - b_B(s_{1B}^{\psi} + s_{2B}^{\psi} + s_{4B}^{inc,\psi} - s_{4B}^{dec,\psi} + m^{\psi})\,, \tag{2.41l}$$

$$y_{AB}^{\psi} = s_{1B}^{\psi} - s_{2A}^{\psi}\,, \tag{2.41m}$$

$$0 \leqslant s_{4A}^{inc,\psi} \perp - a_A + b_A(s_{1A}^{\psi} + s_{2A}^{\psi} + s_{4A}^{inc,\psi} - s_{4A}^{dec,\psi} - m^{\psi}) + C_1 + b_A s_{4A}^{inc,\psi} - b_A s_{4A}^{dec,\psi} + \theta_4^{\psi} R_A \geqslant 0\,, \tag{2.41n}$$

$$0 \leqslant s_{4A}^{dec,\psi} \perp - C_1 + a_A - b_A(s_{1A}^{\psi} + s_{2A}^{\psi} + s_{4A}^{inc,\psi} - s_{4A}^{dec,\psi} - m^{\psi}) + b_A s_{4A}^{dec,\psi} - b_A s_{4A}^{inc,\psi} + \theta_4^{\psi} R_A \geqslant 0\,, \tag{2.41o}$$

$$0 \leqslant s_{4B}^{inc,\psi} \perp - a_B^{\psi} + b_B(s_{1B}^{\psi} + s_{2B}^{\psi} + s_{4B}^{inc,\psi} - s_{4B}^{dec,\psi} + m^{\psi}) + (\Pr(\Omega_a)C_1 + \Pr(\Omega_b)C_2) + b_B s_{4B}^{inc,\psi} - b_B s_{4B}^{dec,\psi} + \theta_4^{\psi} R_B \geqslant 0\,, \tag{2.41p}$$

$$0 \leqslant s_{4B}^{dec,\psi} \perp - (\Pr(\Omega_a)C_1 + \Pr(\Omega_b)C_2) + a_B^{\psi} - b_B(s_{1B}^{\psi} + s_{2B}^{\psi} + s_{4B}^{inc,\psi} - s_{4B}^{dec,\psi} + m^{\psi}) + b_B s_{4B}^{dec,\psi} - b_B s_{4B}^{inc,\psi} + \theta_4^{\psi} R_B \geqslant 0\,, \tag{2.41q}$$

$$0 \leqslant \theta_4^{\psi} \perp S_4 - R_A s_{4A}^{inc,\psi} - R_B s_{4B}^{inc,\psi} - R_A s_{4A}^{dec,\psi} - R_B s_{4B}^{dec,\psi} \geqslant 0\,, \tag{2.41r}$$

Because of the removal of the FTR stage, the structure of this game is changed from a MPEC to a Mixed Complementarity Problem (MCP).

2.3.2.6 Case 6 (Benchmark): Two Cournot Generators, Two Cournot Traders (without FTR)

In Case 6, we remove the FTR position from Trader 3. Trader 3's formulation is modified as follows:

$$\underset{s_{3A}^{inc,\psi},s_{3A}^{dec,\psi},s_{3B}^{inc,\psi},s_{3B}^{dec,\psi}}{\text{maximize}} \quad \mathbb{E}[(p_A^\psi(d_A^\psi) - p_A^\omega)s_{3A}^{inc,\psi} + (p_B^\psi(d_B^\psi) - p_B^\omega)s_{3B}^{inc,\psi} + (p_A^\omega - p_A^\psi(d_A^\psi))s_{3A}^{dec,\psi} + (p_B^\omega - p_B^\psi(d_B^\psi))s_{3B}^{dec,\psi}] \tag{2.42a}$$

$$\text{subject to} \quad s_{3A}^{inc,\psi} \geqslant 0\,, \tag{2.42b}$$

$$s_{3A}^{dec,\psi} \geqslant 0\,, \tag{2.42c}$$

$$s_{3B}^{inc,\psi} \geqslant 0\,, \tag{2.42d}$$

$$s_{3B}^{dec,\psi} \geqslant 0\,, \tag{2.42e}$$

$$R_A s_{3A}^{inc,\psi} + R_A s_{3A}^{dec,\psi} + R_B s_{3B}^{inc,\psi} + R_B s_{3B}^{dec,\psi} \leqslant S_3\,,\ (\theta_3^\psi) \tag{2.42f}$$

The KKT conditions for every realization of ψ for this case is listed below:

$$0 \leqslant s_{1A}^\psi \perp C_1 - a_A + b_A(s_{1A}^\psi + s_{2A}^\psi + s_{3A}^{inc,\psi} + s_{4A}^{inc,\psi} - s_{3A}^{dec,\psi} - s_{4A}^{dec,\psi} - m^\psi) + b_A s_{1A}^\psi + \mu_1^\psi \geqslant 0\,, \tag{2.43a}$$

$$0 \leqslant s_{1B}^\psi \perp C_1 - a_B^\psi + b_B(s_{1B}^\psi + s_{2B}^\psi + s_{3B}^{inc,\psi} + s_{4B}^{inc,\psi} - s_{3B}^{dec,\psi} - s_{4B}^{dec,\psi} + m^\psi) + w_{AB}^\psi + b_B s_{1B}^\psi + \mu_1^\psi \geqslant 0\,, \tag{2.43b}$$

$$0 \leqslant \mu_1^\psi \perp K_1 - s_{1A}^\psi - s_{1B}^\psi \geqslant 0\,, \tag{2.43c}$$

$$0 \leqslant s_{2A}^\psi \perp C_2 - a_A + b_A(s_{1A}^\psi + s_{2A}^\psi + s_{3A}^{inc,\psi} + s_{4A}^{inc,\psi} - s_{3A}^{dec,\psi} - s_{4A}^{dec,\psi} - m^\psi) - w_{AB}^\psi + b_A s_{2A}^\psi - \Pr(\Omega_a)(C_2 - C_1) + \mu_2^\psi \geqslant 0\,, \tag{2.43d}$$

$$0 \leqslant s_{2B}^\psi \perp C_2 - a_B^\psi + b_B(s_{1B}^\psi + s_{2B}^\psi + s_{3B}^{inc,\psi} + s_{4B}^{inc,\psi} - s_{3B}^{dec,\psi} - s_{4B}^{dec,\psi} + m^\psi) + b_B s_{2B}^\psi - \Pr(\Omega_a)(C_2 - C_1) + \mu_2^\psi \geqslant 0\,, \tag{2.43e}$$

$$0 \leqslant \mu_2^\psi \perp K_2 - s_{2A}^\psi - s_{2B}^\psi \geqslant 0\,, \tag{2.43f}$$

$$w_{AB}^\psi - \lambda_{AB}^\psi + \lambda_{BA}^\psi = 0\,, \tag{2.43g}$$

$$p_B^\psi - p_A^\psi - \lambda_{AB}^\psi + \lambda_{BA}^\psi = 0\,, \tag{2.43h}$$

$$0 \leqslant \lambda^{\psi}_{AB} \perp T_{AB} - y^{\psi}_{AB} - m^{\psi} \geqslant 0\,, \tag{2.43i}$$

$$0 \leqslant \lambda^{\psi}_{BA} \perp T_{AB} + y^{\psi}_{AB} + m^{\psi} \geqslant 0\,, \tag{2.43j}$$

$$p^{\psi}_{A} = a_A - b_A(s^{\psi}_{1A} + s^{\psi}_{2A} + s^{inc,\psi}_{3A} + s^{inc,\psi}_{4A} - s^{dec,\psi}_{3A} - s^{dec,\psi}_{4A} - m^{\psi})\,, \tag{2.43k}$$

$$p^{\psi}_{B} = a^{\psi}_{B} - b_B(s^{\psi}_{1B} + s^{\psi}_{2B} + s^{inc,\psi}_{3B} + s^{inc,\psi}_{4B} - s^{dec,\psi}_{3B} - s^{dec,\psi}_{4B} + m^{\psi})\,, \tag{2.43l}$$

$$y^{\psi}_{AB} = s^{\psi}_{1B} - s^{\psi}_{2A}\,, \tag{2.43m}$$

$$\begin{aligned} 0 \leqslant\ & s^{inc,\psi}_{3A} \perp - a_A + b_A(s^{\psi}_{1A} + s^{\psi}_{2A} + s^{inc,\psi}_{3A} + s^{inc,\psi}_{4A} - s^{dec,\psi}_{3A} - s^{dec,\psi}_{4A} - m^{\psi}) \\ & + C_1 + b_A s^{inc,\psi}_{3A} - b_A s^{dec,\psi}_{3A} + \theta^{\psi}_{3} R_A \geqslant 0\,, \end{aligned} \tag{2.43n}$$

$$\begin{aligned} 0 \leqslant\ & s^{dec,\psi}_{3A} \perp - C_1 + a_A - b_A(s^{\psi}_{1A} + s^{\psi}_{2A} + s^{inc,\psi}_{3A} + s^{inc,\psi}_{4A} - s^{dec,\psi}_{3A} - s^{dec,\psi}_{4A} - m^{\psi}) \\ & + b_A s^{dec,\psi}_{3A} - b_A s^{inc,\psi}_{3A} + \theta^{\psi}_{3} R_A \geqslant 0\,, \end{aligned} \tag{2.43o}$$

$$\begin{aligned} 0 \leqslant\ & s^{inc,\psi}_{3B} \perp - a^{\psi}_{B} + b_B(s^{\psi}_{1B} + s^{\psi}_{2B} + s^{inc,\psi}_{3B} + s^{inc,\psi}_{4B} - s^{dec,\psi}_{3B} - s^{dec,\psi}_{4B} + m^{\psi}) \\ & + (\Pr(\Omega_a)C_1 + \Pr(\Omega_b)C_2) + b_B s^{inc,\psi}_{3B} - b_B s^{dec,\psi}_{3B} + \theta^{\psi}_{3} R_B \geqslant 0\,, \end{aligned} \tag{2.43p}$$

$$\begin{aligned} 0 \leqslant\ & s^{dec,\psi}_{3B} \perp a^{\psi}_{B} - b_B(s^{\psi}_{1B} + s^{\psi}_{2B} + s^{inc,\psi}_{3B} + s^{inc,\psi}_{4B} - s^{dec,\psi}_{3B} - s^{dec,\psi}_{4B} + m^{\psi}) \\ & - (\Pr(\Omega_a)C_1 + \Pr(\Omega_b)C_2) + b_B s^{dec,\psi}_{3B} - b_B s^{inc,\psi}_{3B} + \theta^{\psi}_{3} R_B \geqslant 0\,, \end{aligned} \tag{2.43q}$$

$$0 \leqslant \theta^{\psi}_{3} \perp S_3 - R_A s^{inc,\psi}_{3A} - R_B s^{inc,\psi}_{3B} - R_A s^{dec,\psi}_{3A} - R_B s^{dec,\psi}_{3B} \geqslant 0\,, \tag{2.43r}$$

$$\begin{aligned} 0 \leqslant\ & s^{inc,\psi}_{4A} \perp - a_A + b_A(s^{\psi}_{1A} + s^{\psi}_{2A} + s^{inc,\psi}_{3A} + s^{inc,\psi}_{4A} - s^{dec,\psi}_{3A} - s^{dec,\psi}_{4A} - m^{,\psi}) \\ & + C_1 + b_A s^{inc,\psi}_{4A} - b_A s^{dec,\psi}_{4A} + \theta^{\psi}_{4} R_A \geqslant 0\,, \end{aligned} \tag{2.43s}$$

$$\begin{aligned} 0 \leqslant\ & s^{dec,\psi}_{4A} \perp - C_1 + a_A - b_A(s^{\psi}_{1A} + s^{\psi}_{2A} + s^{inc,\psi}_{3A} + s^{inc,\psi}_{4A} - s^{dec,\psi}_{3A} - s^{dec,\psi}_{4A} - m^{\psi}) \\ & + b_A s^{dec,\psi}_{4A} - b_A s^{inc,\psi}_{4A} + \theta^{\psi}_{4} R_A \geqslant 0\,, \end{aligned} \tag{2.43t}$$

$$\begin{aligned} 0 \leqslant\ & s^{inc,\psi}_{4B} \perp - a^{\psi}_{B} + b_B(s^{\psi}_{1B} + s^{\psi}_{2B} + s^{inc,\psi}_{3B} + s^{inc,\psi}_{4B} - s^{dec,\psi}_{3B} - s^{dec,\psi}_{4B} + m^{\psi}) \\ & + (P(\Omega_a)C_1 + P(\Omega_b)C_2) + b_B s^{inc,\psi}_{4B} - b_B s^{dec,\psi}_{4B} + \theta^{\psi}_{4} R_B \geqslant 0\,, \end{aligned} \tag{2.43u}$$

$$\begin{aligned} 0 \leqslant\ & s^{dec,\psi}_{4B} \perp a^{\psi}_{B} - b_B(s^{\psi}_{1B} + s^{\psi}_{2B} + s^{inc,\psi}_{3B} + s^{inc,\psi}_{4B} - s^{dec,\psi}_{3B} - s^{dec,\psi}_{4B} + m^{\psi}) \\ & - (\Pr(\Omega_a)C_1 + \Pr(\Omega_b)C_2) + b_B s^{dec,\psi}_{4B} - b_B s^{inc,\psi}_{4B} + \theta^{\psi}_{4} R_B \geqslant 0\,, \end{aligned} \tag{2.43v}$$

$$0 \leqslant \theta^{\psi}_{4} \perp S_4 - R_A s^{inc,\psi}_{4A} - R_B s^{inc,\psi}_{4B} - R_A s^{dec,\psi}_{4A} - R_B s^{dec,\psi}_{4B} \geqslant 0\,, \tag{2.43w}$$

Similar to Case 5, Case 6 is also a Mixed Complementarity Problem (MCP).

2.3.2.7 Case 7 (Benchmark): Two Cournot Generators, Two Competitive Traders (One with FTR)

In Case 7, we assume both generators behave à la Cournot, while both financial traders behave competitively. This problem formulation is as follows:

- Demand at Node A

$$p_A^\psi = p_A^\psi(d_A^\psi) = a_A - b_A(s_{1A}^\psi + s_{2A}^\psi + s_{3A}^{inc,\psi} + s_{4A}^{inc,\psi} - s_{3A}^{dec,\psi} - s_{4A}^{dec,\psi} - m^\psi) \tag{2.44a}$$

- Demand at Node B

$$p_B^\psi = p_B^\psi(d_B^\psi) = a_B^\psi - b_B(s_{1B}^\psi + s_{2B}^\psi + s_{3B}^{inc,\psi} + s_{4B}^{inc,\psi} - s_{3B}^{dec,\psi} - s_{4B}^{dec,\psi} + m^\psi) \tag{2.45a}$$

- Generator 1

$$\begin{aligned}
\underset{s_{1A}^\psi, s_{1B}^\psi}{\text{maximize}} \quad & \mathbb{E}[p_A^\omega s_{1A}^\omega + (p_B^\omega - w_{AB}^\omega)s_{1B}^\omega + p_A^\psi(d_A^\psi)s_{1A}^\psi + (p_B^\psi(d_B^\psi) - w_{AB}^\psi)s_{1B}^\psi \\
& - C_1(s_{1A}^\omega + s_{1B}^\omega + s_{1A}^\psi + s_{1B}^\psi)] && (2.46a) \\
\text{subject to} \quad & s_{1A}^\psi + s_{1B}^\psi \leqslant K_1\,,\ (\mu_1^\psi) && (2.46b) \\
& s_{1A}^\psi \geqslant 0\,, && (2.46c) \\
& s_{1B}^\psi \geqslant 0\,, && (2.46d)
\end{aligned}$$

- Generator 2

$$\begin{aligned}
\underset{s_{2A}^\psi, s_{2B}^\psi}{\text{maximize}} \quad & \mathbb{E}[(p_A^\omega + w_{AB}^\omega)s_{2A}^\omega + p_B^\omega s_{2B}^\omega + (p_A^\psi(d_A^\psi) + w_{AB}^\psi)s_{2A}^\psi + p_B^\psi(d_B^\psi)s_{2B}^\psi \\
& - C_2(s_{2A}^\omega + s_{2B}^\omega + s_{2A}^\psi + s_{2B}^\psi)] && (2.47a) \\
\text{subject to} \quad & s_{2A}^\psi + s_{2B}^\psi \leqslant K_2\,,\ (\mu_2^\psi) && (2.47b) \\
& s_{2A}^\psi \geqslant 0\,, && (2.47c) \\
& s_{2B}^\psi \geqslant 0\,, && (2.47d)
\end{aligned}$$

- Financial Trader 3

$$\begin{aligned}
\underset{s_{3A}^{inc,\psi}, s_{3A}^{dec,\psi}, s_{3B}^{inc,\psi}, s_{3B}^{dec,\psi}}{\text{maximize}} \quad & \mathbb{E}[(p_A^\psi - p_A^\omega)s_{3A}^{inc,\psi} + (p_B^\psi - p_B^\omega)s_{3B}^{inc,\psi} \\
& + (p_A^\omega - p_A^\psi)s_{3A}^{dec,\psi} + (p_B^\omega - p_B^\psi)s_{3B}^{dec,\psi} && (2.48a) \\
& + f_{3AB}(p_B^\psi - p_A^\psi - (c_f/2, 160))]
\end{aligned}$$

$$\text{subject to} \quad s_{3A}^{inc,\psi} \geqslant 0\,, \tag{2.48b}$$
$$s_{3A}^{dec,\psi} \geqslant 0\,, \tag{2.48c}$$
$$s_{3B}^{inc,\psi} \geqslant 0\,, \tag{2.48d}$$
$$s_{3B}^{dec,\psi} \geqslant 0\,, \tag{2.48e}$$
$$R_A s_{3A}^{inc,\psi} + R_A s_{3A}^{dec,\psi} + R_B s_{3B}^{inc,\psi} + R_B s_{3B}^{dec,\psi} \leqslant S_3\,,\ (\theta_3^{\psi}) \tag{2.48f}$$

- Financial Trader 4

$$\underset{s_{4A}^{inc,\psi}, s_{4A}^{dec,\psi}, s_{4B}^{inc,\psi}, s_{4B}^{dec,\psi}}{\text{maximize}} \quad \begin{aligned}&\mathbb{E}[(p_A^{\psi} - p_A^{\omega}) s_{4A}^{inc,\psi} + (p_B^{\psi} - p_B^{\omega}) s_{4B}^{inc,\psi} \\ &+ (p_A^{\omega} - p_A^{\psi}) s_{4A}^{dec,\psi} + (p_B^{\omega} - p_B^{\psi}) s_{4B}^{dec,\psi}]\end{aligned} \tag{2.49a}$$
$$\text{subject to} \quad s_{4A}^{inc,\psi} \geqslant 0\,, \tag{2.49b}$$
$$s_{4A}^{dec,\psi} \geqslant 0\,, \tag{2.49c}$$
$$s_{4B}^{inc,\psi} \geqslant 0\,, \tag{2.49d}$$
$$s_{4B}^{dec,\psi} \geqslant 0\,, \tag{2.49e}$$
$$R_A s_{4A}^{inc,\psi} + R_A s_{4A}^{dec,\psi} + R_B s_{4B}^{inc,\psi} + R_B s_{4B}^{dec,\psi} \leqslant S_4\,,\ (\theta_4^{\psi}) \tag{2.49f}$$

- ISO

$$\underset{y_{AB}^{\psi}, m^{\psi}}{\text{maximize}} \quad w_{AB}^{\psi} y_{AB}^{\psi} + (p_B^{\psi} - p_A^{\psi}) m^{\psi} \tag{2.50a}$$
$$\text{subject to} \quad y_{AB}^{\psi} + m^{\psi} \leqslant T_{AB}\,,\ (\lambda_{AB}^{\psi}) \tag{2.50b}$$
$$y_{AB}^{\psi} + m^{\psi} \geqslant -T_{AB}\,,\ (\lambda_{BA}^{\psi}) \tag{2.50c}$$

- Market clearing

$$y_{AB}^{\psi} = s_{1B}^{\psi} - s_{2A}^{\psi} \tag{2.51a}$$

The KKT conditions for every realization of ψ in this case is listed below:

$$\begin{aligned}&0 \leqslant s_{1A}^{\psi} \perp C_1 - a_A + b_A(s_{1A}^{\psi} + s_{2A}^{\psi} + s_{3A}^{inc,\psi} + s_{4A}^{inc,\psi} - s_{3A}^{dec,\psi} - s_{4A}^{dec,\psi} - m^{\psi}) \\ &+ b_A s_{1A}^{\psi} + \mu_1^{\psi} \geqslant 0\,,\end{aligned} \tag{2.52a}$$
$$0 \leqslant s_{1B}^{\psi} \perp C_1 - a_B^{\psi} + b_B(s_{1B}^{\psi} + s_{2B}^{\psi} + s_{3B}^{inc,\psi} + s_{4B}^{inc,\psi} - s_{3B}^{dec,\psi} - s_{4B}^{dec,\psi} + m^{\psi})$$

$$+ w^{\psi}_{AB} + b_B s^{\psi}_{1B} + \mu^{\psi}_1 \geqslant 0\,, \tag{2.52b}$$

$$0 \leqslant \mu^{\psi}_1 \perp K_1 - s^{\psi}_{1A} - s^{\psi}_{1B} \geqslant 0\,, \tag{2.52c}$$

$$0 \leqslant s^{\psi}_{2A} \perp C_2 - a_A + b_A(s^{\psi}_{1A} + s^{\psi}_{2A} + s^{inc,\psi}_{3A} + s^{inc,\psi}_{4A} - s^{dec,\psi}_{3A} - s^{dec,\psi}_{4A} - m^{\psi})$$
$$- w^{\psi}_{AB} + b_A s^{\psi}_{2A} - \Pr(\Omega_a)(C_2 - C_1) + \mu^{\psi}_2 \geqslant 0\,, \tag{2.52d}$$

$$0 \leqslant s^{\psi}_{2B} \perp C_2 - a^{\psi}_B + b_B(s^{\psi}_{1B} + s^{\psi}_{2B} + s^{inc,\psi}_{3B} + s^{inc,\psi}_{4B} - s^{dec,\psi}_{3B} - s^{dec,\psi}_{4B} + m^{\psi})$$
$$+ b_B s^{\psi}_{2B} - \Pr(\Omega_a)(C_2 - C_1) + \mu^{\psi}_2 \geqslant 0\,, \tag{2.52e}$$

$$0 \leqslant \mu^{\psi}_2 \perp K_2 - s^{\psi}_{2A} - s^{\psi}_{2B} \geqslant 0\,, \tag{2.52f}$$

$$w^{\psi}_{AB} - \lambda^{\psi}_{AB} + \lambda^{\psi}_{BA} = 0\,, \tag{2.52g}$$

$$p^{\psi}_B - p^{\psi}_A - \lambda^{\psi}_{AB} + \lambda^{\psi}_{BA} = 0\,, \tag{2.52h}$$

$$0 \leqslant \lambda^{\psi}_{AB} \perp T_{AB} - y^{\psi}_{AB} - m^{\psi} \geqslant 0\,, \tag{2.52i}$$

$$0 \leqslant \lambda^{\psi}_{BA} \perp T_{AB} + y^{\psi}_{AB} + m^{\psi} \geqslant 0\,, \tag{2.52j}$$

$$p^{\psi}_A = a_A - b_A(s^{\psi}_{1A} + s^{\psi}_{2A} + s^{inc,\psi}_{3A} + s^{inc,\psi}_{4A} - s^{dec,\psi}_{3A} - s^{dec,\psi}_{4A} - m^{\psi})\,, \tag{2.52k}$$

$$p^{\psi}_B = a^{\psi}_B - b_B(s^{\psi}_{1B} + s^{\psi}_{2B} + s^{inc,\psi}_{3B} + s^{inc,\psi}_{4B} - s^{dec,\psi}_{3B} - s^{dec,\psi}_{4B} + m^{\psi})\,, \tag{2.52l}$$

$$y^{\psi}_{AB} = s^{\psi}_{1B} - s^{\psi}_{2A}\,, \tag{2.52m}$$

$$0 \leqslant s^{inc,\psi}_{3A} \perp - p^{\psi}_A + C_1 + \theta^{\psi}_3 R_A \geqslant 0\,, \tag{2.52n}$$

$$0 \leqslant s^{dec,\psi}_{3A} \perp - C_1 + p^{\psi}_A + \theta^{\psi}_3 R_A \geqslant 0\,, \tag{2.52o}$$

$$0 \leqslant s^{inc,\psi}_{3B} \perp - p^{\psi}_B + (\Pr(\Omega_a)C_1 + \Pr(\Omega_b)C_2) + \theta^{\psi}_3 R_B \geqslant 0\,, \tag{2.52p}$$

$$0 \leqslant s^{dec,\psi}_{3B} \perp - (\Pr(\Omega_a)C_1 + \Pr(\Omega_b)C_2) + p^{\psi}_B + \theta^{\psi}_3 R_B \geqslant 0\,, \tag{2.52q}$$

$$0 \leqslant \theta^{\psi}_3 \perp S_3 - R_A s^{inc,\psi}_{3A} - R_B s^{inc,\psi}_{3B} - R_A s^{dec,\psi}_{3A} - R_B s^{dec,\psi}_{3B} \geqslant 0\,, \tag{2.52r}$$

$$0 \leqslant s^{inc,\psi}_{4A} \perp - p^{\psi}_A + C_1 + \theta^{\psi}_4 R_A \geqslant 0\,, \tag{2.52s}$$

$$0 \leqslant s^{dec,\psi}_{4A} \perp - C_1 + p^{\psi}_A + \theta^{\psi}_4 R_A \geqslant 0\,, \tag{2.52t}$$

$$0 \leqslant s^{inc,\psi}_{4B} \perp - p^{\psi}_B + (\Pr(\Omega_a)C_1 + \Pr(\Omega_b)C_2) + \theta^{\psi}_4 R_B \geqslant 0\,, \tag{2.52u}$$

$$0 \leqslant s^{dec,\psi}_{4B} \perp - (\Pr(\Omega_a)C_1 + \Pr(\Omega_b)C_2) + p^{\psi}_B + \theta^{\psi}_4 R_B \geqslant 0\,, \tag{2.52v}$$

$$0 \leqslant \theta^{\psi}_4 \perp S_4 - R_A s^{inc,\psi}_{4A} - R_B s^{inc,\psi}_{4B} - R_A s^{dec,\psi}_{4A} - R_B s^{dec,\psi}_{4B} \geqslant 0\,, \tag{2.52w}$$

In the upper level, financial trader is choosing its FTR position to maximize

profit. The financial trader's problem is formulated below:

$$\underset{f_{3AB},s^{\psi}_{ji},m^{\psi},\mu^{\psi}_{j},\eta^{\psi}_{j},\zeta^{\psi}_{j},w^{\psi}_{AB},\lambda^{\psi}_{AB},\lambda^{\psi}_{BA},p^{\psi}_{j},y^{\psi}_{AB},s^{inc,\psi}_{3A},s^{dec,\psi}_{3A},s^{inc,\psi}_{3B},s^{dec,\psi}_{3B},s^{inc,\psi}_{4A},s^{dec,\psi}_{4A},s^{inc,\psi}_{4B},s^{dec,\psi}_{4B},\theta^{\psi}_{3},\theta^{\psi}_{4},\epsilon}{\text{maximize}}$$
$$\begin{aligned}&\mathbb{E}_{\psi,\omega}[(p^{\psi}_{A}-p^{\omega}_{A})s^{inc,\psi}_{3A}+(p^{\psi}_{B}-p^{\omega}_{B})s^{inc,\psi}_{3B}\\&+(p^{\omega}_{A}-p^{\psi}_{A})s^{dec,\psi}_{3A}+(p^{\omega}_{B}-p^{\psi}_{B})s^{dec,\psi}_{3B}+f_{3AB}(p^{\psi}_{B}-p^{\psi}_{A}-(c_f/2,160))]\end{aligned} \tag{2.53a}$$

subject to:

- FTR Position Limit

$$-T_{AB}\leqslant f_{3AB}\leqslant T_{AB}\,, \tag{2.54}$$

- KKT conditions of the DA problem

The variables $(s^{\psi}_{ji}, m^{\psi}, \mu^{\psi}_{j}, \eta^{\psi}_{j}, \zeta^{\psi}_{j}, w^{\psi}_{AB}, \lambda^{\psi}_{AB}, \lambda^{\psi}_{BA}, p^{\psi}_{j}, y^{\psi}_{AB}, s^{inc,\psi}_{3A}, s^{dec,\psi}_{3A}, s^{inc,\psi}_{3B}, s^{dec,\psi}_{3B}, s^{inc,\psi}_{4A}, s^{dec,\psi}_{4A}, s^{inc,\psi}_{4B}, s^{dec,\psi}_{4B}, \theta^{\psi}_{3}, \theta^{\psi}_{4})$ represent a solution to the lower-level day-ahead problem, and solve its associated KKT system as in Equations 2.52.

2.3.2.8 Case 8: Two Cournot Generators, Two Cournot Traders with FTRs

In this last case, we assume both financial traders have access to FTR. The day-ahead model formulation is the same as Case 3 except for Trader 4's problem. Trader 4's problem now becomes:

- Financial Trader 4

$$\begin{aligned}\underset{s^{inc,\psi}_{4A},s^{dec,\psi}_{4A},s^{inc,\psi}_{4B},s^{dec,\psi}_{4B}}{\text{maximize}}\quad&\mathbb{E}[(p^{\psi}_{A}(d^{\psi}_{A})-p^{\omega}_{A})s^{inc,\psi}_{4A}+(p^{\psi}_{B}(d^{\psi}_{B})-p^{\omega}_{B})s^{inc,\psi}_{4B}\\&+(p^{\omega}_{A}-p^{\psi}_{A}(d^{\psi}_{A}))s^{dec,\psi}_{4A}+(p^{\omega}_{B}-p^{\psi}_{B}(d^{\psi}_{B}))s^{dec,\psi}_{4B}\\&+f_{4AB}(p^{\psi}_{B}(d^{\psi}_{B})-p^{\psi}_{A}(d^{\psi}_{A})-(c_f/2,160))]\end{aligned} \tag{2.55a}$$

$$\text{subject to}\quad s^{inc,\psi}_{4A}\geqslant 0\,, \tag{2.55b}$$

$$s^{dec,\psi}_{4A}\geqslant 0\,, \tag{2.55c}$$

$$s^{inc,\psi}_{4B}\geqslant 0\,, \tag{2.55d}$$

$$s_{4B}^{dec,\psi} \geqslant 0\,, \tag{2.55e}$$
$$R_A s_{4A}^{inc,\psi} + R_A s_{4A}^{dec,\psi} + R_B s_{4B}^{inc,\psi} + R_B s_{4B}^{dec,\psi} \leqslant S_4\,,\ (\theta_4^{\psi}) \tag{2.55f}$$

The KKT conditions for Trader 4's day-ahead problem are listed below:

$$\begin{aligned} &0 \leqslant s_{4A}^{inc,\psi} \perp -a_A + b_A(s_{1A}^{\psi} + s_{2A}^{\psi} + s_{3A}^{inc,\psi} + s_{4A}^{inc,\psi} - s_{3A}^{dec,\psi} - s_{4A}^{dec,\psi} - m^{\psi}) \\ &+ C_1 + b_A s_{4A}^{inc,\psi} - b_A s_{4A}^{dec,\psi} - f_{4AB} b_A + \theta_4^{\psi} R_A \geqslant 0\,, \end{aligned} \tag{2.56a}$$
$$\begin{aligned} &0 \leqslant s_{4A}^{dec,\psi} \perp -C_1 + a_A - b_A(s_{1A}^{\psi} + s_{2A}^{\psi} + s_{3A}^{inc,\psi} + s_{4A}^{inc,\psi} - s_{3A}^{dec,\psi} - s_{4A}^{dec,\psi} - m^{\psi}) \\ &+ b_A s_{4A}^{dec,\psi} - b_A s_{4A}^{inc,\psi} + f_{4AB} b_A + \theta_4^{\psi} R_A \geqslant 0\,, \end{aligned} \tag{2.56b}$$
$$\begin{aligned} &0 \leqslant s_{4B}^{inc,\psi} \perp -a_B^{\psi} + b_B(s_{1B}^{\psi} + s_{2B}^{\psi} + s_{3B}^{inc,\psi} + s_{4B}^{inc,\psi} - s_{3B}^{dec,\psi} - s_{4B}^{dec,\psi} + m^{\psi}) \\ &+ (\Pr(\Omega_a) C_1 + \Pr(\Omega_b) C_2) + b_B s_{4B}^{inc,\psi} - b_B s_{4B}^{dec,\psi} + f_{4AB} b_B + \theta_4^{\psi} R_B \geqslant 0\,, \end{aligned} \tag{2.56c}$$
$$\begin{aligned} &0 \leqslant s_{4B}^{dec,\psi} \perp a_B^{\psi} - b_B(s_{1B}^{\psi} + s_{2B}^{\psi} + s_{3B}^{inc,\psi} + s_{4B}^{inc,\psi} - s_{3B}^{dec,\psi} - s_{4B}^{dec,\psi} + m^{\psi}) \\ &- (\Pr(\Omega_a) C_1 + \Pr(\Omega_b) C_2) + b_B s_{4B}^{dec,\psi} - b_B s_{4B}^{inc,\psi} - f_{4AB} b_B + \theta_4^{\psi} R_B \geqslant 0\,, \end{aligned} \tag{2.56d}$$
$$0 \leqslant \theta_4^{\psi} \perp S_4 - R_A s_{4A}^{inc,\psi} - R_B s_{4B}^{inc,\psi} - R_A s_{4A}^{dec,\psi} - R_B s_{4B}^{dec,\psi} \geqslant 0\,, \tag{2.56e}$$

In the upper level, the two financial traders choose their FTR positions to maximize profit. Financial trader 3's problem is formulated below:

$$\begin{aligned} &\underset{f_{3AB}, s_{ji}^{\psi}, m^{\psi}, \mu_j^{\psi}, \eta_j^{\psi}, \zeta_j^{\psi}, w_{AB}^{\psi}, \lambda_{AB}^{\psi}, \lambda_{BA}^{\psi}, p_j^{\psi}, y_{AB}^{\psi}, s_{3A}^{inc,\psi}, s_{3A}^{dec,\psi}, s_{3B}^{inc,\psi}, s_{3B}^{dec,\psi}, s_{4A}^{inc,\psi}, s_{4A}^{dec,\psi}, s_{4B}^{inc,\psi}, s_{4B}^{dec,\psi}, \theta_3^{\psi}, \theta_4^{\psi}, \epsilon}{\text{maximize}} \\ &\mathbb{E}_{\psi,\omega}[(p_A^{\psi} - p_A^{\omega}) s_{3A}^{inc,\psi} + (p_B^{\psi} - p_B^{\omega}) s_{3B}^{inc,\psi} \\ &+ (p_A^{\omega} - p_A^{\psi}) s_{3A}^{dec,\psi} + (p_B^{\omega} - p_B^{\psi}) s_{3B}^{dec,\psi} + f_{3AB}(p_B^{\psi} - p_A^{\psi} - (c_f/2, 160))] \end{aligned} \tag{2.57a}$$

Financial trader 4's problem is formulated as follows:

$$\begin{aligned} &\underset{f_{4AB}, s_{ji}^{\psi}, m^{\psi}, \mu_j^{\psi}, \eta_j^{\psi}, \zeta_j^{\psi}, w_{AB}^{\psi}, \lambda_{AB}^{\psi}, \lambda_{BA}^{\psi}, p_j^{\psi}, y_{AB}^{\psi}, s_{3A}^{inc,\psi}, s_{3A}^{dec,\psi}, s_{3B}^{inc,\psi}, s_{3B}^{dec,\psi}, s_{4A}^{inc,\psi}, s_{4A}^{dec,\psi}, s_{4B}^{inc,\psi}, s_{4B}^{dec,\psi}, \theta_3^{\psi}, \theta_4^{\psi}, \epsilon}{\text{maximize}} \\ &\mathbb{E}_{\psi,\omega}[(p_A^{\psi} - p_A^{\omega}) s_{4A}^{inc,\psi} + (p_B^{\psi} - p_B^{\omega}) s_{4B}^{inc,\psi} \\ &+ (p_A^{\omega} - p_A^{\psi}) s_{4A}^{dec,\psi} + (p_B^{\omega} - p_B^{\psi}) s_{4B}^{dec,\psi} + f_{4AB}(p_B^{\psi} - p_A^{\psi} - (c_f/2, 160))] \end{aligned} \tag{2.58a}$$

Both traders' problems are subject to the constraints below:

- FTR Position Limit

$$-T_{AB} \leqslant f_{3AB} + f_{4AB} \leqslant T_{AB}\,, \tag{2.59}$$

- KKT conditions of the DA problem

The variables $(s^{\psi}_{ji}, m^{\psi}, \mu^{\psi}_{j}, \eta^{\psi}_{j}, \zeta^{\psi}_{j}, w^{\psi}_{AB}, \lambda^{\psi}_{AB}, \lambda^{\psi}_{BA}, p^{\psi}_{j}, y^{\psi}_{AB}, s^{inc,\psi}_{3A}, s^{dec,\psi}_{3A}, s^{inc,\psi}_{3B}, s^{dec,\psi}_{3B}, s^{inc,\psi}_{4A}, s^{dec,\psi}_{4A}, s^{inc,\psi}_{4B}, s^{dec,\psi}_{4B}, \theta^{\psi}_{3}, \theta^{\psi}_{4})$ represent a solution to the lower-level day-ahead problem, and solve its associated KKT system as in Equations 2.27, with trader 4's KKT conditions replaced by Equations 2.56. This is an Equilibrium Problem with Equilibrium Constraints as it involves solving two MPECs simultaneously.

2.4 Solution Method and Metrics

We solve the stochastic MPEC (Case 1 to Case 4, and Case 7 to Case 8) and MCP (Case 5 and 6) in GAMS using the sample average approximation method. 100 samples of a^{ψ}_{B} were drawn from a uniform distribution. We start from initial points of all zeros. KNITRO is used to solve the MPEC problems, and PATH is used to solve the MCP problems. Diagonalization is used to solve the EPEC in Case 8.

To understand the impacts of different market behavioral and structural assumptions, we calculate the average procurement cost, market participant profits, consumer surplus as well as social welfare for each case in the following way. Average procurement cost measures the per unit cost of purchasing power, and is obtained by dividing the total expense of purchasing power from both day-ahead and real-time markets, by the total energy consumption at real-time. Profits for generators, financial traders, and ISO are calculated using their objective functions. Day-ahead net consumer surplus at each node is calculated by integrating the day-ahead inverse demand function from zero to total day-ahead demand at that node, subtracting the day-ahead energy cost. If the real-time demand is greater than the day-ahead schedule at one node, we assume that consumers have a constant willingness to pay (WTP) for every megawatt of power they consume in real-time but not bought in day-ahead. Therefore the real-time net consumer surplus at that node is calculated by multiplying the difference between the willingness to pay

and the real-time LMP at that node, to the difference between real-time load and day-ahead schedule at that node. The sum of net day-ahead and real-time consumer surplus is the net consumer surplus at that node (See Figure 2.3). If the real-time demand is less than the day-ahead schedule, we first adjust the net day-ahead consumer surplus by subtracting the net consumer surplus that is not consumed in the real-time. Since the consumers must sell the difference between their day-ahead schedule and real-time consumption at the real-time price, we add the revenue from this sale-back to the adjusted net day-ahead consumer surplus to obtain the net consumer surplus at that node (See Figure 2.4). For cases where Trader 3 has FTR positions, social welfare is calculated by adding up the net consumer surpluses, profits from generators, financial traders and ISO, and subtracting ISO's day-ahead profits (or Trader 3's FTR revenues). This subtraction is necessary to avoid double counting of ISO's day-ahead profits (or Trader 3's FTR revenues) because congestion revenues are the source of the funds to pay FTRs [77]. For Case 5 and 6, where the trader does not have FTR positions, this subtraction is not needed.

Figure 2.3: Consumer Surplus Calculation when Real-time Load is Greater than Day-ahead Load

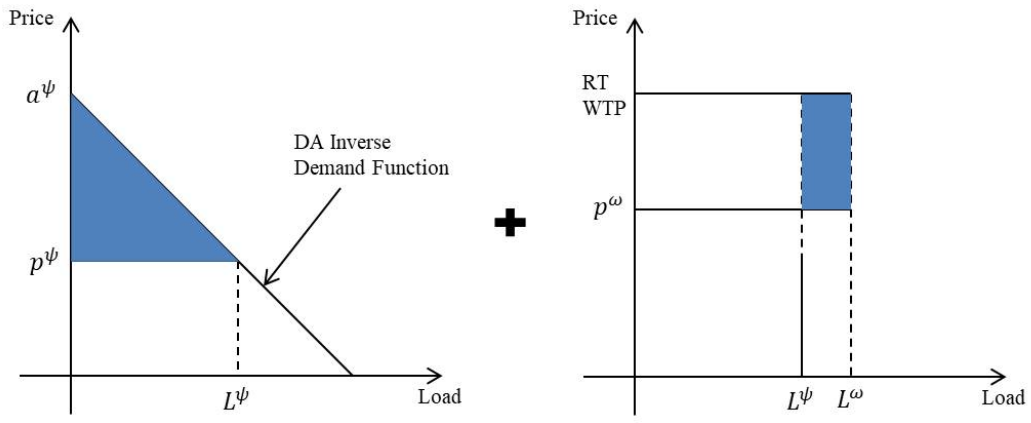

Figure 2.4: Consumer Surplus Calculation when Real-time Load is Less than Day-ahead Load

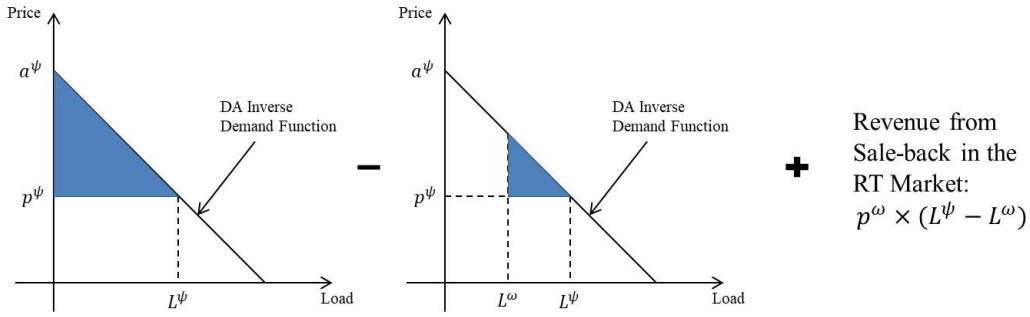

2.5 Results

2.5.1 Short-run MPEC Results

Using parameters in Table 2.4, the simulation results for the short-run base cases are summarized in Table 2.5 and 2.6. Table 2.7 summarizes some of the metrics for each case.

For all the cases where there is an FTR stage, Trader 3 always takes the maximum possible FTR position, which is equal to the capacity of the transmission line. This is because the revenue is always greater than the cost of the FTR for the chosen parameters.

Case 1 is the case where every market participant behaves competitively in the day-ahead market. The result shows that the day-ahead prices at both nodes are equal to their expected real-time levels. Because of this, generators and financial traders make zero profit (except for Trader 3's FTR position). The day-ahead positions placed by each market participant serve to maintain the day-ahead prices at the competitive level, and the numerical solutions to these day-ahead positions are not unique. The competitive case also has the largest consumer surplus and the lowest average procurement cost across all cases.

In Case 2, Trader 3 acts as a Cournot player instead of competitively. The result shows that the day-ahead prices at both nodes are still converging to the expected real-time levels, and neither generators or Trader 4 is bounded by their generation capacities or collateral constraint. This indicates that Trader 3's manipulation attempt would not be successful if other market participants behave competitively

and have enough resources to maintain the day-ahead prices at the competitive levels.

In Case 3, both generators and financial traders act as Cournot players. This raises the day-ahead prices at both nodes above the competitive levels. As a result, consumer surplus at each node is much lower compared to the competitive cases. Despite the fact that the day-ahead price at node B (13.45 $/MWh) is higher than the expected real-time level (12.5 $/MWh), Trader 3 places net virtual demand bids at this node (DEC: 7.55 MW), which yields a negative profit on her virtual position at node B (-$6.04). The reason behind this seemingly counter-intuitive behavior is that, by placing net virtual demand bids at node B, Trader 3 increases the day-ahead price at the sink node of her FTR position, and therefore enhances the value of her FTR. Under the chosen parameters, it is optimal for Trader 3 to lose money on her virtual bids in order to gain larger profits on her FTR positions. This intuition can be better understood when comparing the market outcomes between Case 3 and Case 6 (Benchmark). Case 6 is the scenario where both generators and financial traders behave à la Cournot, yet Trader 3 has no FTR position. In Case 6, Trader 3 is making positive profit ($4.61) by placing net virtual supply offers at node B (INC: 5.85 MW). As a result, we observe a lower day-ahead price at node B in Case 6 (13.08 $/MWh) than that in Case 3 (13.45 $/MWh), and therefore, a higher consumer surplus at that node. For Case 3, Trader 3's uneconomic virtual position at node B further diverges the day-ahead price from its expected real-time level, which is considered an act of price manipulation. At node A, the acquisition of FTR positions gives Trader 3 the incentive to lower the day-ahead price at node A by placing more virtual supply offers at that node (Trader 3 places 42.02 MW of net INC position in Case 3 compared to 28.62 MW of net INC position in Case 6). As a result, day-ahead price at node A is lower in Case 3 (12.50 $/MWh) compared to that in Case 6 (12.86 $/MWh), and consumers at node A is having a larger consumer surplus. Trader 3's net virtual position at node A is not only profitable, but also helping converge the day-ahead price to the expected real-time level at that node. Therefore, Trader 3's behavior at node A is not a act of price manipulation.

In Case 4, we add four more Cournot-type financial traders with smaller budgets and no FTR position to Case 3. In general, more competition will lower the prices at both nodes. However, we observe a drop in day-ahead price from Case 3 to Case 4 only at node A, and the price at node B did not change significantly. This is

because for traders with limited budgets, it is more profitable to acquire virtual supply offers at node A than node B, as the difference between day-ahead price and expected real-time price is higher at node A than that at node B. As a result, consumers at node A enjoy a greater surplus, and the average procurement cost is lower compared to Case 3. It is also worth noting that since the day-ahead price at node A is lowered from Case 3 to Case 4, Trader 3 is having a higher profit from her FTR position and a lower profit from her INC position at node A, resulting in a decrease in her overall profit.

In Case 5 (Benchmark), we remove Trader 3 from Case 6. An immediate effect of lack of Trader 3 is the increase of day-ahead prices at both nodes. In fact, Case 5 has the highest price at each node across all cases, and therefore, the lowest total consumer surplus and highest average procurement cost. This shows the importance of virtual traders in providing liquidity to the market.

In Case 7 (Benchmark), we assume the two generators are Cournot players, and the financial traders behave competitively (including the one with FTR position). Under the chosen parameters, we observe that the Cournot generators are able to push the day-ahead prices at both nodes above the competitive levels to maximize their profits. Not aware of her ability to influence the price at node B through virtual bids, Trader 3 in this case only places virtual supply offers at node A to arbitrage between the day-ahead and expected real-time prices there.

For all the cases where generators behave à la Cournot (Case 3 to Case 7), we observe that each generator's day-ahead sales amounts are the same across both nodes. This is because transmission cost is always equal to the price difference between two nodes, therefore, sales at either nodes results in the same revenues.

2.5.2 Sensitivity Analysis

Figure 2.5 shows the relation between day-ahead price premium at each node and the number of Trader(s) 4 in the Case 4 setting. As the number of Trader(s) 4 increases from 1 to 17, the day-ahead price premium at node A decreases almost linearly from 2.50 $/MWh to 1.31 $/MWh. Meanwhile, the day-ahead price premium at node B does not change significantly as the number of Trader 4 increases. This is because day-ahead price premium at node A presents a better arbitrage opportunity than that at node B. Therefore, Trader(s) 4 would devote most of their resources

in purchasing INCs at node A rather than at node B. Figure 2.6 shows that in the setting of Case 3, Trader 3's loss on her virtual positions at node B becomes larger as the slopes of inverse demand functions increase (from no uneconomic bidding when slopes equal to 0.04 and 0.05, to a loss of 15.59 $ when slope equal to 0.25).

Figure 2.5: Case 4: Day-ahead Price Premium versus Number of Trader(s) 4 (Slope = 0.1)

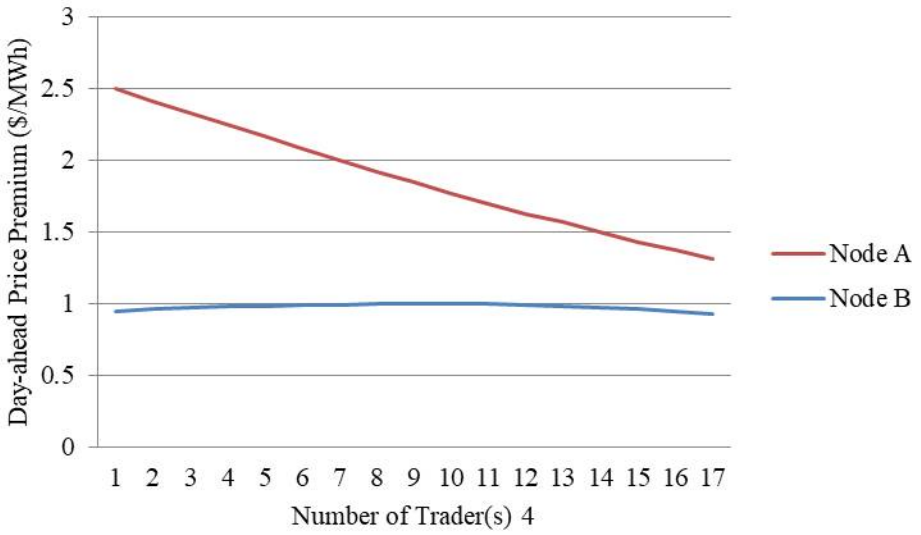

2.5.3 Long-run MPEC Results

Table 2.8 summarizes the hourly long-run results of Case 3 when slopes of the inverse demand functions are random. We assume that in the long-run (a quarter), the slopes of the inverse demand functions can take one of the three numbers (0.05, 0.1 or 0.15) and we assign a probability to each number. The results show that as the day-ahead demand becomes more inelastic, day-ahead price premium (especially at node A) as well as sales from both generators and financial trader 3 decrease (for Trader 3, decrease in sales at node B means an increase in virtual demand bids at that node). Therefore, profits of both generators and financial traders decrease with more inelastic day-ahead demand. Consistent with Figure 2.6, Trader 3's loss on her uneconomic virtual positions at node B also becomes larger as demand becomes more inelastic. Despite the decreased day-ahead price premium, inelastic demand decreases the consumer surplus at both nodes. All of the above contribute to the

Figure 2.6: Case 3: Trader 3's Profit on Virtual Positions at Node B versus Slopes of Inverse Demand Functions

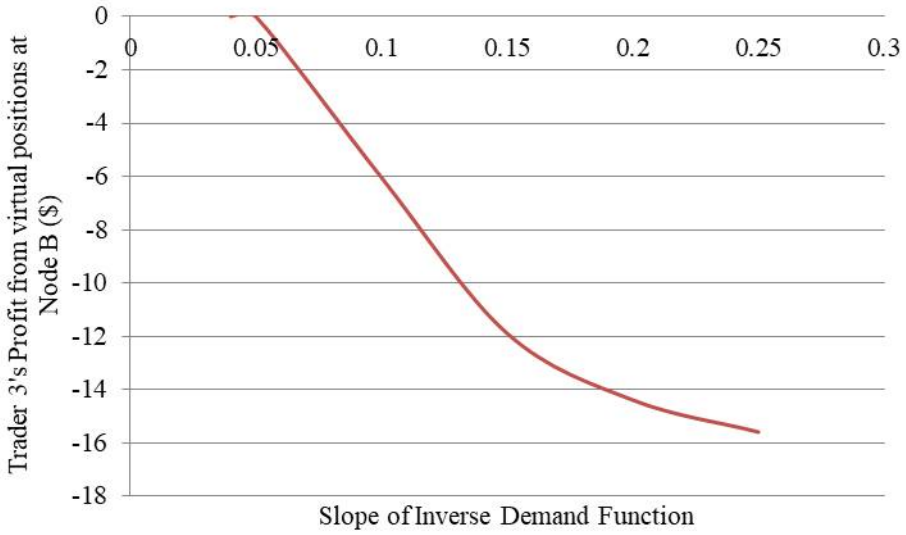

decrease in social welfare as the slopes of inverse demand functions become larger in absolute values. Assuming independence between hours, Table 2.9 amplifies the long-run results to a quarter.

2.5.4 EPEC Results

In this subsection, we discuss the equilibrium results where both strategic financial traders hold FTR contracts. This problem becomes an EPEC. We assume both traders have the same budget with $S_3 = S_4 = 70$, and investigate the equilibrium when the exogenous FTR cost equals \$0 and \$3,000. We start by solving each trader's MPEC problem, assuming the other trader's FTR position is given, and plot her reaction function. Figure 2.7 and 2.8 below show the reaction functions when the FTR cost is \$0 and \$3,000, respectively.

When $c_f = 0$, both traders will take the remaining available FTR position. This results in the overlap of their liner reaction functions, and therefore, a continuum of equilibria.

When $c_f = 3,000$, traders stop acquiring FTR position to its maximum available quantity because of high FTR cost. Take Trader 3 for example: when she believes that Trader 4 is not going to take any FTR position, Trader 3 will only acquire 8.48

MW out of the 20 MW FTR available. As Trader 4's FTR position increases, Trader 3 also has a tendency to increase her FTR position. This is because Trader 4's FTR position now provides an incentive to increase the day-ahead price difference between source and sink nodes. This larger price difference further encourages Trader 3 to acquire more FTR positions. However, this trend will be reversed as the total FTR position is bounded by the capacity of transmission line. This results in a bell-shaped reaction function for each trader. The two reaction functions cross at $f_{3AB} = f_{4AB} = 10$, which is the Nash equilibrium. The EPEC solved by diagonalization also finds this equilibrium point.

Figure 2.7: Reaction Functions when $c_f = 0$

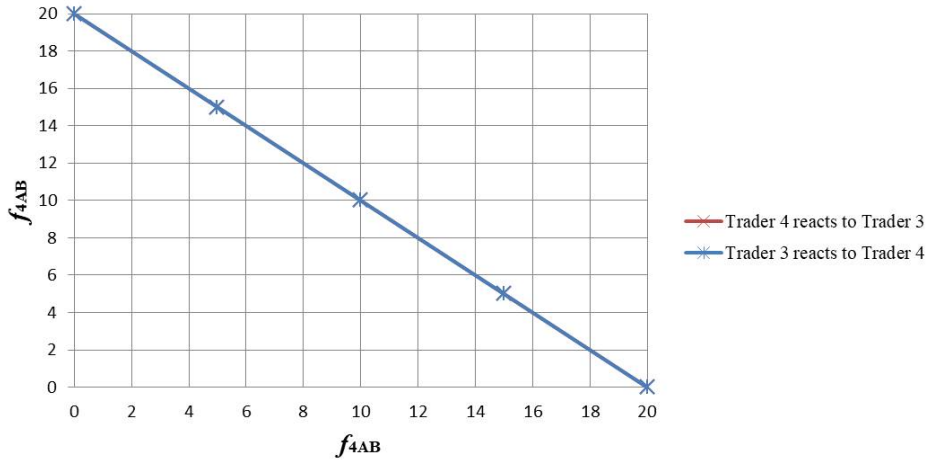

2.6 Conclusions

In this chapter, we develop a three-stage equilibrium model to study cross-product manipulation in FTR and two-settlement energy markets under demand and congestion uncertainty. Numerical results in a two-node setting show that day-ahead price manipulation through uneconomic virtual transactions to profit from FTR positions is sustained only when generators and traders compete in a Cournot game in the day-ahead market. In contrast, this type of manipulation fails when the FTR holder is the only one acting strategically, and generation capacity and credit requirement constraints for other participants are not binding. Manipulation diverges day-ahead and expected real-time prices at the FTR sink, and day-

Figure 2.8: Reaction Functions when $c_f = 3,000$

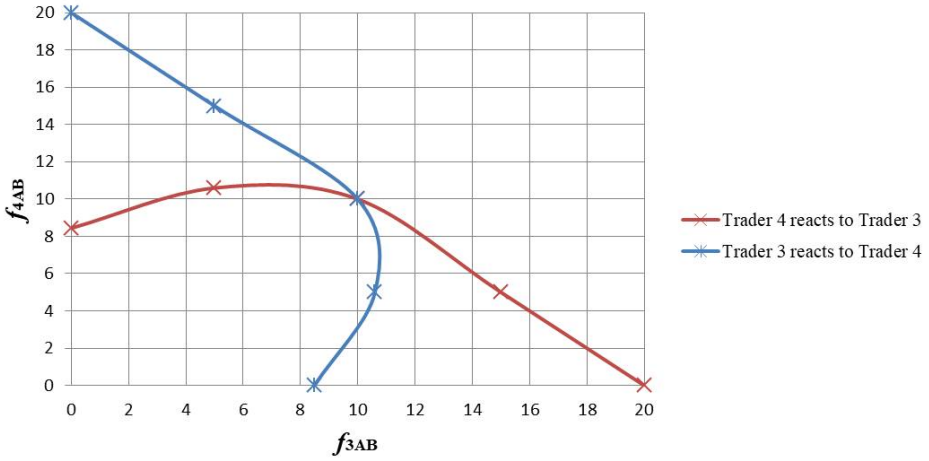

ahead prices at that node increase by 2% to 3%, depending on the benchmark. Welfare implications of cross-product manipulation, as well as its impacts on price convergence at the FTR source and average procurement cost of electricity, critically hinge upon the assumed benchmark. Further, our simulations illustrate that, as day-ahead inverse demand becomes more inelastic, the trader has a greater incentive to lose (on average) on her virtual demand positions at the FTR sink to profit from the FTR. Uneconomic bidding at the contract sink is an equilibrium strategy even when the trader faces uncertainty about day-ahead demand sensitivity to prices.

Table 2.4: Assumed Parameters for Two-generator Cases

C_1 (\$/MWh)	10
C_2 (\$/MWh)	15
K_1 (MW)	100
K_2 (MW)	100
a_A	20
b_A	0.1
a_B^{ψ}	U[14,20]
b_B	0.1
T_{AB} (MW)	20
R_A (\$/MWh)	2
R_B (\$/MWh)	2
S_3 (\$)	100
S_4 (\$)	6
n	5
c_f (\$)	0
$\Pr(\Omega_a)$	0.5
L_a(Unconstrained) (MW)	79
L_b(Unconstrained) (MW)	19
$\Pr(\Omega_b)$	0.5
L_a(Constrained) (MW)	60
L_b(Constrained) (MW)	50

Table 2.5: Numerical Results for Two-generator Case 1 to Case 7 (slope = 0.1), (B) denotes Benchmark cases

Cases	Case 1	Case 2	Case 3	Case 4	Case 5 (B)	Case 6 (B)	Case 7 (B)
Generators	Competitive	Competitive	Cournot	Cournot	Cournot	Cournot	Cournot
Trader 3	Competitive	Cournot	Cournot	Cournot	NA	Cournot	Competitive
Trader 3 with FTR?	Y	Y	Y	Y	NA	N	Y
Trader 4	Competitive	Competitive	Cournot	Cournot	Cournot	Cournot	Competitive
Number of Trader(s) 4	1	1	1	5	1	1	1
Collateral	Y	Y	Y	Y	Y	Y	Y
Solver	KNITRO	KNITRO	KNITRO	KNITRO	PATH	PATH	KNITRO
Variables							
Real-time							
$\mathbb{E}(p_A^\omega)$ (\$/MWh)	10	10	10	10	10	10	10
$\mathbb{E}(p_B^\omega)$ (\$/MWh)	12.5	12.5	12.5	12.5	12.5	12.5	12.5
FTR							
f_{3AB} (MW)	20	20	20	20	NA	NA	20

Table 2.6: Numerical Results for Two-generator Case 1 to Case 7 (slope = 0.1), (B) denotes Benchmark cases

Cases	Case 1	Case 2	Case 3	Case 4	Case 5 (B)	Case 6 (B)	Case 7 (B)
Generators	Competitive	Competitive	Cournot	Cournot	Cournot	Cournot	Cournot
Trader 3	Competitive	Cournot	Cournot	Cournot	NA	Cournot	Competitive
Trader 3 with FTR?	Y	Y	Y	Y	NA	N	Y
Trader 4	Competitive	Competitive	Cournot	Cournot	Cournot	Cournot	Competitive
Number of Trader(s) 4	1	1	1	5	1	1	1
Collateral	Y	Y	Y	Y	Y	Y	Y
Day-ahead (Average over 100 runs)							
p_A^ψ ($/MWh)	10.00	10.00	12.50	12.17	13.54	12.86	12.23
p_B^ψ ($/MWh)	12.50	12.50	13.45	13.48	13.56	13.08	13.19
w_{AB}^ψ ($/MWh)	2.50	2.50	0.95	1.32	0.03	0.22	0.95
s_{1A}^ψ (MW)	54.33	47.41	24.99	21.65	35.35	28.62	22.32
s_{1B}^ψ (MW)	40.73	51.66	24.99	21.65	35.35	28.62	22.32
s_{2A}^ψ (MW)	12.56	17.94	9.48	9.83	10.62	5.85	7.02
s_{2B}^ψ (MW)	12.16	21.80	9.48	9.83	10.62	5.85	7.02
$s_{3A}^{inc,\psi}$ (MW)	29.10	21.27	42.12	40.44	NA	29.88	50.00
$s_{3A}^{dec,\psi}$ (MW)	4.18	1.27	0.10	0.37	NA	1.26	0.00
$s_{3A}^{inc,\psi} - s_{3A}^{dec,\psi}$ (MW)	24.92	20.00	42.02	40.07	NA	28.62	50.00
$s_{3B}^{inc,\psi}$ (MW)	4.66	1.72	0.12	0.11	NA	12.35	0.00
$s_{3B}^{dec,\psi}$ (MW)	8.50	21.72	7.67	8.70	NA	6.50	0.00
$s_{3B}^{inc,\psi} - s_{3B}^{dec,\psi}$ (MW)	-3.84	-20.00	-7.55	-8.59	NA	5.85	0.00
$s_{4A}^{inc,\psi}$ (MW)	0.71	1.38	3.00	3.00	3.00	3.00	3.00
$s_{4A}^{dec,\psi}$ (MW)	0.68	0.45	0.00	0.00	0.00	0.00	0.00
$s_{4A}^{inc,\psi} - s_{4A}^{dec,\psi}$ (MW)	0.03	0.93	3.00	3.00	3.00	3.00	3.00
$s_{4B}^{inc,\psi}$ (MW)	0.67	1.17	0.00	0.00	0.00	0.00	0.00
$s_{4B}^{dec,\psi}$ (MW)	0.65	0.00	0.00	0.00	0.00	0.00	0.00
$s_{4B}^{inc,\psi} - s_{4B}^{dec,\psi}$ (MW)	0.02	1.17	0.00	0.00	0.00	0.00	0.00
y_{AB}^ψ (MW)	28.17	33.72	15.51	11.82	24.73	22.77	15.30
m^ψ (MW)	-8.17	-13.72	4.49	8.18	-15.69	-5.28	4.68
$y_{AB}^\psi + m^\psi$ (MW) (Total Flow)	20.00	20.00	20.00	20.00	9.04	17.49	19.98
μ_1^ψ	0.00	0.00	0.00	0.00	0.00	0.00	0.00
μ_2^ψ	0.00	0.00	0.00	0.00	0.00	0.00	0.00
λ_{AB}^ψ	2.50	2.50	0.95	1.32	0.03	0.22	0.95
λ_{BA}^ψ	0.00	0.00	0.00	0.00	0.00	0.00	0.00
θ_3^ψ	0.00	0.00	0.15	0.08	NA	0.00	1.12
θ_4^ψ	0.00	0.00	1.10	0.93	1.62	1.28	1.12

Table 2.7: Numerical Results for Two-generator Case 1 to Case 7 (slope = 0.1), (B) denotes Benchmark cases

Cases		Case 1	Case 2	Case 3	Case 4	Case 5 (B)	Case 6 (B)	Case 7 (B)
Generators		Competitive	Competitive	Cournot	Cournot	Cournot	Cournot	Cournot
Trader 3		Competitive	Cournot	Cournot	Cournot	NA	Cournot	Competitive
Trader 3 with FTR?		Y	Y	Y	Y	NA	N	Y
Trader 4		Competitive	Competitive	Cournot	Cournot	Cournot	Cournot	Competitive
Number of Trader(s) 4		1	1	1	5	1	1	1
Collateral		Y	Y	Y	Y	Y	Y	Y
$p_A^{\psi} - \mathbb{E}(p_A^{\omega})$ ($/MWh)		0.00	0.00	2.50	2.17	3.54	2.86	2.23
$p_B^{\psi} - \mathbb{E}(p_B^{\omega})$ ($/MWh)		0.00	0.00	0.95	0.98	1.06	0.58	0.69
Generator 1 Production (MW)		89.00	89.00	89.00	89.00	89.00	89.00	89.00
Generator 2 Production (MW)		15.00	15.00	15.00	15.00	15.00	15.00	15.00
Average	Node A	10.00	10.00	12.75	12.49	13.34	12.99	12.54
Procurement	Node B	14.17	14.17	15.06	15.07	15.05	14.83	14.96
Cost ($/MWh)	Total	11.19	11.19	13.33	13.16	13.73	13.39	13.14
% DA Congestion Hours		100.00%	100.00%	100.00%	100.00%	11.00%	49.00%	97.00%
% Node B Uneconomic Hours		0.00%	0.00%	100.00%	100.00%	NA	0.00%	0.00%
Profit for G1 ($)		0.00	0.00	124.99	93.76	251.12	163.99	99.70
Profit for G2 ($)		0.00	0.00	22.31	23.29	24.37	9.23	15.65
Producer Surplus (a) ($)		**0.00**	**0.00**	**147.30**	**117.05**	**275.49**	**173.22**	**115.35**
	Node A	0.00	0.00	104.93	86.69	NA	82.00	111.64
Profit for	Node B	0.00	0.00	-6.04	-7.13	NA	4.61	0.00
Trader 3 ($)	FTR	50.00	50.00	18.98	26.36	NA	NA	19.10
	Total	50.00	50.00	117.87	105.92	NA	86.61	130.74
Profit for	Node A	0.00	0.00	7.50	6.50	10.60	8.58	6.70
(each) Trader 4	Node B	0.00	0.00	0.00	0.00	0.00	0.00	0.00
($)	Total	0.00	0.00	7.50	6.50	10.60	8.58	6.70
Trader Surplus (b) ($)		**50.00**	**50.00**	**125.37**	**138.42**	**10.60**	**95.19**	**137.44**
Consumer Surplus at Node A ($)		753.98	753.98	370.63	393.38	303.58	346.71	389.09
Consumer Surplus at Node B ($)		245.45	245.45	164.44	163.74	168.15	187.51	173.68
Consumer Surplus (c) ($)		**999.43**	**999.43**	**535.07**	**557.12**	**471.73**	**534.22**	**562.77**
ISO Surplus (d) ($)		**50.00**	**50.00**	**18.97**	**26.32**	**27.95**	**10.72**	**19.16**
ISO Day-ahead Surplus (e) ($)		**50.00**	**50.00**	**18.97**	**26.32**	**0.55**	**4.45**	**19.11**
Social Welfare (a+b+c+d-e) ($)		**1049.43**	**1049.43**	**807.74**	**812.59**	**785.77**	**813.35**	**815.61**

The formula for calculating social welfare for Case 6 and 7 is just (a+b+c+d), there is no need to subtract ISO's day-ahead surplus as traders do not have FTR positions in these two cases.

Table 2.8: Sensitivity Analysis for Long-term effects (Case 3, Hourly)

Slopes		Probability		
0.05		1/2	1/3	1/4
0.10		1/4	1/3	1/4
0.15		1/4	1/3	1/2
s_{1A}^{ψ} (MW)		35.27	30.35	26.77
s_{1B}^{ψ} (MW)		35.27	30.35	26.77
s_{2A}^{ψ} (MW)		15.55	13.12	11.66
s_{2B}^{ψ} (MW)		15.55	13.12	11.66
$s_{3A}^{inc,\psi} - s_{3A}^{dec,\psi}$ (MW)		44.38	42.49	40.78
$s_{3B}^{inc,\psi} - s_{3B}^{dec,\psi}$ (MW)		-4.98	-6.64	-8.06
$s_{4A}^{inc,\psi} - s_{4A}^{dec,\psi}$ (MW)		3.00	3.00	3.00
$s_{4B}^{inc,\psi} - s_{4B}^{dec,\psi}$ (MW)		0.00	0.00	0.00
$p_A^{\psi} - \mathbb{E}(p_A^{\omega})$ ($/MWh)		2.85	2.72	2.64
$p_B^{\psi} - \mathbb{E}(p_B^{\omega})$ ($/MWh)		1.08	1.05	1.06
% DA Congestion Hours		100.00%	100.00%	100.00%
Average Procurement Cost ($/MWh)		14.62	14.07	13.71
Profit for G1 ($)		213.24	175.91	151.16
Profit for G2 ($)		41.83	34.67	30.66
Producer Surplus (a) ($)		**255.07**	**210.58**	**181.82**
Profit for Trader 3 ($)	Node A	128.89	117.64	109.62
	Node B	-4.52	-6.02	-7.63
	FTR	14.44	16.65	18.46
	Total	138.81	128.27	120.45
Profit for (each) Trader 4 ($)	Node A	8.56	8.16	7.92
	Node B	0.00	0.00	0.00
	Total	8.56	8.16	7.92
Trader Surplus (b) ($)		**147.37**	**136.43**	**128.37**
Consumer Surplus at Node A ($)		688.00	583.86	533.08
Consumer Surplus at Node B ($)		301.58	252.95	226.26
Consumer Surplus (c) ($)		**989.58**	**836.81**	**759.35**
ISO Surplus (d) ($)		**16.88**	**18.29**	**19.69**
ISO Day-ahead Surplus (e) ($)		**14.44**	**16.66**	**18.47**
Social Welfare (a+b+c+d-e) ($)		**1394.46**	**1185.45**	**1070.76**

Table 2.9: Sensitivity Analysis for Long-term effects (Case 3, Quarterly)

Slopes		Probability		
0.05		1/2	1/3	1/4
0.10		1/4	1/3	1/4
0.15		1/4	1/3	1/2
Profit for G1 ($)		460,598	379,966	326,506
Profit for G2 ($)		90,353	74,887	66,226
Producer Surplus (a) ($)		**550,951**	**454,853**	**392,732**
	Node A	278,402	254,102	236,779
Profit for	Node B	-9,763	-13,003	-16,481
Trader 3 ($)	FTR	31,190	35,964	39,874
	Total	299,829	277,063	260,172
Profit for	Node A	18,490	17,626	17,107
(each) Trader 4	Node B	0	0	0
($)	Total	18,490	17,626	17,107
Trader Surplus (b) ($)		**318,319**	**294,689**	**277,279**
Consumer Surplus at Node A ($)		1,486,080	1,261,138	1,151,453
Consumer Surplus at Node B ($)		651,413	546,372	488,722
Consumer Surplus (c) ($)		**2,137,493**	**1,807,510**	**1,640,174**
ISO Surplus (d) ($)		**36,461**	**39,506**	**42,530**
ISO Day-ahead Surplus (e) ($)		**31,190**	**35,986**	**39,895**
Social Welfare (a+b+c+d-e) ($)		**3,012,034**	**2,560,572**	**2,312,820**

Chapter 3
Cross-product Manipulation in Electricity Markets: A Two-stage, Multi-node Equilibrium Model with Intertemporal Constraints

3.1 Introduction

The model in the previous chapter is able to capture the decision-making process in the three stages of the manipulation game: FTR, day-ahead and real-time markets. However, this comes at the cost of simplifying the network topology, inter-dependence of consecutive trading hours, and market participants' behavior, so that an analytical solution in the real-time stage can be obtained to reduce the three-stage game to a two-stage one. In reality, loop flows in the network and intertemporal constraints that limit units' ability to adjust their output (e.g., unit commitment and ramping constraints) are important factors traders need to consider when placing virtual bids. Moreover, the assumption of generating firms behaving competitively in the real-time market may not always hold. Meanwhile, because of the duration difference between FTR and virtual bids, traders are more often faced with a problem of placing optimal virtual bids given their existing FTR positions than choosing the FTR position upfront. In this chapter, we focus on cross-product manipulation in the presence of loop flows and intertemporal constraints. We also allow generators to behave à la Cournot in the real-time

market. Below is a discussion of how the model in this Chapter builds on the one in Chapter 2.

- Exogenous FTR positions and generator real-time behavior

While virtual bids are generally placed on an hourly basis, FTRs have longer durations. Take California ISO's Congestion Revenue Rights (CRR) for example, the duration of CRR ranges from a month (Monthly CRR) to 10 years (Long Term CRR) [78]. Because of this duration difference, traders are often faced with a problem of maximizing their profits by placing optimal virtual bids given their existing FTR positions. Therefore, this chapter will only focus on day-ahead and real-time markets, and explore if the cross-product manipulation strategy by a financial trader with given FTR positions can be sustained in equilibrium. Importantly, we no longer require generators to behave competitively in the real-time markets to be able to reduce the model from three to two stages.

- Network with loop flows

In Chapter 2, we had a simple network where two nodes are connected by a single transmission line. In that case, it is straightforward that any excessive power generated in one node will be shipped to the other node. However, in a more complicated network with at least three inter-connected buses, how much power flows across each transmission line is dictated by physical laws: Kirchoff's Current Law (KCL) states that the algebraic sum of currents entering and leaving any point in a circuit is equal to zero, and Kirchoff's Voltage Law (KVL) states that the algebraic sum of all voltage drops around a closed loop is equal to zero. This physical constraint of power flows poses additional challenges to a trader engaging in cross-product manipulation. One of the findings from the two-node model in Chapter 2 is that the financial trader has an incentive to place uneconomic virtual demand bids at the sink node of her FTR position to congest the FTR path. In this chapter, we explore how a network with loop flows affects the trader's virtual bidding strategy.

- Unit commitment and ramping constraints in inter-dependent trading hours

In the previous chapter, we assumed trading hours were independent from each other, and focus our attention on a single representative hour in both day-ahead and real-time markets. In reality, consecutive trading hours are unlikely to be independent

because of generator unit commitment decisions and ramping constraints. Unit commitment (UC) problems are generally formulated as an optimization problem that minimizes total costs (including start-up, shut-down and generation costs) or maximizes social welfare, subject to generator capacity, minimum output and ramping constraints. In theory, binary variables are needed to represent generator decision of whether or not to commit a unit. Therefore, much of the literature has focused on finding an efficient formulation and algorithms to solve UC problems as mixed-integer linear programs [79–81]. Less attention has been given to unit commitment models embedded in a complementarity equilibrium framework, where commitment variables are generally treated as continuous. For example, [73] mention the possibility of relaxing the commitment variables to be continuous and in the range of [0,1], while warning about the risk of underestimating the commitment costs if fractional values occur in an equilibrium solution. [82] treated the commitment variables in the same way, but interpreted a fractional solution as committing proportion of the generator capacity. In this chapter, we adopt the same methodology and interpretation as in [82].

Table 3.1 summarizes the differences between the models in Chapter 2 and Chapter 3.

Table 3.1: Modeling Differences between Chapter 2 and Chapter 3

	Chapter 2 (two-node)	**Chapter 3** (n-node)
Loop Flows (Spatial)	No	Yes
Unit Commitment and Ramping Constraints (Temporal)	No	Yes
Generators' Real-time Behavior	Competitive	Competitive or Cournot
Model Structure	FTR, Day-ahead, Real-time	Day-ahead, Real-time

3.2 Model

In this section, we describe the model assumptions and formulations. Superscript ω is used to denote real-time variables, and superscript ψ is used to denote day-ahead

variables. Nodes and generators are indexed by $i \in I$ and $j \in J$, respectively. In particular, node i hosting generator j is denoted by $i(j)$, and generator j located at node i is denoted by $j(i)$.

Assumptions on Game Structure and Market Participant Behavior

We consider a bi-level game in a two-settlement electricity market. On the upper level, a financial trader with given FTR position is the Stackelberg leader. This trader submits virtual bids at each node in the day-ahead market to maximize her total profits from both virtual bids and FTR positions. The lower level games consist of market participants in both day-ahead and real-time markets. In the day-ahead market, generators make bilateral sales to customers with elastic demand, a trader without FTR position submits virtual bids to arbitrage price difference between day-ahead and real-time markets, and a system operator provides transmission services to generators and performs spatial arbitrage (i.e., price differences between nodes). In the day-ahead market, different behavioral assumptions are made for generators and the financial trader without FTR: market participants either act competitively or behave à la Cournot. The spatial arbitrage function of ISO is an essential assumption to ensure the price difference between two nodes is equal to the transmission cost difference between the same two nodes when market participants behave à la Cournot. In the real-time market, generators are also assumed to behave either competitively, or à la Cournot. Different load assumptions are made in the next paragraph. When generators behave competitively in the real-time market, the ISO is assumed to only provide transmission services to generators, as perfectly competitive generators will eliminate spatial arbitrage opportunities. When generators behave à la Cournot in the real-time, we assume the ISO also performs spatial arbitrage for the same reason described above.

Assumptions on Demand

We assume there is deterministic, elastic demand at each node of the network in the day-ahead market for every hour. Elastic demand in the day-ahead market allows bids and offers to influence the day-ahead prices so that a potential manipulation attempt could be sustained in equilibrium. For the real-time demand, we made two distinct assumptions: when generators behave competitively, we assume a stochastic, inelastic demand at each node for every hour; when generators behave à la Cournot, it is necessary to assume elastic real-time demand at each node. The intercepts in this case are assumed to be stochastic to keep randomness in the

real-time market.

Assumptions on Network and Generator Sales Decisions

As can be seen from the model formulation, our model is built on a n-node network with lossless lines. Sales made by generator j to node i at hour t in the day-ahead market is denoted by $s_{ji}^{t,\psi}$. This day-ahead sales schedule can be adjusted in the real-time market by making residual sales $s_{ji}^{t,\omega}$. Based on the principle of superposition, we assume generator j located at node $i(j)$ ships all of its day-ahead (or residual real-time) output to an intermediate hub node at hour t, and gets paid $w_{i(j)}^{t,\psi}$ (or $w_{i(j)}^{t,\omega}$) for every unit of its power output. In turn, power output will be shipped from the hub to each destination node chosen by generator j. Sales made to each node i will incur a per unit cost of $w_i^{t,\psi}$ (or $w_i^{t,\omega}$) in the day-ahead (or real-time) market. For the purpose of numerical simulations, we adopt a three-node network where a low-cost generator 1, a medium-cost generator 2, and a high-cost generator 3 are located at node A, B and C, respectively. The marginal cost of each generator is assumed to be constant and denoted by C_j for generator j ($C_1 < C_2 < C_3$).

Assumptions on Generator Operational Constraints and Unit Commitment Decisions

In addition to sales decisions, generators also make commitment decisions. In this chapter, we allow the commitment decision variables to be fractional as described in [82]. This means generators can commit a percentage of their operational capabilities at the corresponding fractional commitment costs. Similar to the sales schedule, day-ahead commitment decision made by generator j in hour t ($u_j^{t,\psi}$) can be adjusted up in the real-time by making real-time commitment decision ($u_j^{t,\omega} \geqslant 0$). Operational constraints of each generator are explained as follows:

- Maximum generation capacity of generator j is denoted by K_j. Generation capacity of generator j at hour t is discounted by the commitment decision $u_j^{t,\psi}$ (or $u_j^{t,\psi} + u_j^{t,\omega}$) for the day-ahead (or real-time) market.

- Minimum power output of generator j is denoted by k_j. Minimum power output of generator j at hour t is discounted by the commitment decision $u_j^{t,\psi}$ (or $u_j^{t,\psi} + u_j^{t,\omega}$) for the day-ahead (or real-time) market.

- Ramp-up limit of generator j is denoted by R_j^U. Ramp-up limit of generator j from hour $t-1$ to hour t is discounted by the commitment decision in hour t, $u_j^{t,\psi}$ (or $u_j^{t,\psi} + u_j^{t,\omega}$) for the day-ahead (or real-time) market.

- Ramp-down limit of generator j is denoted by R_j^D. Ramp-down limit of generator j from hour $t-1$ to hour t is discounted by the commitment decision in hour $t-1$, $u_j^{t-1,\psi}$ (or $u_j^{t-1,\psi} + u_j^{t-1,\omega}$) for the day-ahead (or real-time) market.

- The cost of bringing generator j from 0% commitment to 100% commitment is C_j^{SU}. The day-ahead commitment cost of generator j at hour t is denoted by $c_j^{t,\psi}$, and is equal to C_j^{SU} discounted by the change of day-ahead commitment status from hour $t-1$ to hour t $(u_j^{t,\psi} - u_j^{t-1,\psi})$ or zero, whichever is larger. The residual real-time commitment cost of generator j at hour t is denoted by $c_j^{t,\omega}$, and the total commitment cost of generator j at hour t $(c_j^{t,\psi} + c_j^{t,\omega})$ is equal to C_j^{SU} discounted by the change of total commitment status $(u_j^{t,\psi} + u_j^{t,\omega} - u_j^{t-1,\psi} - u_j^{t-1,\omega})$ or zero, whichever is larger.

The structure of our bi-level equilibrium model is summarized in 3.1. Below we present detailed model formulations for different behavioral assumptions.

Figure 3.1: Game Structure

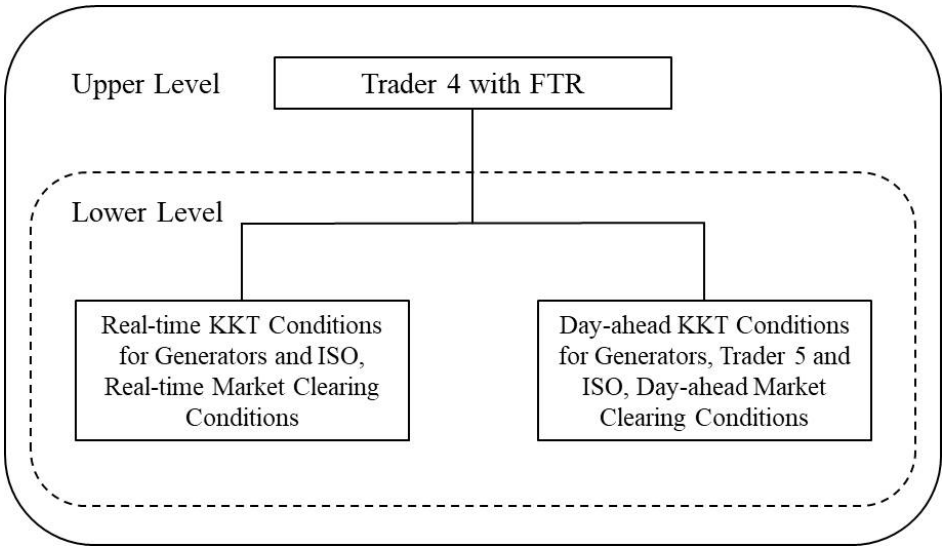

3.2.1 Case 1: Real-time Competitive, Day-ahead Competitive Model Formulation

3.2.1.1 Real-time Market Model Formulation

For every real-time scenario ω, generators j located at node $i(j)$ maximizes her profits from both day-ahead and real-time sales, subject to physical constraints:

$$\begin{aligned}
\underset{s_{ji}^{t,\omega},u_j^{t,\omega},c_j^{t,\omega}}{\text{maximize}} \quad & \sum_{t\in T}\Big[\sum_{i\in I}(p_i^{t,\omega}-w_i^{t,\omega})s_{ji}^{t,\omega}+w_{i(j)}^{t,\omega}(\sum_{i\in I}s_{ji}^{t,\omega})+\sum_{i\in I}(p_i^{t,\psi}-w_i^{t,\psi})s_{ji}^{t,\psi} \\
& + w_{i(j)}^{t,\psi}(\sum_{i\in I}s_{ji}^{t,\psi})-C_j\sum_{i\in I}(s_{ji}^{t,\omega}+s_{ji}^{t,\psi})-c_j^{t,\omega}-c_j^{t,\psi}\Big] && \text{(3.1a)} \\
\text{subject to} \quad & s_{ji}^{t,\omega}+s_{ji}^{t,\psi}\geqslant 0\,,\forall t,i && \text{(3.1b)} \\
& u_j^{t,\omega}\geqslant 0\,,\forall t && \text{(3.1c)} \\
& u_j^{t,\omega}+u_j^{t,\psi}\leqslant 1\,,\forall t && \text{(3.1d)} \\
& c_j^{t,\omega}+c_j^{t,\psi}\geqslant 0\,,\forall t && \text{(3.1e)} \\
& c_j^{t,\omega}+c_j^{t,\psi}\geqslant C_j^{SU}(u_j^{t,\psi}+u_j^{t,\omega}-u_j^{t-1,\psi}-u_j^{t-1,\omega})\,,\forall t && \text{(3.1f)} \\
& \sum_{i\in I}(s_{ji}^{t,\omega}+s_{ji}^{t,\psi})\leqslant(u_j^{t,\psi}+u_j^{t,\omega})K_j\,,\forall t && \text{(3.1g)} \\
& \sum_{i\in I}(s_{ji}^{t,\omega}+s_{ji}^{t,\psi})\geqslant(u_j^{t,\psi}+u_j^{t,\omega})k_j\,,\forall t && \text{(3.1h)} \\
& \sum_{i\in I}(s_{ji}^{t,\omega}+s_{ji}^{t,\psi})-\sum_{i\in I}(s_{ji}^{t-1,\omega}+s_{ji}^{t-1,\psi})\geqslant-(u_j^{t-1,\psi}+u_j^{t-1,\omega})R_j^D\,,\forall t && \text{(3.1i)} \\
& \sum_{i\in I}(s_{ji}^{t,\omega}+s_{ji}^{t,\psi})-\sum_{i\in I}(s_{ji}^{t-1,\omega}+s_{ji}^{t-1,\psi})\leqslant(u_j^{t,\psi}+u_j^{t,\omega})R_j^U\,,\forall t && \text{(3.1j)}
\end{aligned}$$

The ISO's problem is to maximize the value the market receives from the transmission assets, subject to network constraints. In the real-time market, when generators behave competitively, the ISO sells MW of transmission services from the hub node to node i at time t at a price $w_i^{t,\omega}$. When generators behave à la Cournot, the ISO's problem will include the spatial arbitrage decisions. This function is needed to ensure that the price difference between two nodes is equal to the transmission price difference. Conditional on day-ahead transmission services and spatial arbitrage decisions, the parametric real-time optimization problem of

the ISO is defined as follows:

$$\underset{y_i^{t,\omega}}{\text{maximize}} \quad \sum_{t\in T}\Big[\sum_{i\in I} w_i^{t,\omega} y_i^{t,\omega}\Big] \tag{3.2a}$$

$$\text{subject to} \quad -\sum_{i\in I} PTDF_{i,k}(y_i^{t,\omega} + y_i^{t,\psi} + m_i^{t,\psi}) \leqslant T_k\,, \forall t, k \tag{3.2b}$$

$$-\sum_{i\in I} PTDF_{i,k}(y_i^{t,\omega} + y_i^{t,\psi} + m_i^{t,\psi}) \geqslant -T_k\,, \forall t, k \tag{3.2c}$$

where $y_i^{t,\omega}$ denotes real-time transmission services from hub node to node i at hour t, $y_i^{t,\psi}$ denotes transmission services sold to power suppliers in day-ahead for delivery in real-time, and $m_i^{t,\psi}$ is the day-ahead arbitrage sales (i.e., power bought by the system operator at hub node and sold at node i under realization). Since under perfect competition, transmission price differences are equal to nodal price differences, spatial arbitrage in this case is not required. $PTDF_{i,k}$ stand for Power Transfer Distribution Factor, representing the amount of power flowing on transmission line k, given 1 MW of net power injection at node i and withdrawal at the hub node. PTDFs are calculated based on Kirchoff's laws described in 3.1. Since both transmission services and arbitrage sales are formulated as power transfers to node i, they're perceived as power withdrawals at that node. Therefore, a negative sign is added in front of the net withdrawals when calculating power flows. Constraints in the ISO's problem ensure that the sum of day-ahead and real-time transmission services and arbitrage quantities are consistent with physical power flows delivered in real-time on every transmission line k, and satisfy transmission capacity constraints T_k in both directions.

In the real-time competitive case, demand at node i and hour t is exogenous and denoted by $L_i^{t,\omega}$. Market clearing conditions for energy ensure that hourly demand equals supply at each location. Market clearing conditions for transmission services ensure that the MW of transmission delivery provided by the ISO equal the net sales scheduled by the suppliers at each hour. For every hour t, market clearing conditions are listed below:

$$L_i^{t,\omega} = \sum_{j\in J}(s_{ji}^{t,\omega} + s_{ji}^{t,\psi}) + m_i^{t,\psi}\,, \forall i \tag{3.3a}$$

$$y_i^{t,\omega} + y_i^{t,\psi} = \sum_{j\in J}(s_{ji}^{t,\omega} + s_{ji}^{t,\psi}) - \sum_{i\in I}(s_{j(i)i}^{t,\omega} + s_{j(i)i}^{t,\psi})\,, \forall i \tag{3.3b}$$

The above formulation is equivalent to the cost minimization formulation below:

$$\underset{s_{ji}^{t,\omega},u_j^{t,\omega},c_j^{t,\omega},y_i^{t,\omega}}{\text{minimize}} \quad \sum_{t\in T}\sum_{j\in J}\left[C_j\sum_{i\in I}(s_{ji}^{t,\omega}+s_{ji}^{t,\psi})+c_j^{t,\omega}+c_j^{t,\psi}\right] \tag{3.4a}$$

$$\text{subject to} \quad s_{ji}^{t,\omega}+s_{ji}^{t,\psi}\geqslant 0\,,\forall t,i,j,\omega \tag{3.4b}$$

$$u_j^{t,\omega}\geqslant 0\,,\forall t,j,\omega \tag{3.4c}$$

$$u_j^{t,\omega}+u_j^{t,\psi}\leqslant 1\,,\forall t,j,\omega \tag{3.4d}$$

$$c_j^{t,\omega}+c_j^{t,\psi}\geqslant 0\,,\forall t,j,\omega \tag{3.4e}$$

$$c_j^{t,\omega}+c_j^{t,\psi}\geqslant C_j^{SU}(u_j^{t,\psi}+u_j^{t,\omega}-u_j^{t-1,\psi}-u_j^{t-1,\omega})\,,\forall t,j,\omega \tag{3.4f}$$

$$\sum_{i\in I}(s_{ji}^{t,\omega}+s_{ji}^{t,\psi})\leqslant(u_j^{t,\psi}+u_j^{t,\omega})K_j\,,\forall t,j,\omega \tag{3.4g}$$

$$\sum_{i\in I}(s_{ji}^{t,\omega}+s_{ji}^{t,\psi})\geqslant(u_j^{t,\psi}+u_j^{t,\omega})k_j\,,\forall t,j,\omega \tag{3.4h}$$

$$\sum_{i\in I}(s_{ji}^{t,\omega}+s_{ji}^{t,\psi})-\sum_{i\in I}(s_{ji}^{t-1,\omega}+s_{ji}^{t-1,\psi})\geqslant-(u_j^{t-1,\psi}+u_j^{t-1,\omega})R_j^D\,,\forall t,j,\omega \tag{3.4i}$$

$$\sum_{i\in I}(s_{ji}^{t,\omega}+s_{ji}^{t,\psi})-\sum_{i\in I}(s_{ji}^{t-1,\omega}+s_{ji}^{t-1,\psi})\leqslant(u_j^{t,\psi}+u_j^{t,\omega})R_j^U\,,\forall t,j,\omega \tag{3.4j}$$

$$-\sum_{i\in I}PTDF_{i,k}(y_i^{t,\omega}+y_i^{t,\psi}+m_i^{t,\psi})\leqslant T_k\,,\forall t,k,\omega \tag{3.4k}$$

$$-\sum_{i\in I}PTDF_{i,k}(y_i^{t,\omega}+y_i^{t,\psi}+m_i^{t,\psi})\geqslant -T_k\,,\forall t,k,\omega \tag{3.4l}$$

$$L_i^{t,\omega}=\sum_{j\in J}(s_{ji}^{t,\omega}+s_{ji}^{t,\psi})+m_i^{t,\psi}\,,\forall t,i,\omega \tag{3.4m}$$

$$y_i^{t,\omega}+y_i^{t,\psi}=\sum_{j\in J}(s_{ji}^{t,\omega}+s_{ji}^{t,\psi})-\sum_{i\in I}(s_{j(i)i}^{t,\omega}+s_{j(i)i}^{t,\psi})\,,\forall t,i,\omega \tag{3.4n}$$

3.2.1.2 Day-ahead Market Model Formulation

- Day-ahead Demand at Node i

Day-ahead demand at each node of the network is assumed to be elastic, and follows the linear inverse demand function below:

$$p_i^{t,\psi}=p_i^{t,\psi}(d_i^{t,\psi})=$$

$$a_i^t - b_i^t\Big(\sum_{j\in J} s_{ji}^{t,\psi} + s_{4i}^{inc,t,\psi} + s_{5i}^{inc,t,\psi} - s_{4i}^{dec,t,\psi} - s_{5i}^{dec,t,\psi} + m_i^{t,\psi}\Big)\,, \forall t \tag{3.5a}$$

where $p_i^{t,\psi}$ and $d_i^{t,\psi}$ denote the day-ahead price and demand at node i in hour t, respectively. Notation $p_i^{t,\psi}(d_i^{t,\psi})$ is used when price is an explicit function of demand. a_i^t and b_i^t are parameters of the day-ahead inverse demand function.

- Generator j at node $i(j)$

Generator's day-ahead problem is similar to their real-time one, with two differences. First, the real-time profit component in the objective function is expressed in terms of expectation, reflecting the uncertainty of real-time scenarios at day-ahead. Secondly, the constraints only apply to day-ahead variables.

$$\begin{aligned}
\underset{s_{ji}^{t,\psi},u_j^{t,\psi},c_j^{t,\psi}}{\text{maximize}} \quad & \sum_{t\in T}\mathbb{E}_\omega\Big[\sum_{i\in I}(p_i^{t,\omega}-w_i^{t,\omega})s_{ji}^{t,\omega} + w_{i(j)}^{t,\omega}(\sum_{i\in I}s_{ji}^{t,\omega}) - C_j\sum_{i\in I}(s_{ji}^{t,\omega}) - c_j^{t,\omega}\Big] \\
& + \sum_{i\in I}(p_i^{t,\psi}-w_i^{t,\psi})s_{ji}^{t,\psi} + w_{i(j)}^{t,\psi}(\sum_{i\in I}s_{ji}^{t,\psi}) - C_j\sum_{i\in I}(s_{ji}^{t,\psi}) - c_j^{t,\psi} && \text{(3.6a)} \\
\text{subject to} \quad & s_{ji}^{t,\psi} \geqslant 0\,, \forall t, i && \text{(3.6b)} \\
& u_j^{t,\psi} \geqslant 0\,, \forall t && \text{(3.6c)} \\
& u_j^{t,\psi} \leqslant 1\,, \forall t && \text{(3.6d)} \\
& c_j^{t,\psi} \geqslant 0\,, \forall t && \text{(3.6e)} \\
& c_j^{t,\psi} \geqslant C_j^{SU}(u_j^{t,\psi} - u_j^{t-1,\psi})\,, \forall t && \text{(3.6f)} \\
& \sum_{i\in I} s_{ji}^{t,\psi} \leqslant u_j^{t,\psi}K_j\,, \forall t && \text{(3.6g)} \\
& \sum_{i\in I} s_{ji}^{t,\psi} \geqslant u_j^{t,\psi}k_j\,, \forall t && \text{(3.6h)} \\
& \sum_{i\in I} s_{ji}^{t,\psi} - \sum_{i\in I} s_{ji}^{t-1,\psi} \geqslant -u_j^{t-1,\psi}R_j^D\,, \forall t && \text{(3.6i)} \\
& \sum_{i\in I} s_{ji}^{t,\psi} - \sum_{i\in I} s_{ji}^{t-1,\psi} \leqslant u_j^{t,\psi}R_j^U\,, \forall t && \text{(3.6j)}
\end{aligned}$$

- Financial Trader 5

Trader 5 maximizes her profits from virtual bid positions, by choosing the virtual bids placed at each node. $s_{5i}^{inc,\psi}$ and $s_{5i}^{dec,\psi}$ represent the virtual supply offers and virtual demand bids at node i, respectively. Virtual supply offers are settled

using the difference between day-ahead and real-time LMPs, and virtual demand bids are settled using the difference between real-time and day-ahead LMPs.

$$\underset{s_{5i}^{inc,t,\psi},s_{5i}^{dec,t,\psi}}{\text{maximize}} \quad \sum_{t\in T}\mathbb{E}_{\omega}\Big\{\sum_{i\in I}\Big[(p_i^{t,\psi}-p_i^{t,\omega})s_{5i}^{inc,t,\psi}+(p_i^{t,\omega}-p_i^{t,\psi})s_{5i}^{dec,t,\psi}\Big]\Big\} \tag{3.7a}$$

$$\text{subject to} \quad s_{5i}^{inc,t,\psi}\geqslant 0\,,\forall t \tag{3.7b}$$

$$s_{5i}^{dec,t,\psi}\geqslant 0\,,\forall t \tag{3.7c}$$

$$\sum_{t\in T}\sum_{i\in I}\Big(R_i^{inc}s_{5i}^{inc,t,\psi}+R_i^{dec}s_{5i}^{dec,t,\psi}\Big)\leqslant S_5\,, \tag{3.7d}$$

The last constraint in the trader's problem reflects the credit requirement for virtual bidding that is in place at several ISOs, where R_i^{inc} and R_i^{dec} represent the reference price of INCs and DECs at node i, respectively. And S_5 represent Trader 5's collateral. The background of this requirement will be further explained in 3.4.1.

- ISO

$$\underset{y_i^{t,\psi},m_i^{t,\psi}}{\text{maximize}} \quad \sum_{t\in T}\sum_{i\in I}\Big(w_i^{t,\psi}y_i^{t,\psi}+p_i^{t,\psi}m_i^{t,\psi}\Big) \tag{3.8a}$$

$$\text{subject to} \quad \sum_{i\in I}m_i^{t,\psi}=0\,,\forall t \tag{3.8b}$$

$$-\sum_{i\in I}PTDF_{i,k}(y_i^{t,\psi}+m_i^{t,\psi})\leqslant T_k\,,\forall t,k \tag{3.8c}$$

$$-\sum_{i\in I}PTDF_{i,k}(y_i^{t,\psi}+m_i^{t,\psi})\geqslant -T_k\,,\forall t,k \tag{3.8d}$$

- Market clearing

For every hour t, market clearing conditions are listed below:

$$y_i^{t,\psi}=\sum_{j\in J}s_{ji}^{t,\psi}-\sum_{i\in I}s_{j(i)i}^{t,\psi}\,,\forall i \tag{3.9a}$$

The upper level problem is Trader 4's profit optimization problem, which maximizes the profits from both virtual bids and FTR position:

- Financial Trader 4

$$\underset{s_{4i}^{inc,t,\psi}, s_{4i}^{dec,t,\psi}}{\text{maximize}} \quad \sum_{t\in T} \mathbb{E}_\omega \Big\{ \sum_{i\in I} \Big[(p_i^{t,\psi} - p_i^{t,\omega}) s_{4i}^{inc,t,\psi} + (p_i^{t,\omega} - p_i^{t,\psi}) s_{4i}^{dec,t,\psi} \Big] \Big\} + f_{4AB}(p_B^{t,\psi} - p_A^{t,\psi} - c_f) \tag{3.10a}$$

$$\text{subject to} \quad s_{4i}^{inc,t,\psi} \geqslant 0\,, \forall t \tag{3.10b}$$

$$s_{4i}^{dec,t,\psi} \geqslant 0\,, \forall t \tag{3.10c}$$

$$\sum_{t\in T}\sum_{i\in I} \Big(R_i^{inc} s_{4i}^{inc,t,\psi} + R_i^{dec} s_{4i}^{dec,t,\psi} \Big) \leqslant S_4\,, \tag{3.10d}$$

where f_{4AB} denotes Trader 4's FTR position from source node A to sink node B, which is settled using the day-ahead price difference between sink and source nodes. c_f represents the cost of FTR. Trader 4's problem also includes constraints listed in Equations 3.1, 3.2, 3.3, 3.5, 3.6, 3.7, 3.8, 3.9. The entire problem is therefore an MPEC.

3.2.2 Case 2: Real-time Competitive, Day-ahead Cournot Model Formulation

In this subsection, we allow generators and trader 5 to act à la Cournot in the day-ahead by substituting the day-ahead prices with corresponding inverse demand functions in their objectives. The formulations are listed below:

3.2.2.1 Real-time Market Model Formulation

The real-time market formulation is the same as Equations 3.1, 3.2, 3.3.

3.2.2.2 Day-ahead Market Model Formulation

Substituting the day-ahead prices with day-ahead inverse demand functions in generators' and trader 5's objectives, their formulations are listed below:

- Generator j at node $i(j)$

$$\underset{s_{ji}^{t,\psi}, u_j^{t,\psi}, c_j^{t,\psi}}{\text{maximize}} \quad \sum_{t\in T} \mathbb{E}_\omega \Big[\sum_{i\in I} (p_i^{t,\omega} - w_i^{t,\omega}) s_{ji}^{t,\omega} + w_{i(j)}^{t,\omega} (\sum_{i\in I} s_{ji}^{t,\omega}) - C_j \sum_{i\in I} (s_{ji}^{t,\omega}) - c_j^{t,\omega} \Big] + \sum_{i\in I} (p_i^{t,\psi}(d_i^{t,\psi}) - w_i^{t,\psi}) s_{ji}^{t,\psi} + w_{i(j)}^{t,\psi} (\sum_{i\in I} s_{ji}^{t,\psi}) - C_j \sum_{i\in I} (s_{ji}^{t,\psi}) - c_j^{t,\psi} \tag{3.11a}$$

$$\text{subject to} \quad s_{ji}^{t,\psi} \geqslant 0\,, \forall t, i \tag{3.11b}$$

$$u_j^{t,\psi} \geqslant 0\,, \forall t \tag{3.11c}$$

$$u_j^{t,\psi} \leqslant 1\,, \forall t \tag{3.11d}$$

$$c_j^{t,\psi} \geqslant 0\,, \forall t \tag{3.11e}$$

$$c_j^{t,\psi} \geqslant C_j^{SU}(u_j^{t,\psi} - u_j^{t-1,\psi})\,, \forall t \tag{3.11f}$$

$$\sum_{i\in I} s_{ji}^{t,\psi} \leqslant u_j^{t,\psi} K_j\,, \forall t \tag{3.11g}$$

$$\sum_{i\in I} s_{ji}^{t,\psi} \geqslant u_j^{t,\psi} k_j\,, \forall t \tag{3.11h}$$

$$\sum_{i\in I} s_{ji}^{t,\psi} - \sum_{i\in I} s_{ji}^{t-1,\psi} \geqslant -u_j^{t-1,\psi} R_j^D\,, \forall t \tag{3.11i}$$

$$\sum_{i\in I} s_{ji}^{t,\psi} - \sum_{i\in I} s_{ji}^{t-1,\psi} \leqslant u_j^{t,\psi} R_j^U\,, \forall t \tag{3.11j}$$

- Financial Trader 5

$$\underset{s_{5i}^{inc,t,\psi}, s_{5i}^{dec,t,\psi}}{\text{maximize}} \quad \sum_{t\in T} \mathbb{E}_\omega \Big\{ \sum_{i\in I} \Big[(p_i^{t,\psi}(d_i^{t,\psi}) - p_i^{t,\omega}) s_{5i}^{inc,t,\psi} + (p_i^{t,\omega} - p_i^{t,\psi}(d_i^{t,\psi})) s_{5i}^{dec,t,\psi} \Big] \Big\} \tag{3.12a}$$

$$\text{subject to} \quad s_{5i}^{inc,t,\psi} \geqslant 0\,, \forall t \tag{3.12b}$$

$$s_{5i}^{dec,t,\psi} \geqslant 0\,, \forall t \tag{3.12c}$$

$$\sum_{t\in T} \sum_{i\in I} \Big(R_i^{inc,t} s_{5i}^{inc,t,\psi} + R_i^{dec,t} s_{5i}^{dec,t,\psi} \Big) \leqslant S_5\,, \tag{3.12d}$$

The ISO's formulation and other conditions are the same as Equations 3.8, 3.5, 3.9. Trader 4's problem is the same as Equations 3.10, with generators' and trader 5's day-ahead problem replaced by Equations 3.11 and 3.12. Case 3 represents a benchmark characterized by the same behavioral assumptions and participants of Case 2, absent FTR positions.

3.2.3 Case 4: Real-time Cournot, Day-ahead Cournot Model Formulation

In this subsection, we allow generators to behave à la Cournot in the real-time market. Note that this behavioral assumption is not possible in the previous chapter as perfect competition for generators in the real-time market is essential to derive

analytical solution in the real-time stage of the game. The formulations are listed below:

3.2.3.1 Real-time Market Model Formulation

To allow generators behave à la Cournot in the real-time market, real-time inverse demand functions are needed in the formulation. For every real-time scenario ω:

- Real-time Demand at Node i

$$p_i^{t,\omega} = p_i^{t,\omega}(d_i^{t,\omega}) = \\ a_i^{t,\omega} - b_i^{t,\omega}\Big(\sum_{j\in J} s_{ji}^{t,\omega} + m_i^{t,\omega} + \sum_{j\in J} s_{ji}^{t,\psi} + m_i^{t,\psi}\Big)\,, \forall t \tag{3.13a}$$

Substitute the real-time prices with the above real-time inverse demand function, generators' problem formulation are listed as follows:

- Generator j at node $i(j)$

$$\underset{s_{ji}^{t,\omega}, u_j^{t,\omega}, c_j^{t,\omega}}{\text{maximize}} \quad \sum_{t\in T}\Big[\sum_{i\in I}(p_i^{t,\omega}(d_i^{t,\omega}) - w_i^{t,\omega})s_{ji}^{t,\omega} + w_{i(j)}^{t,\omega}(\sum_{i\in I} s_{ji}^{t,\omega}) + \sum_{i\in I}(p_i^{t,\psi} - w_i^{t,\psi})s_{ji}^{t,\psi} \\ + w_{i(j)}^{t,\psi}(\sum_{i\in I} s_{ji}^{t,\psi}) - C_j\sum_{i\in I}(s_{ji}^{t,\omega} + s_{ji}^{t,\psi}) - c_j^{t,\omega} - c_j^{t,\psi}\Big] \tag{3.14a}$$

$$\text{subject to} \quad s_{ji}^{t,\omega} + s_{ji}^{t,\psi} \geqslant 0\,, \forall t, i \tag{3.14b}$$

$$u_j^{t,\omega} \geqslant 0\,, \forall t \tag{3.14c}$$

$$u_j^{t,\omega} + u_j^{t,\psi} \leqslant 1\,, \forall t \tag{3.14d}$$

$$c_j^{t,\omega} + c_j^{t,\psi} \geqslant 0\,, \forall t \tag{3.14e}$$

$$c_j^{t,\omega} + c_j^{t,\psi} \geqslant C_j^{SU}(u_j^{t,\omega} + u_j^{t,\psi} - u_j^{t-1,\omega} - u_j^{t-1,\psi})\,, \forall t \tag{3.14f}$$

$$\sum_{i\in I}(s_{ji}^{t,\omega} + s_{ji}^{t,\psi}) \leqslant (u_j^{t,\omega} + u_j^{t,\psi})K_j\,, \forall t \tag{3.14g}$$

$$\sum_{i\in I}(s_{ji}^{t,\omega} + s_{ji}^{t,\psi}) \geqslant (u_j^{t,\omega} + u_j^{t,\psi})k_j\,, \forall t \tag{3.14h}$$

$$\sum_{i\in I}(s_{ji}^{t,\omega} + s_{ji}^{t,\psi}) - \sum_{i\in I}(s_{ji}^{t-1,\omega} + s_{ji}^{t-1,\psi}) \geqslant -(u_j^{t-1,\omega} + u_j^{t-1,\psi})R_j^D\,, \forall t \tag{3.14i}$$

$$\sum_{i\in I}(s_{ji}^{t,\omega} + s_{ji}^{t,\psi}) - \sum_{i\in I}(s_{ji}^{t-1,\omega} + s_{ji}^{t-1,\psi}) \leqslant (u_j^{t,\omega} + u_j^{t,\psi})R_j^U\,, \forall t \tag{3.14j}$$

- ISO

$$\underset{y_i^{t,\omega}}{\text{maximize}} \quad \sum_{t\in T}\Big[\sum_{i\in I}(w_i^{t,\omega}y_i^{t,\omega}+p_i^{t,\omega}m_i^{t,\omega})\Big] \tag{3.15a}$$

$$\text{subject to} \quad -\sum_{i\in I} PTDF_{i,k}(y_i^{t,\omega}+y_i^{t,\psi}+m_i^{t,\omega}+m_i^{t,\psi}) \leqslant T_k\,, \forall t,k \tag{3.15b}$$

$$-\sum_{i\in I} PTDF_{i,k}(y_i^{t,\omega}+y_i^{t,\psi}+m_i^{t,\omega}+m_i^{t,\psi}) \geqslant -T_k\,, \forall t,k \tag{3.15c}$$

- Market clearing

For every hour t, market clearing conditions are listed below:

$$y_i^{t,\omega}+y_i^{t,\psi} = \sum_{j\in J}(s_{ji}^{t,\omega}+s_{ji}^{t,\psi}) - \sum_{i\in I}(s_{j(i)i}^{t,\omega}+s_{j(i)i}^{t,\psi})\,, \forall i \tag{3.16a}$$

3.2.3.2 Day-ahead Market Model Formulation

Day-ahead market formulations are the same as Section 3.2.2.2. Case 5 represents a benchmark characterized by the same behavioral assumptions and participants of Case 4, absent FTR positions.

3.3 Solution Method and Metrics

We solve the bi-level optimization problems in GAMS using the built-in Extended Mathematical Programming (EMP) tool. EMP reformulates the bi-level optimization problem as a Mathematical Program with Equilibrium Constraints (MPEC) and passes the MPEC on to the KNITRO solver.

Similarly to Chapter 2, we calculate average procurement cost, market participant profits, consumer surplus and social welfare to measure the impacts of different market behavioral assumptions and uneconomic virtual bidding strategy. The calculation for these metrics are the same as in Chapter 2 with one exception. When generators behave à la Cournot in the real-time market, and real-time demand is greater than the day-ahead schedule, the net consumer surplus at each node is calculated by summing up the day-ahead net consumer surplus (integrating the DA inverse demand function from zero to the day-ahead demand at that node) and real-time net consumer surplus, which is obtained by integrating the RT inverse

demand function from the day-ahead load level to the real-time load level at that node (See Figure 3.2). Consumer surplus for other cases follow the same calculation as described in Chapter 2.

Figure 3.2: Consumer Surplus Calculation when Generators Behave à la Cournot in the Real-time Market, and Real-time Load is Greater than Day-ahead Load

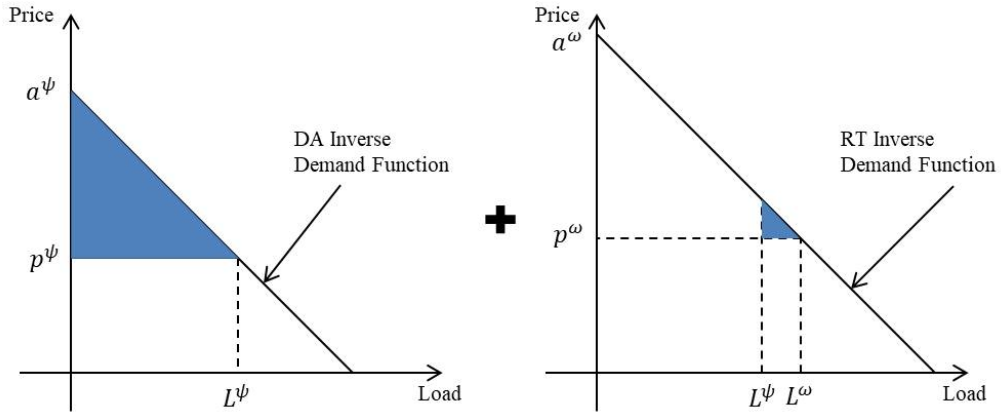

3.4 Parameters and Results

3.4.1 Parameters

Parameters used for the simulation are summarized in Table 3.2, 3.3 and 3.4.

- Power Transfer Distribution Factors (PTDFs) are calculated assuming equal reactances on all transmission lines.
- According to [83], the start-up cost for each generator includes a fuel component and a non-fuel component (i.e., consumption of water, chemicals and auxiliary power for starting the unit). For the fuel component, we use start-up fuel input by technology type from [83] and annual fuel costs for electricity generation from the EIA [84]. For the non-fuel component, we refer to other start-up costs by technology type, also given by [83]. This yields a per-unit start-up cost of 40$/MW, 15$/MW and 1$/MW for generator 1, 2 and 3, respectively, corresponding to a baseload, intermediate load and peak load generator. The per-unit start-up cost is then multiplied by nameplate capacity (in MW) to obtain the start-up cost for each generator, in $ (C_j^{SU}).

- Generation capacity, minimum output level and ramp rates are from [82].
- RTOs and ISOs have different policies for calculating reference prices and setting credit requirements for virtual positions. For instance, in the California ISO (CAISO) market, reference prices are calculated for each node for every three-month period of each year (Jan-Mar, Apr-Jun, Jul-Sep, and Oct-Dec). For one node, the reference price of a virtual supply position (INC) for a quarter is the 95th percentile value of the difference between hourly RT LMP and DA LMP of the same quarter from the previous year. Similarly, the reference price of a virtual demand position (DEC) for a quarter is the 95th percentile value of the difference between hourly DA LMP and RT LMP of the same quarter from the previous year [85, 86]. The reference prices in our simulations are obtained from CAISO and refer to year 2017 [87]. For determining the collateral requirement, we use instead information from PJM Interconnection. In this RTO, the minimum collateral requirements for market participants engaging in virtual and FTR transactions are \$200,000 and \$500,000, respectively [88]. In line with these requirements, we choose a collateral of \$800,000 for each financial market participant under perfect competition. However, to obtain an optimal equilibrium solution under the assumption of Cournot behavior, we must reduce the collateral value of each market participant to \$30,000.
- The FTR positions have to satisfy the simultaneous feasibility test to ensure revenue adequacy (i.e., total congestion charges collected from day-ahead markets must be sufficient to cover the FTR payments). FTRs are modeled as generation at source point and load at sink point. System operator then performs a DC power flow analysis to evaluate if the modeled FTR positions satisfy network constraints [89, 90]. In our case, the FTR path is from node A to node B. Assuming equal reactances for all three lines, one third of the FTR position will flow across line AC, which has a thermal limit of 150 MW. Therefore, the maximum FTR position that can be established on line AB to satisfy simultaneous feasibility is $f_{4AB} = 450MW$ (Figure 3.3).
- For the real-time competitive cases, the loads at each node for the two scenarios are exogenous and given in Table 3.3. Figure 3.4, 3.5 and 3.6 plot real-time load at node A, B and C, respectively. Table 3.4 summarizes the intercepts

Figure 3.3: Illustration on Simultaneous Feasibility Test

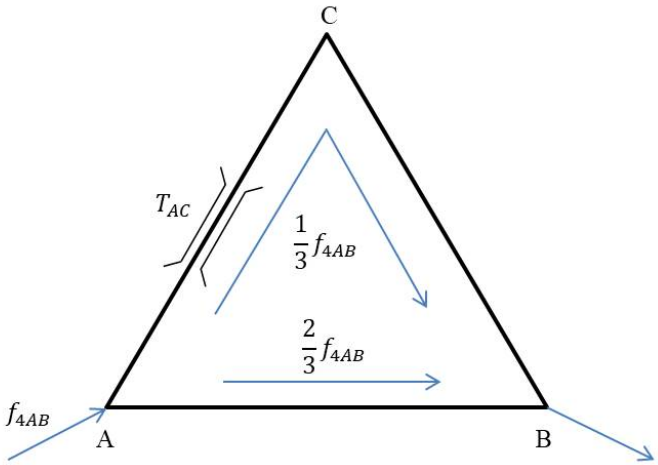

of day-ahead inverse demand functions, which are calibrated so that the day-ahead load follows the same pattern as the real-time load. For real-time Cournot cases, the intercepts of real-time inverse demand functions are equal to the intercepts of day-ahead inverse demand functions of corresponding hour, minus and plus 2 for scenario 1 and 2, respectively. Slopes for all inverse demand functions are set to be 0.1. The willingness to pay (WTP) used to calculate the real-time consumer surplus for an hour is set to be the same as the intercept of day-ahead inverse demand function for that hour.

3.4.2 Results

Table 3.5(a) and 3.5(b) summarize the results and metrics for the five cases simulated. Note that Case 3 and 5 represent benchmarks to assess changes in prices and other equilibrium market outcomes.

In Case 1, all market participants behave competitively in both real-time and day-ahead markets, and both financial traders have enough collateral ($800,000). The results show that the day-ahead prices converge to the expected real-time prices in all three nodes. Because of this, traders make zero profits on their virtual bids. Competitive generators also make zero profit. Case 1 achieves the highest consumer surplus as well as social welfare.

In Case 2, generators behave competitively in the real-time market while act à la Cournot in the day-ahead. Financial traders are also Cournot players in

the day-ahead market. This behavior difference induces price divergence between day-ahead and real-time markets in all three nodes (an averaged of 6.86 $/MWh). As an example, the hourly day-ahead prices and expected real-time prices at node C are plotted in Figure 3.7. This figure shows that the day-ahead price is consistently above the expected real-time price in all hours. A comparison between Case 2 and 3 allows us to see the effects of FTR positions: Trader 4 in Case 2 has given FTR position on line AB, while does not possess any FTR position in Case 3. The most significant contrast is that, Trader 4 is placing net DEC at node B and C in Case 2, despite the fact that day-ahead prices are higher than the expected real-time prices in these two nodes. This results in Trader 4 incurring a loss on her virtual bids at node B and C, therefore making her virtual bids "uneconomic". On the other hand, in Case 3, profitable net INC positions are taken by Trader 4 without FTR. The intuition behind this uneconomic bidding strategy is similar to what we found in the previous chapter: the possession of FTR gives financial traders the incentive to increase the day-ahead price at the sink node (an average DA LMP at node B of 25.30 $/MWh in Case 2 compared to 25.07 $/MWh in Case 3) while decrease that at the source node (an average DA LMP at node A of 18.31 $/MWh in Case 2 compared to 18.60 $/MWh in Case 3). This action is intended to enlarge the day-ahead price gap between sink and source, therefore enhance the value of the FTR position. One difference from this simulation result compared to the two-node case in Chapter 2 is that, with loop flows, price difference between source and sink can be induced by transmission congestions different from the FTR path. In this case, FTR path AB is not congested, yet the congestion on line AC is able to create day-ahead price difference between node A and B, therefore making the FTR position profitable. This also explains Trader 4's behavior of not only placing uneconomic demand bids at the FTR sink (node B), but also at node C, as DECs at node C serves as a direct way of creating congestion on line AC.

Case 4 and 5 simulate the scenarios where generators behave à la Cournot in both real-time and day-ahead markets. Trader 4 has given FTR position in Case 4 but not in Case 5. The result shows similar insight as in Case 2 and 3. Despite consistent day-ahead price premium over expected real-time price at node C (Figure 3.8), Trader 4 places virtual demand bids at this node which results in a loss of $ 2,159. In return, this strategy increases the day-ahead price at both node C and B (FTR sink), with an averaged DA LMP increased from 32.13 $/MWh (Case 5)

to 33.13 $/MWh (Case 4) at node C, and from 25.19 $/MWh (Case 5) to 25.62 $/MWh (Case 4) at node B. Similar to Case 2, FTR path AB is not congested in Case 4, but the congestion of line AC is able to induce price difference between FTR source and sink, making Trader 4's FTR position profitable. We also note that the increase of average forward premium at node C from Case 5 to Case 4 (1.41 $/MWh) is higher than that from Case 3 to Case 2 (0.10 $/MWh). This is because Cournot behavior in the real-time market increases the expected real-time price at node C, narrowing the forward price premium at this node and giving Trader 4 the incentive to place more uneconomic virtual demand positions at node C. This suggests that primary reliance on measures of long-run price convergence, as is often the case, may not be able to effectively detect when manipulation is in the works.

When comparing Case 2 to Case 3, we observe a higher percentage of commitment for generator 2 and 3, and a lower commitment percentage for generator 1. As a result, generator 2 and 3 incur higher commitment cost while generator 1's commitment cost is lower in Case 2. This is because uneconomic virtual demand bids increase day-ahead prices at node B and C, making generators at these nodes commit a higher share of their capacity. On the other hand, economic virtual supply offers at node A decrease the day-ahead price at that node, making generator 1 commit a lower share of its capacity in Case 2. Similar conclusions can be drawn comparing Case 4 and 5.

Figure 3.4: Real-time Load at Node A for RT Competitive Cases

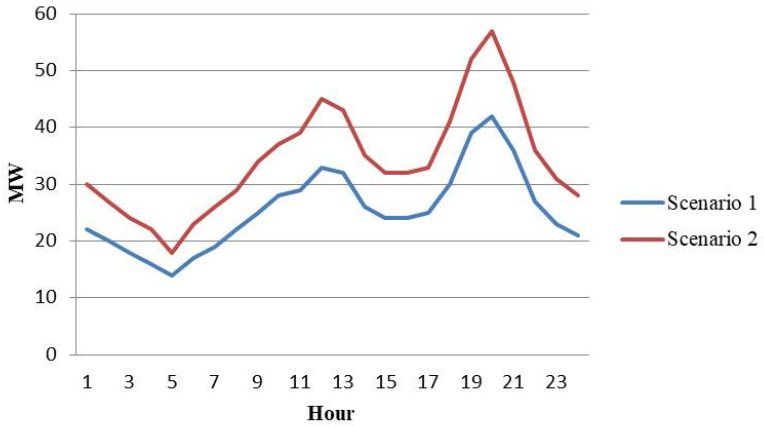

Table 3.2: Assumed Parameters for Base Cases

C_1 (\$/MWh)	10
C_2 (\$/MWh)	20
C_3 (\$/MWh)	30
C_1^{SU} (\$)	20,000
C_2^{SU} (\$)	7,500
C_3^{SU} (\$)	1,000
K_1 (MW)	500
K_2 (MW)	500
K_3 (MW)	1,000
$k_1 = k_2 = k_3$ (MW)	0
$R_1^D = R_1^U$ (MW)	500
$R_2^D = R_2^U$ (MW)	500
$R_3^D = R_3^U$ (MW)	1,000
T_{AB} (MW)	1,000
T_{BC} (MW)	1,000
T_{AC} (MW)	150
$R_A^{inc} = R_B^{inc} = R_C^{inc}$ (\$/MWh)	75
$R_A^{dec} = R_B^{dec} = R_C^{dec}$ (\$/MWh)	11
$S_4 = S_5$ (\$) (Competitive)	800,000
$S_4 = S_5$ (\$) (Cournot)	30,000
c_f/n (\$/MW)	0
f_{4AB} (MW)	450

Figure 3.5: Real-time Load at Node B for RT Competitive Cases

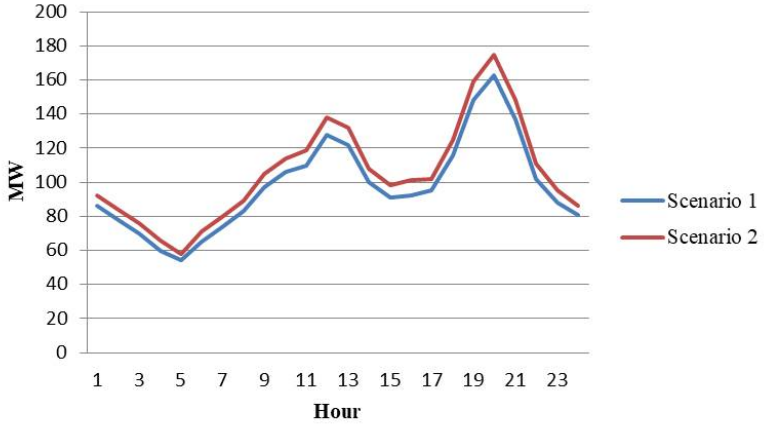

Table 3.3: Hourly Real-time Load (MW)

Hour	Load at A		Load at B		Load at C	
	Scenario 1	Scenario 2	Scenario 1	Scenario 2	Scenario 1	Scenario 2
1	22	30	86	92	171	435
2	20	27	78	84	156	396
3	18	24	70	76	140	357
4	16	22	60	66	125	309
5	14	18	54	58	109	273
6	17	23	65	71	135	334
7	19	26	74	80	151	377
8	22	29	83	89	166	422
9	25	34	97	105	197	494
10	28	37	106	114	213	539
11	29	39	110	119	223	559
12	33	45	128	138	260	650
13	32	43	122	132	249	617
14	26	35	100	108	203	507
15	24	32	91	98	182	458
16	24	32	92	101	187	471
17	25	33	95	102	192	484
18	30	41	116	125	234	588
19	39	52	148	159	301	750
20	42	57	163	175	327	822
21	36	48	137	148	275	692
22	27	36	102	111	208	520
23	23	31	88	95	177	448
24	21	28	81	86	161	409

Figure 3.6: Real-time Load at Node C for RT Competitive Cases

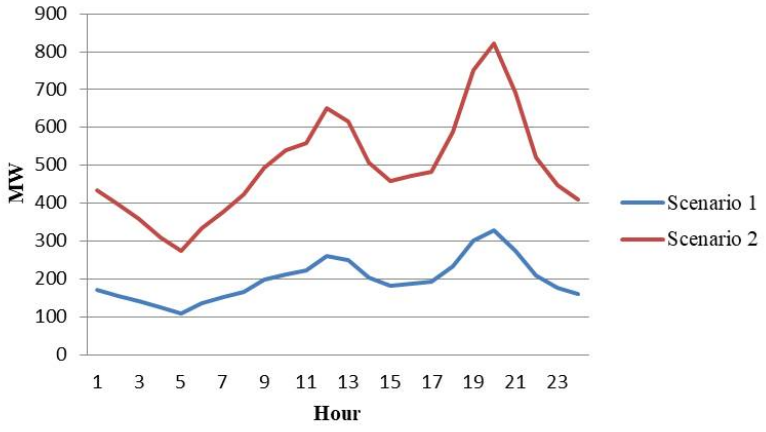

Table 3.4: Intercepts of Hourly Day-ahead Inverse Demand Functions ($/MW)

Hour	**Node** A	**Node** B	**Node** C
1	20.03	32.09	59.13
2	18.88	30.79	55.42
3	19.01	29.55	51.77
4	19.55	28.45	48.25
5	19.57	27.42	44.47
6	19.14	29.03	50.37
7	18.73	30.16	53.75
8	19.93	31.63	57.89
9	20.34	35.08	66.85
10	20.66	36.22	70.27
11	20.66	37.18	72.87
12	20.88	39.90	80.80
13	20.03	39.01	78.09
14	20.45	35.45	67.91
15	20.20	34.25	64.00
16	20.18	34.50	65.01
17	20.28	34.77	66.01
18	20.96	38.05	75.35
19	22.10	43.09	89.57
20	22.58	45.52	95.53
21	21.62	41.24	84.37
22	20.55	35.78	68.92
23	20.13	32.50	60.43
24	18.95	31.21	56.66

Figure 3.7: Price Divergence at Node C for Case 2

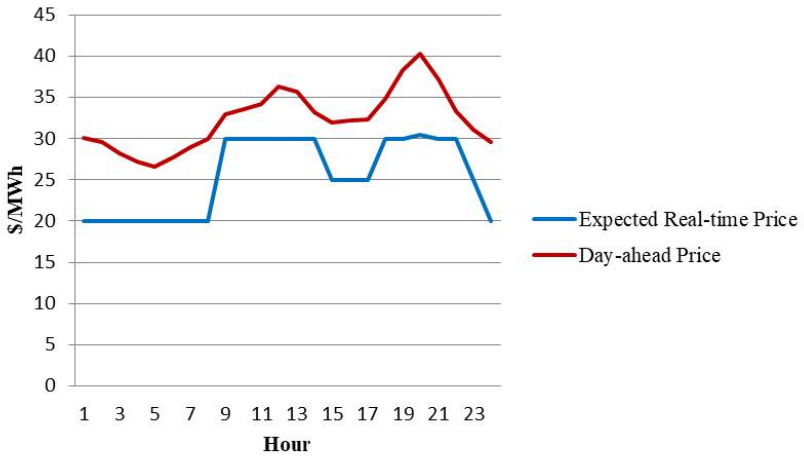

Figure 3.8: Price Divergence at Node C for Case 4

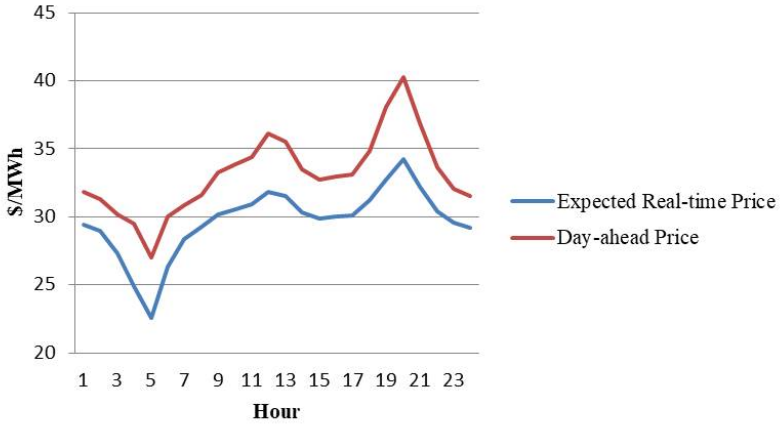

Table 3.5: Numerical Results

(a) Prices, Positions and Selected Metrics

Cases **RT Behavior** **DA Behavior** **Trader 4 with FTR?**		Case 1 Competitive Competitive Y	Case 2 Competitive Cournot Y	Case 3 Competitive Cournot N	Case 4 Cournot Cournot Y	Case 5 Cournot Cournot N
Total Day-ahead Generation (MW)	G1	2,894.48	4,781.76	4,994.88	4,640.64	4,746.72
	G2	795.26	3,366.60	3,197.25	3,595.92	3,289.77
	G3	671.37	1,991.78	1,980.37	2,325.72	2,045.97
Max Commitment	G1	0.455	0.485	0.495	0.525	0.530
	G2	0.485	0.495	0.470	0.440	0.435
	G3	0.330	0.410	0.395	0.375	0.375
Average Expected Real-time Prices ($/MWh)	Node A	11.67	11.44	11.44	13.90	13.86
	Node B	18.56	18.44	18.44	21.79	21.97
	Node C	25.46	25.44	24.78	29.67	30.08
Average Day-ahead Prices ($/MWh)	Node A	11.67	18.31	18.60	18.11	18.26
	Node B	18.56	25.30	25.07	25.62	25.19
	Node C	25.46	32.29	31.53	33.13	32.13
Average Forward Premium ($/MWh)	Node A	0.00	6.87	7.16	4.21	4.40
	Node B	0.00	6.86	6.63	3.83	3.22
	Node C	0.00	6.85	6.75	3.46	2.05
Trader 4 Total Virtual Bids (MW)	Node A	3,001.53	382.47	95.42	299.14	302.86
	Node B	765.53	-78.30	60.79	0.00	31.91
	Node C	2,087.47	-41.24	243.76	-687.67	64.81
Trader 5 Total Virtual Bids (MW)	Node A	2,261.21	137.12	178.16	211.88	265.20
	Node B	851.25	85.94	72.06	95.02	74.68
	Node C	2,326.52	176.99	149.76	93.10	57.96
Trader 4 Max DEC Position (MW)	Node B	-	57.53	-	0.00	0.00
	Node C	-	13.46	-	75.78	0.34
Generator Day-ahead Sales (MW)	Node A	2,301.29	3,380.10	3,390.75	3,520.70	3,360.93
	Node B	1,127.14	3,380.10	3,390.75	3,520.70	3,360.93
	Node C	932.73	3,380.10	3,390.75	3,520.70	3,360.93
Average Procurement Cost ($/MWh)	Node A	12.29	16.51	15.71	15.25	15.13
	Node B	19.58	25.53	25.47	25.01	24.95
	Node C	28.81	36.36	36.38	33.62	33.06
	Total	25.49	32.16	32.07	29.56	29.14
% Node B Uneconomic Bidding Hours		0.00%	8.33%	0.00%	0.00%	0.00%
% Node C Uneconomic Bidding Hours		0.00%	20.83%	0.00%	75.00%	0.00%

Table 3.5: Numerical Results

(b) Welfare

Cases **RT Behavior** **DA Behavior** **Trader 4 with FTR?**		Case 1 Competitive Competitive Y	Case 2 Competitive Cournot Y	Case 3 Competitive Cournot N	Case 4 Cournot Cournot Y	Case 5 Cournot Cournot N
	Revenue ($)	80,238	130,581	132,953	154,152	154,502
	Transmission Gain/Loss ($)	-20,958	-34,109	-32,104	-47,564	-45,772
Generator 1	Commitment Cost ($)	-9,020	-9,643	-9,822	-10,418	-10,545
	Generation Cost ($)	-50,260	-55,065	-55,278	-62,503	-63,270
	Profit ($)	0	31,764	35,749	33,667	34,915
	Revenue ($)	88,811	92,047	90,468	112,011	106,130
	Transmission Gain/Loss ($)	-1,359	-2,117	-3,069	1	3
Generator 2	Commitment Cost ($)	-3,653	-3,712	-3,536	-3,331	-3,256
	Generation Cost ($)	-83,799	-64,955	-64,110	-88,649	-85,149
	Profit ($)	0	21,263	19,753	20,032	17,728
	Revenue ($)	51,336	75,780	75,948	71,267	69,053
	Transmission Gain/Loss ($)	16,984	18,963	19,141	21,813	21,818
Generator 3	Commitment Cost ($)	-324	-410	-402	-375	-372
	Generation Cost ($)	-67,996	-81,848	-82,470	-79,488	-78,537
	Profit ($)	0	12,485	12,217	13,217	11,962
Producer Surplus (a) ($)		**0**	**65,512**	**67,719**	**66,916**	**64,605**
	Node A	19,596	3,001	2,967	3,101	3,228
Consumer	Node B	52,746	14,473	14,766	12,863	13,211
Surplus ($)	Node C	281,807	247,846	248,442	143,676	149,792
	Total (b)	**354,149**	**265,320**	**266,175**	**159,640**	**166,231**
	Node A	0	2,572	800	1,158	1,344
	Node B	0	-526	482	0	140
Profit for	Node C	0	-182	1,954	-2,159	312
Trader 4 ($)	FTR	74,475	75,523	NA	81,077	NA
	Total	74,475	77,387	3,236	80,076	1,796
	Node A	0	1,155	1,525	950	1,172
Profit for	Node B	0	727	594	418	310
Trader 5 ($)	Node C	0	1,673	1,324	469	272
	Total	0	3,555	3,443	1,837	1,754
Trader Surplus (c) ($)		**74,475**	**80,942**	**6,679**	**81,913**	**3,550**
ISO Real-time Surplus (d) ($)		**0**	**0**	**121**	**0**	**-1**
ISO Day-ahead Surplus (e) ($)		**74,475**	**75,523**	**69,789**	**81,077**	**74,902**
Social Welfare (a+b+c+d) ($)		**428,624**	**411,774**	**410,483**	**308,469**	**309,287**

The formula for calculating social welfare for Case 3 and 5 is (a+b+c+d+e), we need to add ISO's day-ahead surplus since Trader 4 does not have FTR position in these two cases.

3.4.3 Sensitivity Analysis

In this section, we conduct several sensitivity analyses to our baseline results. Specifically, our analyses consider Trader 5's collateral, generators' ramping capabilities, Trader 4's FTR position, reference price at node C, and the relationship between Trader 4's profitability and day-ahead load at node C. All simulations in this section are based on Case 4 where Trader 4 holds a FTR position, and generators behave à la Cournot in both real-time and day-ahead markets.

3.4.3.1 Trader 5's Collateral

When increasing the collateral of Trader 5, we observe a slight decrease of the day-ahead price at node C in all hours (Figure 3.9). This helps converge the day-ahead price at node C to the expected real-time level to some extent. However, increasing Trader 5's collateral past $150,000 fails to further close the gap as Trader 5 achieves maximum profits (Figure 3.10).

Figure 3.9: Relationship between Trader 5's Collateral and Day-ahead Price at Node C

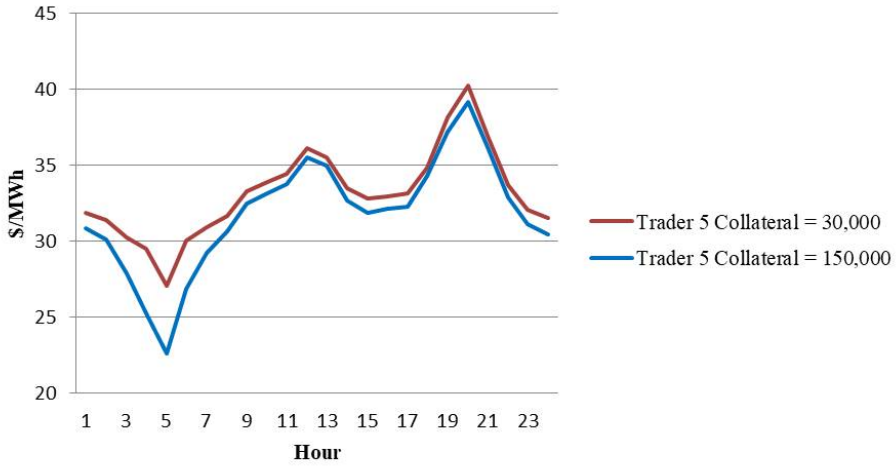

3.4.3.2 Ramping Capabilities

In the base cases, generators' ramping capabilities are assumed to be the same as their generation capacities. In this sensitivity analysis, we decrease both ramp-up and ramp-down rates for Generator 1, 2, and 3 down to 300, 300 and 100

Figure 3.10: Trader 5's Profits vs Collateral

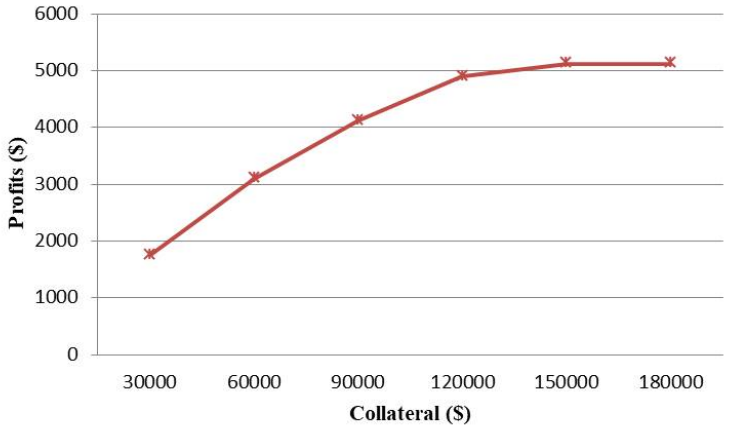

MW/Hour, respectively. Lowering the ramping capabilities prevents the most economical generators to be dispatched at their optimal levels in some hours. This limitation is most obvious in the first hour when generators are turning on. Compared to the base case, simulation results for this sensitivity analysis show that the Hour 1 day-ahead price at node A, B and C is increased by 5.65, 2.86 and 0.09 \$/MWh, respectively.

3.4.3.3 Trader 4's FTR Position

As shown in Table 3.6, when we decrease Trader 4's FTR position on line AB to 20 MW, there is no uneconomic bidding in this case because the FTR position is too small to give Trader 4 the incentive to engage in day-ahead price manipulation (i.e., the trader has no sufficient leverage).

3.4.3.4 Reference Prices at Node C

As described in Section 3.4.1, we obtain the reference prices from CAISO's website. For the year of 2017, the range of reference prices for INCs are between 10 and 75 \$/MWh, and between 11 and 52 \$/MWh for DECs. Table 3.7 summarizes Trader 4's virtual positions and profits using different combinations of reference prices at node C. When the reference price for INCs and DECs are at their upper and lower bound, respectively, Trader 4 places the largest amount of virtual demand bids at node C. Despite the big loss on her virtual position (- \$2,158.95), Trader

Table 3.6: Sensitivity Analysis of Trader 4's FTR Positions

FTR on AB (MW)		450	20
Key Equilibrium Outcomes			
Trader 4 Total	Node A	299.14	331.77
Virtual Bids	Node B	0.00	17.33
(MW)	Node C	-687.67	42.6
Average $\mathbb{E}(p_A^\omega)$ (\$/MWh)		13.90	13.87
Average $\mathbb{E}(p_B^\omega)$ (\$/MWh)		21.79	21.97
Average $\mathbb{E}(p_C^\omega)$ (\$/MWh)		29.67	30.06
Average p_A^ψ (\$/MWh)		18.11	18.24
Average p_B^ψ (\$/MWh)		25.62	25.20
Average p_C^ψ (\$/MWh)		33.13	32.16
Metrics			
% Node C Uneconomic Bidding Hours		75.00%	0.00%
Average Forward	Node A	4.21	4.37
Premium	Node B	3.83	3.23
(\$/MWh)	Node C	3.46	2.10
Profit for Trader 4 (\$)	Node A	1,158	1,460
	Node B	0	78
	Node C	-2,159	252
	FTR	81,077	3,341
	Total	80,076	5,131

4 records the highest FTR revenue (\$81,076.95) among all cases. On the other hand, when the reference price for INCs and DECs are at their lower and upper bound, respectively, Trader 4 places the smallest virtual demand bids at node C. This results in little loss on Trader 4's virtual position (- \$124.48), as well as the smallest FTR revenue (\$75,311.04) among all cases.

Table 3.7: Trader 4's Virtual Positions and Profits under Different Reference Prices at Node C

R_C^{inc} (\$/MWh)	75	75	10	10
R_C^{dec} (\$/MWh)	11	52	11	52
Virtual Position at Node C (MW)	-687.67	-180.60	-607.71	-119.44
Profit at Node C (\$)	-2,158.95	-570.98	-1,635.11	-124.48
Profit on FTR (\$)	81,076.95	78,192.49	78,291.81	75,311.04

3.4.3.5 Relationship between Trader 4's Profitability and Day-ahead Load at Node C

When placing uneconomic virtual demand bids at node C, Trader 4 takes heterogeneous positions across different hours in a day. To better understand what causes Trader 4 to bid more in certain hours, we plot Trader 4's profits as well as the day-ahead demand at node C against the time line. The medium load case corresponds to the intercepts of day-ahead inverse demand function as recorded in Table 3.4, the low and high load cases represent a decrease and increase of 10 from the intercepts of day-ahead inverse demand function at node C in the medium case. As we can see from Figure 3.11, Trader 4 in general has a tendency of losing more money when demand is low. This is consistent with Trader 4's motivation of placing uneconomic virtual bids: when demand is low, more virtual demand bids are needed to cause transmission congestion in the day-ahead market, so that the value of FTR can be enhanced. However, Trader 4 might not pursue uneconomic bidding in hours when demand is too low (Hour 5 of the Low Load case). This is because in these hours, the loss from virtual bids could outweigh the gains from FTR.

3.5 Conclusions

In this chapter, we develop a two-stage equilibrium model to study cross-product manipulation in the presence of loop flows and intertemporal constraints, and evaluate its effects on price convergence and other market outcomes using numerical simulations. Focusing on the day-ahead and real-time markets allows us to extend the model framework from Chapter 2 in several ways. First, a multi-node network can be incorporated in the analysis, enabling us to study the effect of loop flows on a trader's bidding strategy. Secondly, we include generator unit commitment decisions and other intertemporal constraints into the equilibrium framework, in order to capture the inter-dependence of consecutive trading hours. Lastly, instead of assuming away supplier market power in the real-time market, we are now able to let generators behave à la Cournot in both real-time and day-ahead markets. Similarly to the two-node case, numerical results show that a Cournot trader with FTR positions has an incentive to place uneconomic virtual bids to enhance

Figure 3.11: Relationship between Trader 4's Profitability and Day-ahead Load at Node C

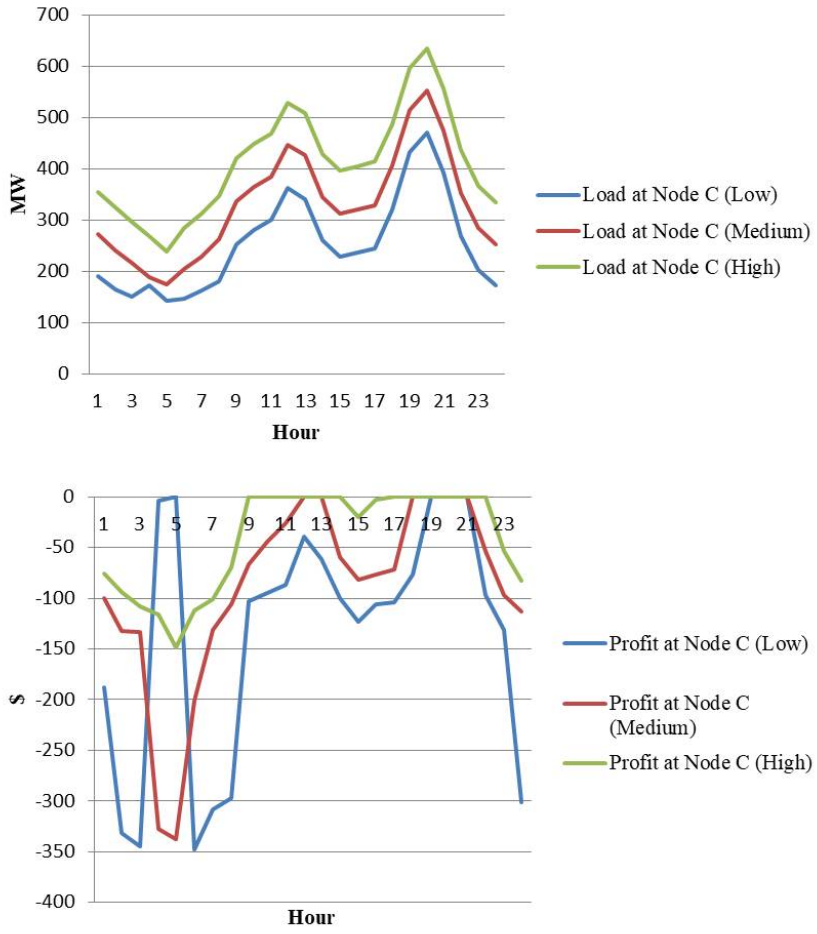

the value of her FTR positions. This uneconomic bidding strategy diverges the day-ahead price from its expected real-time level at the node(s) being manipulated. The model suggests that uneconomic bidding could take place at nodes other than the FTR sink. This is because, when loop flows are introduced, price separation between the source and sink of the FTR path can be induced by congestion of transmission lines different from the FTR path.

Cournot behavior in the real-time market increases the expected real-time price at node C, narrowing the forward price premium at this node but giving the trader holding FTRs the incentive to place more uneconomic virtual demand positions at node C. This suggests that primary reliance on measures of long-run price convergence, as is often the case, may not be able to effectively detect when

manipulation is in the works.

Since uneconomic manipulation increases the day-ahead prices at certain nodes, a higher fraction of capacity from generators located at these nodes will be dispatched, resulting in higher commitment costs for these generators.

We also find that traders tend to engage in uneconomic manipulation when day-ahead demand is low. This is consistent with the fact that more DECs will be needed to create transmission congestion in lower demand scenarios.

Currently, FTR positions in ISO markets are only limited by credit (or collateral) requirements and simultaneous feasibility [90]. Our analysis suggests that limiting trader FTR positions could be effective in preventing price manipulation through uneconomic virtual bids. However, the degree to which this limitation may affect the efficiency of FTR markets should be further investigated. In addition, our models inform market monitors and system operators regarding which factors affect the probability of cross-product manipulation. For example, our results indicate that supplier market power allows cross-product manipulation to succeed and be sustained in equilibrium. This suggests that locations/hours-of-sample where market participants exercise market power are more likely to be vulnerable to cross-product manipulation, and should thus be monitored more closely. Finally, Our model quantifies the price impact of cross-product manipulation. This could be potentially used to determine the amount of disgorgement in price manipulation cases. Future work will focus on revising the formulation of the multi-node model to include binary (or close to binary) commitment decisions.

Bibliography

[1] Energy Information Administration (2016), "U.S. Natural Gas Total Consumption," .
URL https://www.eia.gov/dnav/ng/hist/n9140us2A.htm

[2] ——— (2016), "U.S. Dry Natural Gas Production," .
URL https://www.eia.gov/dnav/ng/hist/n9070us2A.htm

[3] ——— (2016), "U.S. Dry Natural Gas Production by States," .
URL https://www.eia.gov/dnav/ng/NG_PROD_SUMPD_A_EPG0_FPD_MMCF_A.htm

[4] Ikonnikova, S., J. Browning, G. Gulen, K. Smye, and S. W. Tinker (2015) "Factors influencing shale gas production forecasting: Empirical studies of Barnett, Fayetteville, Haynesville, and Marcellus Shale plays," *Economics of Energy and Environmental Policy*, **4(1)**, pp. 19–35.

[5] Williams (2016), "Transco Operational Capacity," .
URL http://www.1line.williams.com/Transco/index.html

[6] Marcellus Gas (2016), "Well Information in Marcellus," .
URL https://www.marcellusgas.org/

[7] Gabriel, S. A., S. Kiet, and J. Zhuang (2005) "A Mixed Complementarity-Based Equilibrium Model of Natural Gas Markets," *Operations Research*, **53(5)**, pp. 799–818.

[8] Gabriel, S. A., J. Zhuang, and S. Kiet (2005) "A Large-Scale Complementarity Model of the North American Natural Gas Market," *Energy Economics*, **27**, pp. 639–665.

[9] Gabriel, S. A., K. E. Rosendahl, R. Egging, H. G. Avetisyan, and S. Siddiqui (2012) "Cartelization in Gas Markets: Studying the Potential for a "Gas OPEC"," *Energy Economics*, **34**, pp. 137–152.

[10] Egging, R., F. Holz, and S. A. Gabriel (2010) "The World Gas Model — A Multi-Period Mixed Complementarity Model for the Global Natural Gas Market," *Energy*, **35**, pp. 4016–4029.

[11] Egging, R., S. A. Gabriel, F. Holz, and J. Zhuang (2008) "A Complementarity Model for the European Natural Gas Market," *Energy Policy*, **36**, pp. 2385–2414.

[12] Lise, W. and B. F. Hobbs (2008) "Future Evolution of the Liberalised European Gas Market: Simulation Results with a Dynamic Model," *Energy*, **33(7)**, pp. 989–1004.

[13] Zwart, G. T. (2009) "European Natural Gas Markets: Resource Constraints and Market Power," *The Energy Journal*, **30**, pp. 151–165.

[14] Hartley, P. and K. B. Medlock (2006) "The Baker Institute World Gas Trade Model," in *Natural Gas and Geopolitics: From 1970 to 2040* (D. G. Victor, A. M. Jaffe, and M. H. Hayes, eds.), Cambridge University Press, pp. 357–406.

[15] Rosendahl, K. E. and E. L. Sagen (2009) "The Global Natural Gas Market: Will Transport Cost Reductions Lead to Lower Prices?" *The Energy Journal*, **30(2)**, pp. 17–39.

[16] Aune, F. R., K. E. Rosendahl, and E. L. Sagen (2009) "Globalisation of Natural Gas Markets: Effects on Prices and Trade Patterns," *The Energy Journal*, **30**, pp. 39–53.

[17] De Vany, A. and W. D. Walls (1996) "The Law of One Price in a Network: Arbitrage and Price Dynamics in Natural Gas City Gate Markets," *Journal of Regional Science*, **36(4)**, pp. 555–570.

[18] Kleit, A. N. (1998) "Did Open Access Integrate Natural Gas Markets? An Arbitrage Cost Approach," *Journal of Regulatory Economics*, **14**, pp. 19–33.

[19] ——— (2001) "Defining Electricity Markets: An Arbitrage Cost Approach," *Resource and Energy Economics*, **23**, pp. 259–270.

[20] Joutz, F., R. Trost, D. Shin, and B. McDowell (2009) "Estimating Regional Short-Run and Long-Run Price Elasticities of Residential Natural Gas Demand in the U.S." *Social Science Research Network Working Paper*.

[21] Energy Information Administration (2006), "Reduced Form Energy Model Elasticities from EIA's Regional Short-Term Energy Model," .
URL `https://www.eia.gov/forecasts/steo/special/pdf/elasticities.pdf`

[22] Huntington, H. G. (2007) "Industrial Natural Gas Consumption in the United States: An Empirical Model for Evaluating Future Trends," *Energy Economics*, **29**, pp. 743–759.

[23] Energy Information Administration (2012), "Fuel Competition in Power Generation and Elasticities of Substitution," .
URL `https://www.eia.gov/analysis/studies/fuelelasticities/pdf/eia-fuelelasticities.pdf`

[24] Hausman, C. and R. Kellogg (2015) "Welfare and Distributional Implications of Shale Gas," *NBER Working Paper 21115*.

[25] Federal Energy Regulatory Commission Order No. 888 (1996), "Promoting Wholesale Competition Through Open Access Non-discriminatory Transmission Services by Public Utilities; Recovery of Stranded Costs by Public Utilities and Transmitting Utilities," .
URL `http://www.ferc.gov/legal/maj-ord-reg/land-docs/order888.asp`

[26] Federal Energy Regulatory Commission Order No. 889 (1996), "Open Access Same-Time Information System (formerly Real-Time Information Networks) and Standards of Conduct," .
URL `http://www.ferc.gov/legal/maj-ord-reg/land-docs/order889.asp`

[27] Federal Energy Regulatory Commission Order No. 2000 (1999), "Regional Transmission Organizations," .
URL `http://www.ferc.gov/legal/maj-ord-reg/land-docs/RM99-2A.pdf`

[28] Kury, T. J. (2013) "Price Effects of Independent Transmission System Operators in the United States Electricity Market," *Journal of Regulatory Economics*, **43(2)**, pp. 147–167.

[29] ISO/RTO Council (2015), "IRC History," .
URL `http://www.isorto.org/about/irchistory`

[30] Fabra, N., N.-H. von der Fehr, and D. Harbord (2006) "Designing Electricity Auctions," *The RAND Journal of Economics*, **37(1)**, pp. 23–46.

[31] Schweppe, F. C., M. C. Caramanis, R. D. Tabors, and R. E. Bohn (1988) *Spot Pricing of Electricity*, Kluwer Academic Publishers.

[32] Helman, U., B. F. Hobbs, and R. P. O'Neill (2008) "The Design of U.S. Wholesale Energy and Ancillary Service Auction Markets: Theory and Practice," in *Competitive Electricity Markets: Design, Implementation, Performance* (F. P. Sioshansi, ed.), chap. 5, Elsevier, pp. 179–243.

[33] Borenstein, S., J. Bushnell, C. R. Knittel, and C. Wolfram (2008) "Inefficiencies and Market Power in Financial Arbitrage: A Study of California's Electricity Markets," *The Journal of Industrial Economics*, **56(2)**, pp. 347–378.

[34] Ledgerwood, S. D. and J. P. Pfeifenberger (2013) "Using Virtual Bids to Manipulate the Value of Financial Transmission Rights," *The Electricity Journal*, **26(9)**, pp. 9–25.

[35] PJM Interconnection (2015), "Virtual Transactions in the PJM Energy Markets," .
URL http://www.pjm.com/~/media/documents/reports/20151012-virtual-bid-report.ashx

[36] Monitoring Analytics (2015), "State of the Market Report for PJM," .
URL http://www.monitoringanalytics.com/reports/PJM_State_of_the_Market/2015/2015-som-pjm-volume2-sec3.pdf

[37] Potomac Economics (2015), "State of the Market Report for the New York ISO Markets," .
URL http://www.nyiso.com/public/webdocs/markets_operations/documents/Studies_and_Reports/Reports/Market_Monitoring_Unit_Reports/2015/NYISO2015SOMReport_5-23-2016-CORRECTED.pdf

[38] California ISO (2014), "Annual Report on Market Issues and Performance," .
URL http://www.caiso.com/Documents/2014AnnualReport_MarketIssues_Performance.pdf

[39] ——— (2015), "Annual Report on Market Issues and Performance," .
URL http://www.caiso.com/Documents/2015AnnualReportonMarket\\IssuesandPerformance.pdf

[40] Potomac Economics (2014), "Assessment of the ISO New England Electricity Markets," .
URL https://www.potomaceconomics.com/uploads/isone_reports/isone_2014_emm_report_6_16_2015_final.pdf

[41] ——— (2015), "Assessment of the ISO New England Electricity Markets," .
URL https://www.potomaceconomics.com/uploads/isone_reports/ISONE_2015_EMM_Report_final_6-14-16.pdf

[42] Midcontinent ISO (2015), "January 2015 Informational Forum," .
URL https://www.misoenergy.org/Library/Repository/MeetingMaterial/Stakeholder/InformationalForum/2015/20150120/20150120InformationalForumPresentation.pdf

[43] ——— (2016), "January 2016 Informational Forum," . URL https://www.misoenergy.org/Library/Repository/MeetingMaterial/Stakeholder/InformationalForum/2016/20160126/20160126InformationalForumPresentation.pdf

[44] Hogan, W. W. (1992) "Contract Networks for Electric Power Transmission," *Journal of Regulatory Economics*, **4(3)**, pp. 211–242.

[45] Rosellón, J. and T. Kristiansen (2013) *Financial Transmission Rights: Analysis, Experiences and Prospects*, Springer.

[46] Isemonger, A. G. (2006) "The Benefits and Risks of Virtual Bidding in Multi-settlement Markets," *The Electricity Journal*, **19(9)**, pp. 26–36.

[47] Celebi, M., A. Hajos, and P. Q. Hanser (2010) "Virtual Bidding: the Good, the Bad and the Ugly," *The Electricity Journal*, **23(5)**, pp. 16–25.

[48] Parsons, J. E., C. Colbert, J. Larrieu, T. Martin, and E. Mastrangelo (2015) "Financial Arbitrage and Efficient Dispatch in Wholesale Electricity Markets," *MIT Center for Energy and Environmental Policy Research Working Paper 15-002*.

[49] Lo Prete, C., B. Liu, and J. Wang (2018) "Cross-product Manipulation in Electricity Markets: Insights from Strategic Trade Models of Asymmetric Information," *Working Paper*.

[50] Kumar, P. and D. J. Seppi (1992) "Futures Manipulation with "Cash Settlement"," *The Journal of Finance*, **47(4)**, pp. 1485–1502.

[51] Klemperer, P. and M. Meyer (1989) "Supply Function Equilibria in Oligopoly under Uncertainty," *Econometrica*, **57(6)**, pp. 1243–1277.

[52] Green, R. and D. M. Newbery (1992) "Competition in the British Electricity Spot Market," *Journal of Political Economy*, **100(5)**, pp. 929–953.

[53] von der Fehr, N. and D. Harbord (1993) "Spot Market Competition in the UK Electricity Industry," *The Economic Journal*, **103(418)**, pp. 531–546.

[54] Newbery, D. M. (1998) "Competition, Contracts, and Entry in the Electricity Spot Market," *The RAND Journal of Economics*, pp. 726–749.

[55] Allaz, B. (1992) "Oligopoly, Uncertainty and Strategic Forward Transactions," *International Journal of Industrial Organization*, **10(2)**, pp. 297–308.

[56] Allaz, B. and J.-L. Vila (1993) "Cournot Competition, Forward Markets and Efficiency," *Journal of Economic Theory*, **59(1)**, pp. 1–16.

[57] Powell, A. (1993) "Trading Forward in an Imperfect Market: The Case of Electricity in Britain," *The Economic Journal*, **103(417)**, pp. 444–453.

[58] Saravia, C. (2003) "Speculative Trading and Market Performance: The Effect of Arbitrageurs on Efficiency and Market Power in the New York Electricity Market," *Center for the Study of Energy Markets (CSEM) Working Paper*.

[59] Yao, J., I. Adler, and S. S. Oren (2008) "Modeling and Computing Two-settlement Oligopolistic Equilibrium in A Congested Electricity Network," *Operations Research*, **56(1)**, pp. 34–47.

[60] Yao, J., S. S. Oren, and I. Adler (2004) "Computing Cournot Equilibria in Two-settlement Electricity Markets with Transmission Constraint," *Proceedings of the 37th Annual Hawaii International Conference on System Sciences*.

[61] ——— (2007) "Two-settlement Electricity Markets with Price Caps and Cournot Generation Firms," *European Journal of Operational Research*, **181(3)**, pp. 1279–1296.

[62] Shanbhag, U. V., G. Infanger, and P. W. Glynn (2011) "A Complementarity Framework for Forward Contracting under Uncertainty," *Operations Research*, **59(4)**, pp. 810–834.

[63] Cardell, J. B., C. C. Hitt, and W. W. Hogan (1997) "Market Power and Strategic Interaction in Electricity Networks," *Resource and Energy Economics*, **19(1)**, pp. 109–137.

[64] Hobbs, B. F., C. B. Metzler, and J.-S. Pang (2000) "Strategic Gaming Analysis for Electric Power Systems: An MPEC Approach," *IEEE Transactions on Power Systems*, **15(2)**, pp. 638–645.

[65] Kamat, R. and S. S. Oren (2004) "Two-settlement Systems for Electricity Markets under Network Uncertainty and Market Power," *Journal of Regulatory Economics*, **25(1)**, pp. 5–37.

[66] Hu, X. and D. Ralph (2007) "Using EPECs to Model Bilevel Games in Restructured Electricity Markets with Locational Prices," *Operations Research*, **55(5)**, pp. 809–827.

[67] Murphy, F. and Y. Smeers (2010) "On the Impact of Forward Markets on Investments in Oligopolistic Markets with Reference to Electricity," *Operations Research*, **58(3)**, pp. 515–528.

[68] ——— (2012) "Withholding Investments in Energy Only Markets: Can Contracts Make A Difference?" *Journal of Regulatory Economics*, **42(2)**, pp. 159–179.

[69] Sauma, E. E. and S. S. Oren (2006) "Proactive Planning and Valuation of Transmission Investments in Restructured Electricity Markets," *Journal of Regulatory Economics*, **30(3)**, pp. 261–290.

[70] Ruiz, C., S. J. Kazempour, and A. J. Conejo (2012) "Equilibria in Futures and Spot Electricity Markets," *Electric Power Systems Research*, **84(1)**, pp. 1–9.

[71] Hu, J., J. E. Mitchell, J. S. Pang, K. P. Bennett, and G. Kunapuli (2008) "On the Global Solution of Linear Programs with Linear Complementarity Constraints," *SIAM Journal on Optimization*, **19(1)**, pp. 445–471.

[72] Pang, J. S. and M. Fukushima (2005) "Quasi-variational Inequalities, Generalized Nash Equilibria, and Multi-leader-follower Games," *Computational Management Science*, **2(1)**, pp. 21–56.

[73] Gabriel, S. A., A. J. Conejo, J. D. Fuller, B. F. Hobbs, and C. Ruiz (2012) *Complementarity Modeling in Energy Markets*, Springer Science & Business Media.

[74] Su, C. L. (2005) "Equilibrium Problems with Equilibrium Constraints: Stationarities, Algorithms, and Applications," *Stanford University*.

[75] Leyffer, S. and T. Munson (2005) "Solving Multi-leader-follower Games," *Preprint ANL/MCS-P1243-0405*.

[76] Su, C. L. (2007) "Analysis on the Forward Market Equilibrium Model," *Operations Research*, **35(1)**, pp. 74–82.

[77] Monitoring Analytics (2017), "State of the Market Report for PJM," . URL `http://www.monitoringanalytics.com/reports/PJM_State_of_the_Market/2017/2017q2-som-pjm-sec13.pdf`

[78] California Independent System Operator (2017), "Business Practice Manual for Congestion Revenue Rights," .

[79] Dillon, T. S., K. W. Edwin, H. D. Kochs, and R. J. Taud (1978) "Integer Programming Approach to the Problem of Optimal Unit Commitment with Probabilistic Reserve Determination," *IEEE Transactions on Power Apparatus and Systems*, **(6)**, pp. 2154–2166.

[80] Arroyo, J. M. and A. J. Conejo (2000) "Optimal Response of A Thermal Unit to An Electricity Spot Market," *IEEE Transactions on Power Systems*, **15(3)**, pp. 1098–1104.

[81] Carrion, M. and J. M. Arroyo (2006) "A Computationally Efficient Mixed-integer Linear Formulation for the Thermal Unit Commitment Problem," *IEEE Transactions on Power Systems*, **21(3)**, pp. 1371–1378.

[82] Kazempour, J. and B. F. Hobbs (2018) "Value of Flexible Resources, Virtual Bidding, and Self-Scheduling in Two-Settlement Electricity Markets with Wind Generation," *IEEE Transactions on Power Systems*, **33(1)**, pp. 749–759.

[83] Kumar, N., P. Besuner, S. Lefton, D. Agan, and D. Hilleman (2012) "Power plant cycling costs (No. NREL/SR-5500-55433)," *National Renewable Energy Laboratory (NREL), Golden, CO.*

[84] Energy Information Administration (2018), "Average Cost of Fossil Fuels for Electricity Generation," `https://www.eia.gov/electricity/data.php`.

[85] Li, R., A. J. Svoboda, and S. S. Oren (2015) "Efficiency Impact of Convergence Bidding in the California Electricity Market," *Journal of Regulatory Economics*, **48(3)**, pp. 245–284.

[86] California Independent System Operator (2016), "Business Practice Manual for Credit Management & Market Clearing," .

[87] California ISO (CAISO) (2017), "Reference Prices," `http://oasis.caiso.com/mrioasis/logon.do`.

[88] PJM Interconnection (2017), "Credit Overview and Supplement to the PJM Credit Policy," .
URL `http://www.pjm.com/~/media/documents/agreements/pjm-credit-overview.ashx`

[89] Transpower (2012), "FTR Design as Implemented September 2002," .
URL `https://www.transpower.co.nz/sites/default/files/plain-page/attachments/transpower-ftr-design-R1-0.pdf`

[90] PJM Interconnection (2017), "PJM Manual 06: Financial Transmission Rights," .
URL `https://www.pjm.com/~/media/documents/manuals/m06.ashx`

Vita

Nongchao Guo

Education

The Pennsylvania State University — University Park, PA
Ph.D. in Energy Management and Policy — August 2018

Northeastern University — Shenyang, China
B.Eng. in Biological Engineering — June 2011

Work Experience

New York Independent System Operator — Rensselaer, NY
Associate Economist — April 2018 – Present

California Independent System Operator — Folsom, CA
Market and Infrastructure Policy Intern — June 2017 – August 2017

KPMG — Shenyang, China
Auditor — October 2011 – April 2012

Teaching Experience

TA for EBF 483: Introduction to Electricity Markets	FA 2016
TA for EBF 401: Strategic Corporate Finance	FA 2015 & SP 2015
TA for EGEE 411: Energy Science and Engineering Lab	FA 2014 & FA 2013
Lab Instructor for PNG 451: Drilling Laboratory	SP 2014
TA for EGEE 101: Energy and the Environment	SP 2013
TA for EGEE 102: Energy Conservation for Environmental Protection	FA 2012

Working Papers

Lo Prete, C., **N. Guo**, and U. V. Shanbhag (2018) "Virtual Bidding and Financial Transmission Rights: An Equilibrium Model for Cross-Product Manipulation in Electricity Markets." (*under review*)

Kleit, A. N., C. Lo Prete, S. Blumsack, and **N. Guo** (2018) "Weather or Not? Welfare Impacts of Natural Gas Pipeline Expansion in the Northeastern U.S." (*under review*)

Honors & Awards

Outstanding Graduate Teaching Assistant Award	SP 2017 & SP 2015
EBF Scholarship in Honor of Dr. Richard Gordon	SP 2015
Funds for Excellence in Graduate Recruitment	FA 2012